Matematik ve Fen Bilimleri Üzerine Araştırmalar-III

Research on Mathematics and Science- III

Editör: Doç. Dr. Adile Akpınar

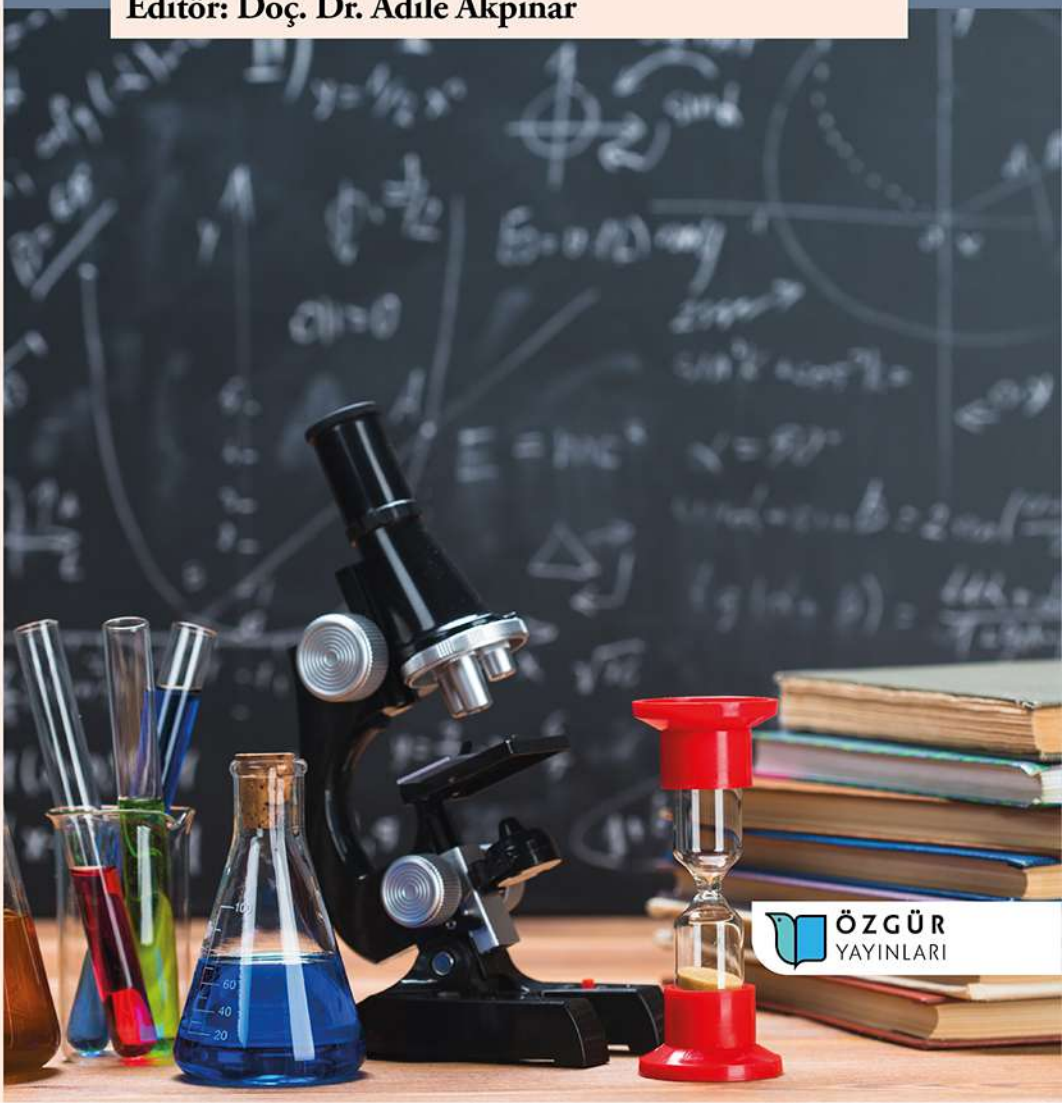

ÖZGÜR YAYINLARI

Matematik ve Fen Bilimleri Üzerine Araştırmalar-III

Editör:

Doç. Dr. Adile Akpınar

ÖZGÜR YAYINLARI

Published by
Özgür Yayın-Dağıtım Co. Ltd.
Certificate Number: 45503

15 Temmuz Mah. 148136. Sk. No: 9 Şehitkamil/Gaziantep
+90.850 260 09 97
+90.532 289 82 15
www.ozguryayınlari.com
info@ozguryayinlari.com

Matematik ve Fen Bilimleri Üzerine Araştırmalar-III

Research on Mathematics and Science- III

Editör: Doç. Dr. Adile Akpınar

Language: Turkish-English
Publication Date: 2023
Cover design by Mehmet Çakır
Cover design and image licensed under CC BY-NC 4.0
Print and digital versions typeset by Çizgi Medya Co. Ltd.

ISBN (PDF): 978-975-447-766-5

DOI: https://doi.org/10.58830/ozgur.pub252

Suggested citation:
Akpınar, A. (ed) (2023). *Matematik ve Fen Bilimleri Üzerine Araştırmalar-III.* Özgür Publications.
DOI: https://doi.org/10.58830/ozgur.pub252. License: CC-BY-NC 4.0

The full text of this book has been peer-reviewed to ensure high academic standards. For full review policies, see https://www.ozguryayinlari.com/

ÖZGÜR YAYINLARI

Önsöz

Matematik ve Fen bilimleri Üzerine Araştırmalar' başlıklı kitabın hazırlanmasındaki temel amaç, matematik, fizik, kimya, biyoloji gibi temel bilimlere ait güncel bilgileri veya araştırma bulgularını bir araya getirmektir. Kitap ile sunulan bölümler, sonrasındaki çalışmalar için kaynak niteliğinde olup yeni araştırmalar ve fikirler için ışık tutacaktır. Farklı disiplinleri bira araya getiren bu kitap ile başta lisans öğrencileri olmak üzere akademisyenlerin ve araştırmacıların çalışmalarına önemli katkılar sağlayacaktır. Kitabın hazırlanmasında emeği geçen tüm bölüm yazarlarına ve kitabı okuyucuları ile buluşturma fırsatı sunan 'Özgür Yayınları"nın tüm bireylerine teşekkür ederim.

Doç. Dr. Adile Akpınar

Preface

The main purpose of preparing the book titled 'Research on Mathematics and Science' is to bring together current information or research findings in basic sciences such as mathematics, physics, chemistry and biology. The chapters presented in the book will be a source for future studies and will be light on new research and ideas. This book, which brings together different disciplines, will make significant contributions to the studies of academics and researchers, especially undergraduate students. I would like to thank all the authors of the chapters who contributed to the preparation of the book, and all the individuals of 'Özgür Yayınları' who provided the opportunity to bring the book together with its readers.

Assoc. Prof. Adile Akpınar

İçindekiler

Bölüm 1

Amanita caesarea ve *Boletus reticulatus* Özütlerini İçeren Yenebilir Film Üretimi

Mukaddes Gökyermez[1]

Özge Süfer[2]

Fuat Bozok[3]

Özet

Bu çalışmanın amacı, Osmaniye ili Zorkun bölgesi Karıncalı yaylası toplanan *Amanita caesarea* (AC) ve *Boletus reticulatus* (BR) makrofunguslarından elde edilen ekstraktların yenebilir filmlere ilavesinin yol açtığı etkilerin araştırılmasıdır. Bu ekstraktlardan farklı oranlarda (25, 50 ve 100 mg) filmler hazırlanarak, filmlerin bazı fiziksel ve kimyasal özellikleri incelenmiştir. Çalışmanın bulguları, AC mantarının BR mantarına kıyasla daha yüksek toplam fenolik bileşen içeriğe sahip olduğunu ortaya koymuştur. AC ekstraktı içeren filmler kontrol grubuna göre daha ince bulunurken, sadece BR100 filmi daha kalın şekilde ölçülmüştür. Her iki mantar özütü kullanılarak üretilen filmlerin nem içeriği, kontrol filminden daha düşük seyretmiştir. Filmlerin suda çözünürlüğü mantar ekstraktının düşük konsantrasyonlarında azalmış, ancak daha yüksek konsantrasyonlarda artmıştır. Filmlerin şeffaflığını gösteren L* değerinin kontrol filminde en yüksek, AC100 film örneğinde ise en düşük olması kontrol filminin daha şeffaf olduğunu gözler önüne sermiştir. Ayrıca, mantar ekstraktlarından gelen biyoaktif bileşenler, yenebilir filmlerin opaklığının ve UV bariyer özelliklerinin artmasına neden olmuştur.

1 Yüksek Lisans Öğrencisi, Biyoloji Bölümü, Fen Bilimleri Enstitüsü, Osmaniye Korkut Ata Üniversitesi, 80000, Osmaniye, Türkiye, drgkyrmz@hotmail.com

2 Doç. Dr., Gıda Mühendisliği Bölümü, Mühendislik Fakültesi, Osmaniye Korkut Ata Üniversitesi, 80000, Osmaniye, Türkiye, ozgesufer@osmaniye.edu.tr, Orcid: 0000-0001-8337-6318

3 Doç. Dr., Biyoloji Bölümü, Fen-Edebiyat Fakültesi, Osmaniye Korkut Ata Üniversitesi, 80000, Osmaniye, Türkiye, fbozok@osmaniye.edu.tr, Orcid: 0000-0002-9370-7712

https://doi.org/10.58830/ozgur.pub252.c1212

1. Giriş

Ülkemiz, kendine özgü topografyası ve iklim özelliklerinin bir sonucu olarak, çok çeşitli makro ve mikro mantarı barındırmaktadır (Dündar vd., 2016). Bugüne kadar Türkiye'de yaklaşık 2500 mantar türü tespit edilmiş olup, bu türlerin yaklaşık %85'i bazidli mantarlar sınıfına girmektedir. Her gün bu alemin yeni ve ilgi çekici üyeleri keşfedilerek listeye eklenmektedir (Sesli ve Denchev, 2014; Bozok vd., 2018 ve 2020; Doğan vd., 2018; Altuntaş vd., 2021).

Dünya genelinde, gıda endüstrisinde yaygın olarak kullanılan makromantarların 70.000'den fazla türünün olduğu ve bunlardan 2000 kadarının yenebilir olduğu belirtilmektedir (Naeem vd., 2020). Bu yenebilir mantarlar, özellikle Çin gibi bazı Uzak Doğu ülkelerinde sağlıklı ve dengeli beslenme için önemli bir diyet bileşeni olarak kullanılmaktadır. Çünkü hayvansal gıdalarda bulunan bazı aminoasitler ve vitaminler bitkisel ürünlerde bulunmamaktadır. Ayrıca, düşük karbonhidrat, düşük yağ ve dolayısıyla düşük kalori fakat yüksek lif içeriği nedeniyle diyet yapan kişilerin de kilo vermelerine yardımcı olabilirler (Badalyan ve Zambonelli, 2019).

Fenolik bileşikler, besinlerin duyusal özelliklerine katkıda bulunan sekonder metabolitler olarak bilinir ve birçok meyvede bol miktarda bulunur (Rice-Evans vd., 1997). Bu bileşikler, besin değeri taşımasa da hipertansiyonun olumsuz etkilerini azaltma, düşük yoğunluklu lipoprotein oksidasyonunu engelleme, tümör gelişimini önleme ve glikoz emilimini düzenlemede rol oynamaktadır (Stacewicz-Sapuntzakis vd., 2001; Del Caro vd., 2004).

Bitkilerden elde edilen doğal polimerler, petrolden yapılan sentetik ambalaj malzemelerinin çevre dostu ve toksik olmayan bir ikamesi olarak kullanılmaktadır. Kitinin deasetilasyonu yoluyla elde edilen doğal bir polimer olan kitosan, biyolojik olarak parçalanabilirliği ve çevre dostu özellikleri nedeniyle yenebilir filmlerin formülasyonunda yaygın olarak kullanılmaktadır (Priyadarshi ve ark., 2018). Önceki araştırmalar, toksik olmayan ve biyouyumlu bir madde olan kitosanın başarılı antioksidan ve antimikrobiyal özelliklerini göstermiştir (Bégin ve Van Calsteren, 1999; Xie vd., 2001; Rabea vd., 2003; Yen vd., 2008; Goy vd., 2009; Raafat ve Sahl, 2009; Kong vd., 2010; Siripatrawan ve Harte, 2010; Leceta vd., 2013; Ke vd., 2021). Sonuç olarak kitosan, yenebilir filmlerin üretimi için umut verici bir malzeme olarak ortaya çıkmaktadır. Ancak, mantar özütleri içeren kitosan bazlı yenebilir filmler hakkında şu anda sınırlı literatür bilgisi bulunmaktadır. Bu eksiklikten yola çıkılarak bu çalışmanın amacı, Osmaniye ilinden temin

edilen *Amanita caesarea* ve *Boletus reticulatus* ekstraktlarını içeren kitosan bazlı yenebilir filmleri üretmek ve elde edilen filmlerin bazı fiziksel ve kimyasal özelliklerini araştırmak olarak belirlenmiştir (Gökyermez, 2022).

2. MATERYAL VE YÖNTEM

2.1. Materyal

2.1.1. Mantar Materyali

Amanita caesarea ve *Boletus reticulatus* makrofungusları Osmaniye ili Zorkun bölgesi Karıncalı yaylasından toplanmıştır. Toplamadan önce, arazide makrofungusların fotoğrafları çekilmiş, GPS koordinatları, yükseklik ve çevredeki bitki örtüsü gibi ayrıntıları kaydedilmiştir. Toplanan makrofungus örnekleri daha sonra Kangye (Çin) marka sebze kurutucusu kullanılarak, 50°C sıcaklıkta 24 saat süreyle kurutulmuştur. Daha sonra, kurutulmuş mantarları öğütmek için Waring (Almanya) firmasına ait bir öğütücü kullanılmıştır. Kurutulan örnekler kilitli torbalarda özenle buzdolabında +4°C'de analiz edilinceye kadar muhafaza edilmiştir. Toplanan makromantarların konumları ve genel özellikleri aşağıda verilmektedir (Gökyermez, 2022);

08.10.2021 tarihinde Osmaniye, Zorkun, Karıncalı yaylasında 36°57'35.9" K, 36°20'05.9"D koordinatlarında ve 1324 m rakımda *Amanita caesarea* toplanmıştır (Şekil 1). Mantarın şapkasının çapı 50-140 (190) mm'dir ve parlak turuncu-kırmızı ila soluk turuncu bir renk sergilemektedir, renk olgunlaştıkça solmaktadır. Başlangıçta, şapka dışbükey ve sonunda düz hale gelmeden önce yarım küre şeklindedir. Yüzey biraz yapışkandır ve kenar boşlukları kısa çizgilidir. Koruyucu bir doku olan volva, fark edilir derecede büyük ve kalındır. Mantarın eti beyaz, şapkanın alt tarafı sarıdır. Gövde 60-130 × 15-25 mm boyutlarında ve silindirik olup, aşağı doğru genişlemektedir. Sarı renklidir, halkasının alt tarafı düzdür. Halkanın kendisi geniş, kalın ve zarımsıdır, yukarısında hafif çizgiler sergilemektedir. Bu mantar türü Akdeniz bölgesinde yaygın olarak tüketilmektedir (Neville ve Poumarat 2004).

Boletus reticulatus mantar türü, 8 Ekim 2021 tarihinde Osmaniye'de Zorkun Karıncalı yaylasında 36°57'43.0" K ve 36°19'56.5" D koordinatlarında 1240 m rakımda toplanmıştır (Şekil 2). Mantarın şapkası 20 cm'ye kadar bir çapa ulaşabilir ve yarım küre şeklinde başlamakta, daha sonra dışbükey veya düz hale gelmektedir. Tipik olarak kurudur ancak özellikle yağışlı havalarda biraz yapışkan hale gelebilir. Şapka genellikle ince veya kaba çatlaklar gösterir ve rengi soluk kahverengi, kahverengi, koyu sarımsı, grimsi-koyu kahverengiden neredeyse tamamen beyazımsıya

kadar değişebilir. Bu tür, zarar gördüğünde mavi bir renklenme göstermez. Gövde, çubuk şeklinde ve silindiriktir, bazen şapkanın rengiyle uyumludur. Mantarın eti beyazdır, bazen sapın tabanından kaynaklanan kahverengi bir leke vardır ve havaya maruz kaldığında renk değiştirmez. Başlangıçta, tüpler beyaz görünür ancak daha sonra krem veya soluk sarı bir renk tonuna geçer. Bazı yazarlar bu türe *B. aestivalis* olarak da atıfta bulunmakta ve yaygın olarak Avrupa kıtasının güney bölgelerinde *B. reticulatus*'a rastlanılmaktadır (kaynak: https://boletales.com).

Şekil 1. Amanita caesarea makromantarının arazide çekilmiş bir fotoğrafı (Gökyermez, 2022)

Şekil 2. Boletus reticulatus makromantarının arazide çekilmiş bir fotoğrafı (Gökyermez, 2022)

2.2. Yöntem

2.2.1. Ekstrakt Elde Edilmesi

5 gram kurutulmuş ve toz haline getirilmiş makrofungus 100 ml distile suya ilave edilmiş ve 2 saat süreyle 100 °C'de kaynamaya bırakılmıştır. Daha sonra elde edilen Whatman No.1 filtre kâğıdı kullanılarak süzülen sıvı, buharlaştırılmış ve makromantar ekstraktı üretilmiştir. Elde edilen özütler, kitosan bazlı yenebilir filmlerin yapısında kullanılana kadar buzdolabında +4 °C'de saklanmıştır (Gökyermez, 2022).

2.2.2. Filmlerin Üretilmesi

Her iki mantar özütünün farklı konsantrasyonları (25, 50 ve 100 mg) kullanılarak yenebilir film hazırlanmıştır. Her bir yenebilir film üretmek için aşağıdaki basamaklar takip edilmiştir (Şekil 3).

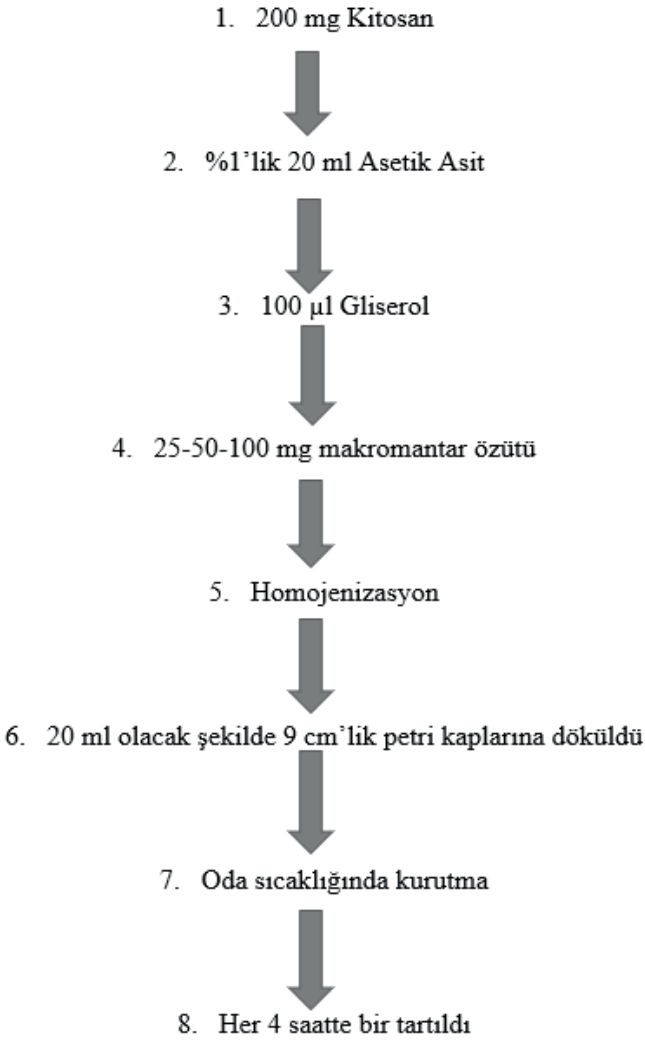

Şekil 3. Yenebilir film üretim aşamaları (Gökyermez, 2022)

2.2.3. Fourier Dönüşümlü Kızılötesi Spektroskobu (FTIR) ile Analiz

Numunelerin FTIR spektrumları, zayıflatılmış toplam yansıtma aksesuarı ile donatılmış bir FTIR spektrofotometresi (Perkin Elmer 65, Waltham, MA, ABD) kullanılarak elde edilmiştir. Veri toplama için 4000-400 cm^{-1} dalga boyu aralığı kullanılmıştır. Her bir spektrumu elde etmek için toplamda 16 tarama gerçekleştirilmiştir.

2.2.4.Taramalı Elektron Mikroskobu ile Analiz

Filmin yüzeyini ve enine kesitini incelemek için, taramalı elektron mikroskobu kullanılmıştır. Kullanılan mikroskop Almanya, Jena üretimli Zeiss Evo 50 modelidir. Filmi daha iletken hale getirmek için ABD çıkışlı Electron Microscopy Sciences markalı sprey kaplayıcı numuneleri altın/paladyum ile kaplamıştır. 15 kV hızlanan voltajda film örneklerinin görüntüleri alınmıştır.

2.2.5. Kalınlık Ölçümü

Filmlerin beş farklı noktasından bir dijital kumpas yardımıyla kalınlıkları ölçülmüş ve bu beş değerin ortalaması alınmıştır.

2.2.6. Nem İçeriği ve Suda Çözünürlük

Film örnekleri makas kullanılarak 2 × 2 cm'lik parçalar halinde kesilmiş ve hassas terazide tartılmıştır. Kesilen filmler daha sonra alüminyum kaplara konularak 105ºC hava sirkülasyonlu bir fırında (Binder, ED 115, ABD) 24 saat bekletilmiştir. Filmler fırından çıkarıldıktan sonra, tekrar ağırlıkları ölçülmüştür. Doğruluğu sağlamak için bu işlem üç kez tekrarlanmıştır. Filmlerin nem içeriği aşağıda belirtilen formül kullanılarak, yüzde olarak hesaplanmıştır;

$$\%\,\text{Nem} = (M1 - M2)/M1 \times 100 \qquad (1)$$

M1 : Örneğin ilk ağırlığı (g)

M2 : Örneğin son ağırlığı (g)

Filmlerin suda ne kadar iyi çözündüğünü anlayabilmek için, kurutulan filmler 50 ml distile su içerisine konularak 25°C'de 24 saat ağırlık kaybı durana kadar çalkalanmıştır. Filmin çözünmeyen kısımları daha sonra 105ºC'de 24 saat etüvde (Binder, ED 115, ABD) bırakılmıştır. Filmlerin sudaki çözünürlüğü, eşitlik 2 yardımıyla belirlenmiştir.

$$\%\,\text{Suda çözünürlük} = (W1 - W2)/W1 \times 100 \qquad (2)$$

W1 : Örneğin ilk ağırlığı (g)

W2 : Örneğin son ağırlığı (g)

2.2.7 Renk ve Opaklık

Filmlerin rengi portatif bir kolorimetre (Konica-Minolta CR-400, Japonya) kullanılarak ölçülmüştür. L* (açıklık), a* (kırmızılık-yeşillik) ve b* (sarılık-mavilik) değerleri, her filmdeki dört farklı noktadan okumaların ortalaması alınarak elde edilmiştir. Filmlerin toplam renk değişimleri (ΔE) aşağıdaki formül kullanılarak tespit edilmiştir;

$$\Delta E = \sqrt{[(L^* - L^*_{ref})^2 + (a^* - a^*_{ref})^2\ ] + (b^* - b^*_{ref})^2} \quad (3)$$

"Ref" ile belirtilmiş olan parametreler, mantar özütü içermeyen örneğe; diğerleri ise mantar özütü içeren numuneye aittir.

Beyazlık (BI) ve sarılık (SI) indeksleri ise sırasıyla eşitlik 4 ve 5 kullanılarak tayin edilmiştir;

$$BI = 100 - \sqrt{(100 - L^*)^2 + (a^*)^2 + (b^*)^2} \quad (4)$$

$$SI = \frac{142.86 \times b^*}{L^*} \quad (5)$$

Filmler, 4.5 × 1.2 cm boyutlarında kesilmiş, bir kuvarts küvet içine yerleştirilmiş ve absorbansları spektrofotometre kullanılarak (Shimadzu, UV 1800, Japonya) 600 nm dalga boyunda ölçülmüştür. Opaklık, elde edilen absorbans değerlerinin filmin kalınlığına bölünmesi ile tespit edilmiştir (Noshirvani vd., 2017).

2.2.8.UV-VIS Analizi

Kitosan bazlı ve mantar özütü içeren yenebilir filmlerin optik geçirgenliği, 250 ile 850 nm arasında değişen dalga boylarında analiz edilmiştir. Optik ölçümler, spektrofotometre kullanılarak yapılmış ve filmlerin geçirgenliği yüzde transmittans olarak belirlenmiştir (Sady et. al., 2021).

2.2.9. Toplam Fenolik Bileşen (TFB) Tayini

Bu çalışmada toplam fenolik bileşen (TFB) tayini için Folin-Ciocalteu yönteminden yararlanılmıştır (Li vd., 2015). Ekstrakte edilen maddeden 0.5 ml alınarak 0.5 ml Folin-Ciocalteu reaktifi ile birleştirilmiş, ardından 3 ml %10'luk $NaCO_3$ çözeltisi eklenmiştir. Karışım daha sonra 30 dakika boyunca

karanlık bir ortamda bırakılmış, ardından spektrofotometre yardımıyla 760 nm dalga boyunda karışımın absorbansı ölçülmüştür. %80 metanol solüsyonu kör çözelti olarak kullanılmıştır. Sonuçlar, özütün gram kuru maddesi ya da filmin gramı başına miligram galik asit eşdeğeri olarak rapor edilmiştir. Analiz üç tekrarlı olarak yapılmıştır.

2.2.10. Antioksidan Aktivite Tayini (DPPH, FRAP ve ABTS Yöntemi)

0.1 ml özüt, 0.025 g/l konsantrasyonda %100 metanol içindeki 2 ml 1,1-difenil-2-pikrilhidrazil (DPPH) solüsyonuna ilave edilmiştir. Elde edilen karışım 30 dakika süreyle karanlık bir ortamda bekletilmiştir. Daha sonra absorbanslar, 517 nm'lik dalga boyunda spektrofotometrede ölçülmüştür. Kontrol olarak hizmet etmesi için %80'lik metanol solüsyonu kullanılmıştır. Sonuçlar, Aghraz vd., (2018) tarafından açıklanan yöntem izlenerek troloks eşdeğeri cinsinden rapor edilmiştir. Analiz üç kez tekrarlanmıştır.

FRAP testini gerçekleştirmek için şu bileşenler kullanılmıştır; 10 mM konsantrasyonda 40 Mm HCI içinde hazırlanan 2,5 ml 2,4,6-Tris(2-piridil)-s-triazin (TPTZ), 2.5 ml 20 mM $FeCl_3$ solüsyonu ve 25 ml 0.1 M pH değeri 3.6 olan asetat tamponu. Hazırlanmış 2 ml FRAP reaktifine, her bir mantar ekstraktından ayrı ayrı 0.3 ml ilave edilmiş ve nihai karışım, 10 ml'lik hacme tamamlanmıştır. Karanlıkta 10 dakikalık inkübasyon süresinin ardından numunelerin absorbansları spektrofotometre (Shimadzu, UV 1800, Japonya) kullanılarak 593 nm dalga boyunda ölçülmüştür. Şahit olarak 2 ml FRAP reaktifi ve 8 ml damıtılmış sudan oluşan bir numune hazırlanmıştır. Elde edilen sonuçlar Szydłowska-Czerniak vd. (2008)'e göre μmol TE/g KM cinsinden hesaplanmıştır.

1:1 oranında 7.4 mmol/L ABTS ve 2.6 mM $K_2S_2O_8$ içeren başlangıç stok solüsyonu ABTS analizi öncesinden hazırlanmıştır. Bu çözelti daha sonra etanol ile absorbansı 734 nm'de 1100 ± 0.005 nm olana kadar seyreltilmiştir. Her 0.15 ml mantar ya da film ekstraktı için 2.85 ml ABTS solüsyonu ortama ilave edilmiş ve karışım karanlık ortamda 2 saat bekletilmiştir. Son numunelerin absorbansları, spektrofotometre kullanılarak ölçülmüş ve bulgular, Thaipong vd. (2006) tarafından açıklanan metodolojiye göre μmol TE/g KM olarak ifade edilmiştir. Referans örnek bu analizde %80 etanoldür.

2.2.11. İstatistiksel Analiz

Sonuçlar, Statistical Package for the Social Sciences (SPSS) programı (IBM Statistics, ABD) (Sürüm 18.0) kullanılarak tek yönlü varyans analizi yoluyla değerlendirilmiştir. Bu amaçla %95 güven aralığında Duncan testi

yapılmıştır. Ek olarak, değişkenlerin çıktılar üzerindeki etkisi, iki yönlü varyans analizi kullanılarak belirlenmiştir.

3. BULGULAR VE TARTIŞMA

3.1. Mantar Özütlerinin Biyoaktif Potansiyeli

Amanita caesarea (AC) ve *Boletus reticulatus* (BR) mantarlarının TFB içerikleri (mg GAE/g KM) ile DPPH, FRAP ve ABTS yöntemleriyle (μmol TE/g KM) belirlenen antioksidan aktiviteleri Çizelge 1'de verilmiştir (Gökyermez, 2022).

Çizelge 1. Mantar özütlerinin toplam fenolik madde miktarları ve antioksidan bileşen potansiyelleri (Gökyermez, 2022)

Örnek	TFB	DPPH	FRAP	ABTS
Amanita caesarea	32.65±4.96	288.90±22.28	141.62±19.52	75.91±06.06
Boletus reticulatus	20.92±1.45	117.50±08.16	66.63±01.84	53.10±11.01

AC mantarının TFB değeri 32.65 mg GAE/g KM iken, BR mantarı için bu değer 20.92 mg GAE/g KM'dir. AC mantar özütünün, DPPH, FRAP ve ABTS yöntemleriyle belirlenen antioksidan aktiviteleri sırasıyla 288.90, 141.62 ve 75.91 μmol TE/g KM iken, BR mantar özütü, 117.50, 66.63 ve 53.10 μmol TE/g KM'lik antioksidan davranış sergilemiştir (Gökyermez, 2022). Sharma ve Gautam tarafından 2015 yılında yapılan araştırmada, AC'nin TFB miktarı 63.32 mg/100 g GAE, DPPH radikali süpürme aktivitesi 2.02 mg/ml, ABTS radikali indirgeme potansiyeli 1.45 mg/ml, FRAP yöntemiyle demir iyonunu indirgeme yeteneği 1.86 mol Fe^{+2}/g KM olarak bulunmuştur. Heleno vd. (2011) ise, Avrupa ülkelerinde bulunan çeşitli Boletus türlerinin antioksidan özelliklerini inceleyen bir çalışma yürütmüştür. Araştırma aynı zamanda bu türlerin TFB analizini de içermektedir. Makalede BR'nin TFB konsantrasyonu (ekstrenin gramı başına miligram galik asit eşdeğeri olarak) ve ayrıca DPPH süpürme ve indirgeme gücü kapasiteleri (mililitre başına miligram olarak) sırasıyla 12.08, 0.38 ve 0.96 olarak tespit edilmiştir. Macáková vd. (2009), BR'nin TFB'sini 23.0 mg GAE/g olarak belgelemiştir. Bu araştırma ile önceki araştırmalar arasında coğrafi konum, süre, kurutma prosedürleri ve ekstraksiyon tekniklerindeki farklılıklara atfedilebilecek farklılıklar bulunduğunu söylemek gereklidir.

3.2. Filmlerin Bazı Fiziksel Karakteristikleri

Çizelge 2, değişen konsantrasyonlarda (25, 50 ve 100 mg) AC ve BR makrofunguslarından elde edilen özütlerin ilave edildiği yenebilir filmlerin bazı fiziksel özelliklerine ilişkin verileri sunmaktadır. AC ekstraktı içeren tüm filmlerinin kalınlığının, kontrol filminden daha düşük olduğu gözlenmiştir. Ek olarak, 25 ve 50 mg oranında BR ekstraktı içeren filmlerin kalınlığı da kontrole göre daha düşükken, 100 mg ekstrakt içeren filmin kalınlığı daha yüksektir. AC ekstraktını barındıran filmlerin kalınlığı 0.060-0.062 mm arasında değişirken, BR özütlü filmler 0.067-0.102 mm arasında değişen kalınlık değerleri sergilemiştir (Gökyermez, 2022).

Kontrol filminin nem içeriği %34.75 olarak belirlenmiştir. Hem AC hem de BR ekstraktlarını içeren filmlerin, kontrol filmine göre daha düşük nem içeriğine sahip olduğu bulunmuştur. Bununla birlikte, mantar özütlerinin film içerisinde konsantrasyonları arttıkça, nem miktarının bir dereceye kadar azaldığı gözlenmiştir. Çizelge 2 incelendiğinde, BR100 filminin en yüksek suda çözünürlük değerine sahip olduğu, BR50 filminin ise en düşük değeri gösterdiği ortaya çıkmaktadır. Ayrıca AC ekstraktı içeren filmlerin suda çözünürlüğünün, mantar ekstraktı içeriği arttıkça belirli oranlarda azaldığı da gözlenmiştir (Gökyermez, 2022).

Çizelge 2. Filmlerin kalınlık, nem ve suda çözünürlük değerleri (Gökyermez, 2022)

Film Çeşidi	Kalınlık (mm)	Nem (%)	Suda Çözünürlük (%)
Kontrol	$0.093^{ab}\pm0.015$	$34.75^{a}\pm0.01$	$62.19^{a}\pm0.93$
AC25	$0.060^{cd}\pm0.010$	$28.57^{b}\pm0.05$	$63.63^{a}\pm1.64$
AC50	$0.054^{d}\pm0.006$	$19.04^{bc}\pm0.06$	$61.80^{a}\pm3.83$
AC100	$0.062^{cd}\pm0.001$	$18.18^{bc}\pm0.75$	$60.16^{a}\pm1.68$
BR25	$0.067^{cd}\pm0.016$	$18.18^{bc}\pm0.01$	$60.83^{a}\pm3.53$
BR50	$0.077^{bc}\pm0.008$	$15.55^{c}\pm0.02$	$59.98^{a}\pm1.25$
BR100	$0.102^{a}\pm0.018$	$15.76^{c}\pm0.01$	$64.28^{a}\pm0.00$

Aynı sütundaki farklı harfler istatistiksel olarak anlamlı farklılıkları göstermektedir ($p<0.05$).

Geniş çapta bir literatür taraması yapıldığında, bugüne kadar mantar özütü içeren kitosan bazlı yenebilir filmler üzerine belgelenmiş tek bir çalışmaya rastlanmıştır. Bu araştırmada, Koc vd., (2020), *Tricholoma terreum* sulu özütü içeren ve içermeyen kitosan bazlı filmlerin kalınlığını sırasıyla 0.19 ve 0.06 mm olarak ölçmüşlerdir. Suda çözünürlük özellikleri açısından

T. terreum ekstraktı içermeyen kitosan bazlı filmin 25ºC sıcaklıkta 48 saat sonra suda tamamen çözündüğü, *T. terreum* ekstraktı içeren filmin ise %34.9 oranında çözünürlüğe sahip olduğu belirtilmiştir.

3.3. Filmlerin Renk Özellikleri

AC ve BR özütlerini içeren kitosan polimeri bazlı yenebilir filmlerin bazı optik karakteristikleri Çizelge 3'te verilmiştir.

L* değeri parlaklık seviyesini belirtir ve 0 (siyahlığı temsil eder) ile 100 (beyazlığı gösterir) arasında değişir. Film örnekleri arasında gözlemlenen en düşük L* değeri AC100'e (54.42) ait olurken, en yüksek değer ise kontrol numunesinde (79.85) kaydedilmiştir. Filmlerin L* değerleri, her iki mantar ekstraktının konsantrasyonu arttıkça belirli oranlarda düşüş göstermiştir. Bu bulgulara dayanarak, kontrol filminin daha yüksek derecede parlaklığa sahip olduğu sonucuna varılabilir (Gökyermez, 2022).

a* için negatif bir değer yeşil tonların varlığını, pozitif bir değer ise kırmızı tonların varlığını gösterir. AC ekstraktı eklendiğinde, filmler pozitif değerler sergilemiş ve kontrole kıyasla daha kırmızı bir renk tonu göstermişlerdir. BR25 ve BR50 filmleri ise referans filme benzer negatif değerlere sahiptir, ancak BR100 numunesi için pozitif bir a* kaydedilmiştir (Gökyermez, 2022).

b* değeri, sarılık ve mavilik derecesinin bir ölçüsü olarak işlev görmektedir. Test edilen film örneklerinde gözlemlenen değer aralığı 6.60 ila 38.51 arasında değişmiştir. Mantar ekstraktı içermeyen kontrol filminde, b* değeri 6.60 olup, numuneler arasında en yüksek mavilik seviyesine haiz film olma özelliğine sahiptir. Mantar ekstraktlarının miktarı arttıkça, sarılık değeri giderek yükselmiştir. AC100 filmi en yüksek b* değerini sergilemiştir (Gökyermez, 2022).

Çizelge 3. Filmlerin açıklık, kırmızılık-yeşillik, sarılık-mavilik değerleri ile toplam renk değişimleri (Gökyermez, 2022)

Film Çeşidi	L*	a*	b*	ΔE
Kontrol	$82.04^{a}\pm3.56$	$-1.72^{d}\pm0.20$	$6.60^{f}\pm0.50$	0^{c}
AC25	$73.44^{b}\pm1.65$	$0.19^{c}\pm0.87$	$25.10^{c}\pm5.45$	$13.98^{a}\pm5.20$
AC50	$65.39^{c}\pm2.51$	$3.41^{b}\pm0.80$	$33.98^{ab}\pm2.14$	$13.22^{a}\pm2.31$
AC100	$54.42^{d}\pm2.11$	$11.29^{a}\pm1.83$	$38.51^{a}\pm2.24$	$15.72^{a}\pm1.89$
BR25	$74.05^{b}\pm6.22$	$-1.60^{d}\pm0.36$	$12.58^{e}\pm1.76$	$06.57^{b}\pm5.22$
BR50	$72.24^{bc}\pm4.32$	$-1.47^{d}\pm0.18$	$19.69^{d}\pm1.96$	$06.73^{b}\pm2.66$
BR100	$70.49^{bc}\pm2.61$	$0.29^{c}\pm0.09$	$31.74^{b}\pm2.49$	$08.09^{b}\pm4.06$

Aynı sütundaki farklı harfler istatistiksel olarak anlamlı farklılıkları göstermektedir ($p<0.05$).

Toplam renk farklılığı, referans kabul edilen yani özüt içermeyen filme göre hesaplandığından dolayı, kontrol filminin ΔE değeri sıfır olarak belirlenmiştir. Herhangi bir ürün/materyal için ΔE değeri sıfırdan ne kadar uzaklaşırsa, o ürün/materyal orjinalinden renk açısından o denli uzaklaşmaktadır. O halde ΔE miktarı en büyük olan AC100 filmi, kontrol filminden renk açısından en farklı olan numunedir. Ayrıca, AC özütünü içeren filmlerin ΔE değerleri, her konsantrasyonda BR ekstraktını içeren yenebilir filmlerden daha yüksektir. En düşük toplam renk farklılığına (6.57) sahip olan örnek 25 mg BR özütü içeren filmidir. Özüt konsantrasyonu arttıkça BR film grubunda ΔE kademeli olarak artarken, AC grubunda aynı etki gözlenmemiştir (Gökyermez, 2022).

3.4. Filmlerin Beyazlık ve Sarılık İndeksleri ile Opaklık Değerleri

AC ve BR makromantar ekstraktlarını içeren yenebilir filmlerin beyazlık ve sarılık indeksleri (BI ve SI) ile opaklıklarına ait veriler Çizelge 4'te gösterilmiştir.

Çizelge 4. Filmlerin renk indeksleri ve opaklıkları (Gökyermez, 2022)

Film Çeşidi	BI	SI	Opaklık
Kontrol	$80.77^{a} \pm 0.90$	$012.34^{e} \pm 00.66$	$1.28^{de} \pm 0.05$
AC25	$63.25^{c} \pm 4.15$	$048.91^{c} \pm 10.87$	$1.35^{cd} \pm 0.28$
AC50	$51.32^{d} \pm 2.39$	$074.34^{b} \pm 05.49$	$1.76^{b} \pm 0.19$
AC100	$39.19^{e} \pm 1.84$	$101.14^{a} \pm 05.46$	$2.17^{a} \pm 0.40$
BR25	$71.33^{b} \pm 5.89$	$023.66^{d} \pm 02.12$	$0.91^{e} \pm 0.10$
BR50	$65.74^{bc} \pm 3.36$	$038.62^{c} \pm 03.26$	$1.14^{de} \pm 0.11$
BR100	$56.44^{d} \pm 4.22$	$065.03^{b} \pm 09.32$	$1.72^{bc} \pm 0.19$

Aynı sütundaki farklı harfler istatistiksel olarak anlamlı farklılıkları göstermektedir ($p<0.05$).

Çizelge 4'te sunulan verilerle kanıtlandığı gibi, mantar özlerinin film bileşimine dâhil edilmesi, BI değerlerinde dikkate değer bir azalma ile sonuçlanmıştır. Kontrol filmi en yüksek BI değerini (80.77) gösterirken, AC100 film numunesi ise en düşük değeri (39.19) sergilemiştir. Bununla birlikte mantar ekstraktlarının, filmlerin BI değerlerini konsantrasyon artışına bağlı olarak farklı oranlarda düşürdüğü tespit edilmiştir (Gökyermez, 2022).

Çizelge 4, değişen oranlarda formülasyona ilave edilen makromantar ekstraktlarının, konsantrasyona bağlı olarak, filmlerin SI değerlerini arttırdığını ortaya koymaktadır. SI değerleri analiz edildiğinde, kontrol filminin en düşük değeri (12.34) gösterdiği, AC100 film örneğinin ise

en yüksek değeri (101.14) gösterdiği ortaya çıkmıştır. AC ekstraktı içeren filmlerin SI değerleri 48.91 ile 101.14 arasında değişirken, BR ekstraktı içeren filmlerin SI değerleri ise 23.66 ile 65.03 arasında değişmiştir (Gökyermez, 2022).

Opaklık, gıdaların paketlenmesinde kullanılan yenebilir filmlerin önemli bir özelliğidir. Bu filmlere ışığa duyarlı bileşenlerin dâhil edilmesinin, ışık iletimini potansiyel olarak azaltabileceği varsayılmaktadır (Zhang vd., 2020). Çizelge 4'te de gösterildiği üzere, mantar özü konsantrasyonlarının artmasıyla filmlerin opaklığı artmıştır. Bununla birlikte, BR25 olarak belirtilen film en düşük opaklık değerini (0.91) sergilerken, AC100 film örneği ise en yüksek opaklık değerine (2.17) sahip olmuştur (Gökyermez, 2022).

3.5. Filmlerin UV Işığını Engelleme Yeteneği

AC ve BR makromantar ekstraktlarını içeren yenebilir filmlerin optik transmittansları sırasıyla Şekil 4 ve Şekil 5'de gösterilmiştir.

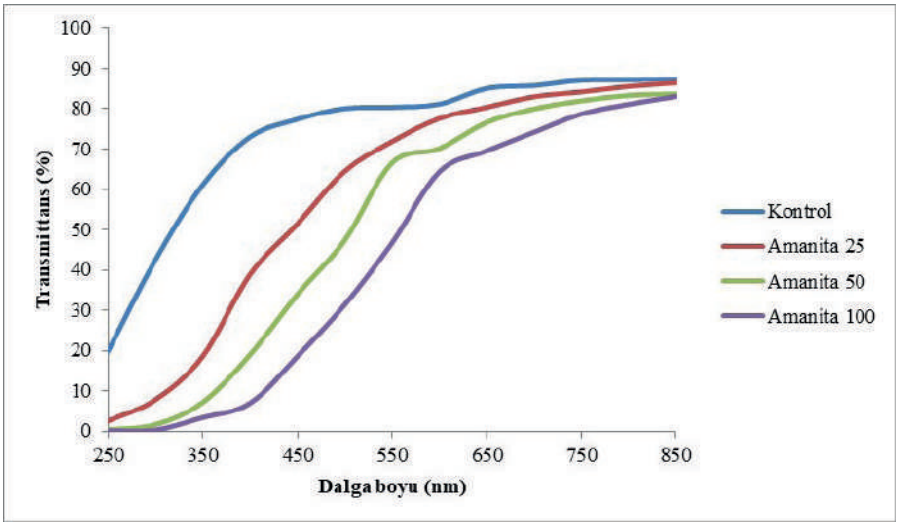

Şekil 4. Farklı oranlarda** Amanita caesarea **özütü içeren filmlerin UV-görünür bölgedeki % transmittans değerleri (Gökyermez, 2022)

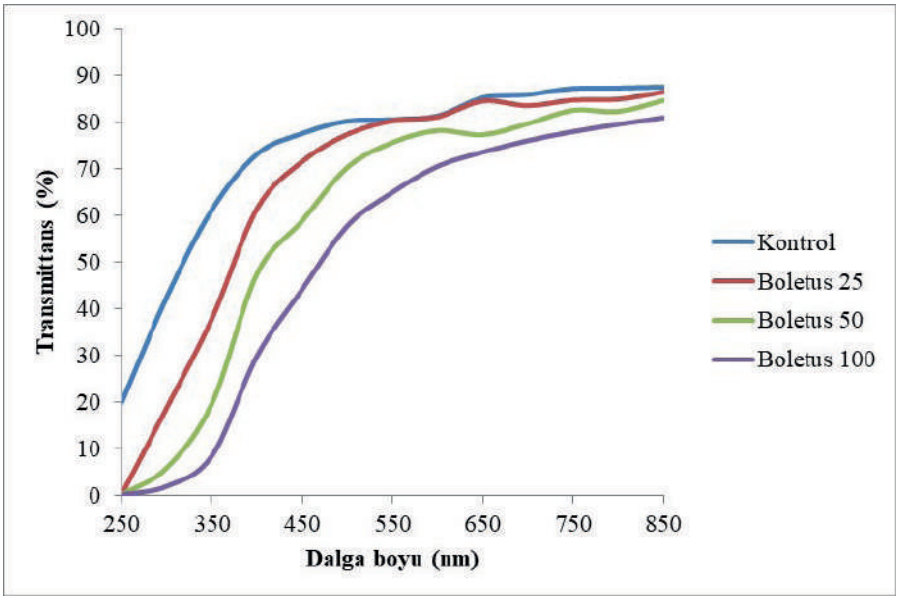

Şekil 5. Farklı miktarlarda** Boletus reticulatus **özütü içeren filmlerin UV-görünür bölgedeki % transmittans değerleri (Gökyermez, 2022)

Lipitler gibi ışığa duyarlı gıda bileşenleri için kullanılan ambalaj malzemelerinin UV-engelleme özellikleri, Sady vd. (2021) tarafından vurgulandığı gibi büyük önem taşımaktadır. Analiz, kontrol filminin en yüksek UV-Vis ışık geçirgenliğini sergilediğini ortaya çıkarmıştır. Ayrıca hem AC hem de BR ekstraktlarının artan konsantrasyonları ile geçirgenlik değerlerinin belirli oranlarda kademeli olarak düştüğü de gözlenmiştir. Özellikle BR100 film numunesi, UV ışığı en etkili engelleme kapasitesine sahiptir (Gökyermez, 2022).

3.6. FTIR ile Filmlerdeki Fonksiyonel Grupların Tespiti

AC ve BR makromantar ekstraktlarını içeren yenebilir filmlerin 4000-600 cm^{-1} dalga boyu aralığındaki FTIR spektrumları Şekil 6 ve Şekil 7'de verilmiştir.

Her iki şekilde de hem AC hem de BR özütü içeren film örneklerini benzer pik davranışı sergilediği görülmektedir. Her iki mantar özütünü içeren filmlerin FTIR spektrumunda 850-924 cm^{-1} seviyelerinde piklerin olması, mantarların yapısında da bulunan polisakkaritlerden β-glukanın varlığına işaret etmektedir. 1028-1086 cm^{-1} band aralığı CO ve C-O-C gruplarına, 1400 cm^{-1} ve civarının birincil alkolik grupların O-H bağlarına, 1554 cm^{-1} bandının ve civarının amid I O-H bağlarına, 1600 cm^{-1} ve civarının amid II

O-H bağlarına, 3290 cm^{-1} ve civarı amit A gruplarına, 2870 cm^{-1} ve civarı ise CH gerilmesine işaret etmektedir (Martins vd., 2012; Bonilla ve Sobral, 2016; Mahcene vd., 2020; Silva-Rodrigues vd., 2020).

Kontrol filmi, değişen konsantrasyonlarda AC ve BR ekstraktları içeren filmlerle karşılaştırıldığında, belirli piklerin hafif kaymalar gösterdiği gözlemlenmiştir. Spesifik olarak, kontrol filminde 2876 cm^{-1}'deki pik, mantar özlerinin eklenmesi üzerine 2862-2866 cm^{-1} aralığına kaymıştır. Benzer şekilde, kontrol filminde 1028 cm^{-1}'deki pik, mantar ekstraktları eklendiğinde 1030-1086 cm^{-1} aralığında bulunmuştur (Gökyermez, 2022).

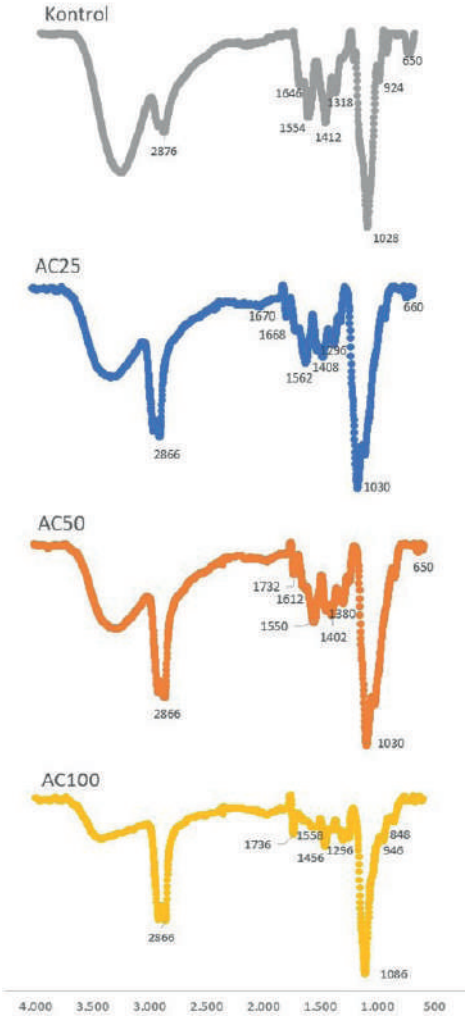

Şekil 6. Farklı oranlarda** Amanita caesarea **ekstraktı içeren filmlerin FTIR spektrumları (Gökyermez, 2022)

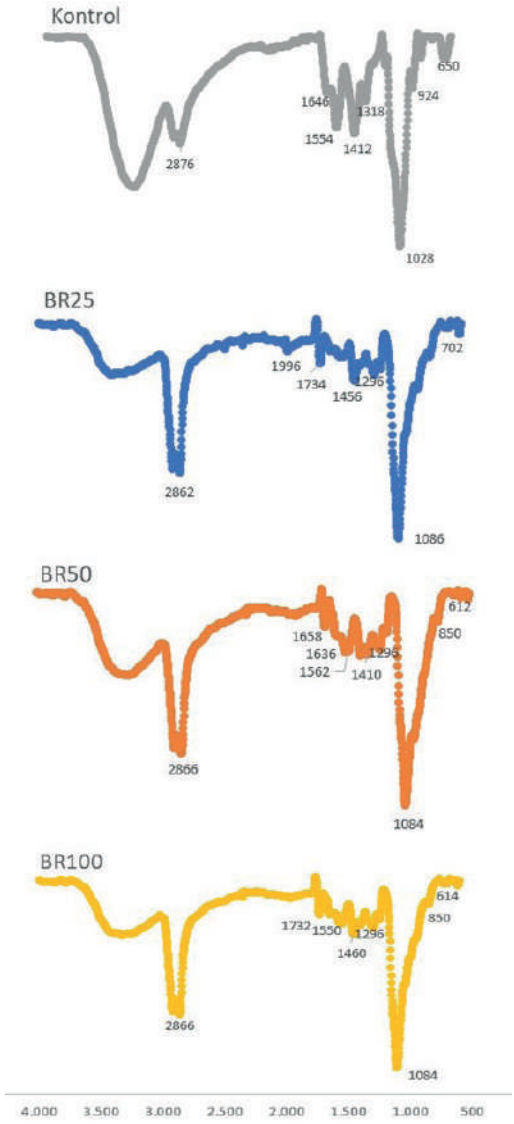

Şekil 7. Farklı oranlarda** Boletus reticulatus **ekstraktı içeren filmlerin FTIR spektrumları (Gökyermez, 2022)

3.7. Filmlerin Antioksidan Aktiviteleri

AC ve BR makromantar ekstraktlarını içeren yenebilir filmlerin DPPH ve ABTS yöntemiyle belirlenen antioksidan aktiviteleri filmlerin gramı başına olmak üzere, Çizelge 5'de gösterilmiştir. Mantar özütü içeren filmlerin TFB miktarları ile demir iyonunu indirgeme yeteneğinin bir göstergesi olan FRAP

yöntemiyle antioksidan aktivite tayin verileri, filmlerdeki ilgili bileşiklerin konsantrasyonları standart eğrilerin konsantrasyon değerlerinin altlarında kaldığı için hesaplanamamıştır (Gökyermez, 2022).

Çizelge 5. Mantar özütü içeren film örneklerinin toplam fenolik madde içerikleri ve antioksidan madde içerikleri (Gökyermez, 2022)

Film Çeşidi	DPPH yöntemiyle AA (μmol TE/g film)	ABTS yöntemiyle AA (μmol TE/g film)
Kontrol	11.94^{c}±0.94	Belirlenemedi
AC25	12.57^{c}±1.56	Belirlenemedi
AC50	15.17^{b}±1.93	05.09^{e}±0.00
AC100	27.45^{a}±2.37	37.05^{a}±2.06
BR25	14.49^{c}±3.41	00.84^{de}±0.62
BR50	19.27^{c}±1.46	04.22^{cd}±0.47
BR100	25.38^{a}±0.64	29.92^{b}±5.04

TE: Troloks eşdeğeri

Aynı sütundaki farklı harfler istatistiksel olarak anlamlı farklılıkları göstermektedir ($p<0.05$).

Çizelge 5 incelendiğinde, mantar ekstraktlarının konsantrasyonu arttıkça filmlerin DPPH ve ABTS radikalini süpürme aktivitelerinin kademeli olarak arttığı görülmektedir. AC100 filmi en yüksek DPPH indirgeme aktivitesi sergilerken, kontrol filmi en düşük potansiyele sahip olmuştur. Buna karşılık, BR100 film numunesi en fazla ABTS indirgeme davranışı sergilerken, kontrol ve AC25 filmlerinin aynı radikalle tepkimeye girme potansiyelleri tanımlanamamıştır (Gökyermez, 2022).

3.8. Filmlerin Morfolojisi

Şekil 8'deki SEM görüntüleri, değişen seviyelerde mantar ekstraktı içeren yenebilir filmlerin mikroyapılarını göstermektedir. Yapılan incelemede mantar özü içermeyen kontrol filminin yapısının, diğerlerine göre daha muntazam ve pürüzsüz olduğu görülmektedir. Her iki mantar özütünün de düşük konsantrasyonlarda film matriksine dahil edildiği durumlarda, 50 ve 100 kodlu filmlere oranla, kontrol filmine daha yakın bir yapıya sahip filmlerin elde edildiği belirlenmiştir. Ancak mantar özü konsantrasyonu arttıkça filmler daha düzensiz bir yapı sergilemiştir (Gökyermez, 2022). Koç vd. (2020)'nin, *T. terreum* ekstresi içeren kitosan bazlı filmlerin mikro

yapısını incelenmesi sonucunda, ekstrakt içermeyen kitosan filmin yüzeyinin daha pürüzsüz bir doku sergilediği, oysa *T. terreum* ekstraktı içeren filmin kontrol filmine kıyasla daha fazla sertliğe ve biraz daha pürüzlü bir dokuya sahip olduğu ortaya çıkmıştır.

4. Sonuçlar ve Öneriler

Bu çalışmada, Osmaniye ilinin Zorkun, Karıncalı Yaylası mevkiinden temin edilen *Amanita caesarea* ve *Boletus reticulatus* özütleri farklı oranlarda (25, 50 ve 100 mg) kitosan bazlı yenebilir filmlerin formülasyonlarına eklenmiştir. Filmlerin bazı fiziksel ve kimyasal özelliklerinin incelenmesi sonucunda elde edilen bulgular şu şekilde özetlenmiştir (Gökyermez, 2022);

- ✓ *Amanita caesarea* (AC), *Boletus reticulatus* (BR)'a nazaran daha fazla toplam fenolik maddeye sahiptir.
- ✓ AC özütü içeren bütün filmler kontrole göre daha düşük kalınlıktadır.
- ✓ Nem içerikleri kıyaslandığında, her iki mantar özütünün ayrı ayrı ilave edilmesiyle elde edilen bütün filmlerin nem miktarları, referansın nem içeriğine göre daha düşük seviyelerdedir.
- ✓ Suda çözünürlük, 25 ve 50 mg'lık mantar özütü konsantrasyonlarında azalırken, 100 mg'lık konsantrasyonda ise artmıştır.
- ✓ Renk parlaklığı, en yüksek değerini kontrol filminde, en düşük değerini ise AC100 film örneğinde almıştır.

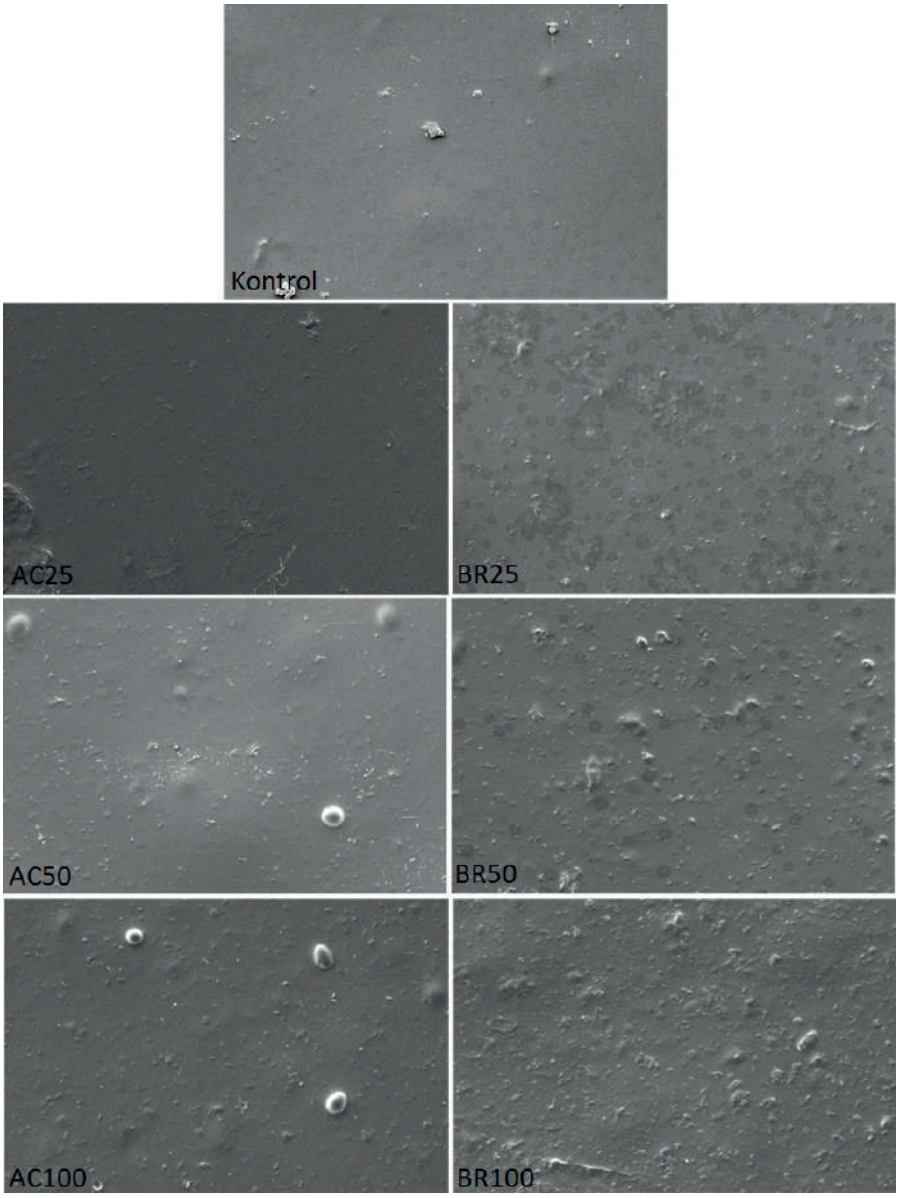

Şekil 8. Farklı oranlarda (25, 50 ve 100 mg) AC ve BR özütü içeren yenebilir filmlerin SEM görüntüleri (Gökyermez, 2022)

- ✓ Biyoaktif bileşenler içeren mantar ekstraktı ilavesi, yenebilir filmlerin opaklık değerlerini arttırmıştır.
- ✓ Mantar özütü ilave edilmiş örneklerin UV bariyer özellikleri daha iyidir.

Yukarıdaki bilgiler ışığında, her iki mantar özütünün de kontrol filmine dahil edilmesinin antioksidan aktivitenin artmasına neden olduğu belirlenmiştir. Bununla birlikte gelecekteki araştırmalarda, film yapımında daha farklı mantar özütlerinin kullanılması ve özütlerin filmlerin çeşitli kalite niteliklerinde değişikliklere neden olup olmadığının araştırılması tavsiye edilmektedir (Gökyermez, 2022). Özellikle daha açık bir renge sahip olan filmlerin üretilmesi, tüketicilerin ilgisini daha çok çekebilir. Bunun için de farklı mantar türlerinin konu edilmesi ve/veya başarılı optimizasyon çalışmalarının yürütülmesi elzemdir. Ayrıca, üretilen yenebilir filmlerin gıda maddelerinin ambalajlanmasında kullanılması ve depolama sırasında elde edilen veriler, filmlerin kullanım potansiyellerinin açığa çıkartılabilmesi bakımından önem taşıyacaktır.

Teşekkür

Bu çalışmayı destekleyen OKÜ Bilimsel Araştırma Projeleri Birimine (Proje No: OKÜBAP-2021-PT3-004) teşekkürlerimizi sunarız.

Yayın Etiği Beyanı

Bu çalışma Doç. Dr. Fuat Bozok ve Doç. Dr. Özge Süfer danışmanlığında, Eylül 2022 tarihinde Mukaddes Gökyermez tarafından tamamlanan, "Osmaniye'de Yayılış Gösteren *Amanita caesarea* ve *Boletus reticulatus* Makromantarlarının Özütleri Kullanılarak Kitosan Temelli Yenebilir Film Üretilmesi ve Antioksidan Aktivitelerinin Araştırılması" başlıklı yüksek lisans tezi esas alınarak hazırlanmıştır (Osmaniye Korkut Ata Üniversitesi, Osmaniye, Türkiye, 2022).

Çıkar Çatışması Beyanı

Yazarlar hem birbirleriyle hem de herhangi bir kurum/kuruluş ile çıkar çatışmaları olmadığını beyan ederler.

5. Kaynaklar

Aghraz, A., Gonçalves, S., Rodríguez-Solana, R., Dra, L. A., Di Stefano, V., Dugo, G., Romano, A., Antioxidant activity and enzymes inhibitory properties of several extracts from two Moroccan Asteraceae species. South African Journal of Botany, 118, 58-64, 2018.

Altuntaş, D., Bozok, F., Taşkın, H., Kabaktepe, Ş., Alli, H., Akata, I. New additions to Turkish mycota from Ankara, Balıkesir, and Kütahya provinces. Turkish Journal of Botany, 45(1), 83-94, 2021.

Badalyan, S.M., Zambonelli, A., Biotechnological Exploitation of Macrofungi for the Production of Food, Pharmaceuticals and Cosmeceuticals (Chapter 9) in book of Advances in Macrofungi: Diversity, Ecology and Biotechnology, Edited by Ramaiah Sridhar and Sunil Kumar, CRC Press, 366, 2019.

Barros, L., Calhelha, R. C., Vaz, J. A., Ferreira, I. C., Baptista, P., Estevinho, L. M. Antimicrobial activity and bioactive compounds of Portuguese wild edible mushrooms methanolic extracts. European Food Research and Technology, 225(2), 151-156, 2007.

Bégin, A., Van Calsteren, M. R. Antimicrobial films produced from chitosan. International Journal of Biological Macromolecules, 26(1), 63-67, 1999.

Bilbao-Sainz, C., Chiou, B. S., Williams, T., Wood, D., Du, W. X., Sedej, I., McHugh, T. Vitamin D-fortified chitosan films from mushroom waste. Carbohydrate Polymers, 167, 97-104, (2017).

Bonilla, J., Sobral, P. J., Investigation of the physicochemical, antimicrobial and antioxidant properties of gelatin-chitosan edible film mixed with plant ethanolic extracts. Food Bioscience, 16, 17-25, 2016.

Bozok, F., Taşkın, H., Büyükalaca, S., Doğan, H. H., Assyov, B. *Cryptomarasmius corbariensis* (Physalacriaceae, Agaricales) in Turkey with first molecular data on the species from Eurasia. Nova Hedwigia, 107(1-2), 110-116, 2018.

Bozok, F., Assyov, B., Taskin, H., Dogan, H. H., Buyukalaca, S. Molecular phylogenetic studies of Turkish boletes with emphasis on some recently described species. Nowa Hedwigia, 110(1-2), 99-129, 2020.

Cheung, L. M., Cheung, P. C., Ooi, V. E. Antioxidant activity and total phenolics of edible mushroom extracts. Food Chemistry, 81(2), 249-255, 2003.

Crognale, S., Russo, C., Petruccioli, M., D'annibale, A. Chitosan production by fungi: current state of knowledge, future opportunities and constraints. Fermentation, 8(2), 76. 2022.

Del Caro, A., Piga, A., Pinna, I., Fenu, PM., Agabbio, M., Effect of drying conditions and storage period on polyphenolic content, antioxidant capacity, and ascorbic acid of prunes. Journal of Agricultural and Food Chemistry, 52, 4780-4784, 2004.

Doğan, H. H., Bozok, F., Taşkın, H. A new species of Barssia (Ascomycota, Helvellaceae) from Turkey. Turkish Journal of Botany, 42(5), 636-643, 2018.

Dündar, Ö., Demircioğlu, H., Özkaya, O., Dündar, B. Kültür mantarlarının muhafazası ve kalite özellikleri üzerine yapılan araştırmalar. Türk Tarım-Gıda Bilim ve Teknoloji Dergisi, 4(3), 150-154, 2016.

Erdem, B. G., Diblan, S., Kaya, S. Development and structural assessment of whey protein isolate/sunflower seed oil biocomposite film. Food and Bioproducts Processing, 118, 270-280, 2019.

Fadhil, A., Mous, E. F. Some characteristics and functional properties of chitin produced from local mushroom *Agaricus bisporus*. In IOP Conference Series: Earth and Environmental Science, 761(1), 012127, 2021.

Gao, Y., Tang, W., Gao, H. E., Chan, E., Lan, J., Li, X., Zhou, S. Antimicrobial activity of the medicinal mushroom Ganoderma. Food Reviews International, 21(2), 211-229, 2005.

Gezer, K., Duru, M. E., Kivrak, I., Turkoglu, A., Mercan, N., Turkoglu, H., Gulcan, S. Free-radical scavenging capacity and antimicrobial activity of wild edible mushroom from Turkey. African Journal of Biotechnology, 5(20),1924-1928, 2006.

Goy, R. C., Britto, D. D., Assis, O. B. A review of the antimicrobial activity of chitosan. Polímeros, 19, 241-247, 2009.

Gökyermez, M., Osmaniye'de Yayılış Gösteren *Amanita caesarea* ve *Boletus reticulatus* Makromantarlarının Özütleri Kullanılarak Kitosan Temelli Yenebilir Film Üretilmesi ve Antioksidan Aktivitelerinin Araştırılması. Osmaniye Korkut Ata Üniversitesi, Fen Bilimleri Enstitüsü, Biyoloji Ana Bilim Dalı, Yüksek Lisans Tezi, 45 sayfa, 2022.

Heleno, S. A., Barros, L., Sousa, M. J., Martins, A., Santos-Buelga, C., Ferreira, I. C. Targeted metabolites analysis in wild Boletus species. LWT-Food Science and Technology, 44(6), 1343-1348, 2011.

Janesch, J., Jones, M., Bacher, M., Kontturi, E., Bismarck, A., Mautner, A. Mushroom-derived chitosan-glucan nanopaper filters for the treatment of water. Reactive and Functional Polymers, 146, 104428, 2020.

Jayakumar, T., Thomas, P. A., Geraldine, P. In-vitro antioxidant activities of an ethanolic extract of the oyster mushroom, *Pleurotus ostreatus*. Innovative Food Science & Emerging Technologies, 10(2), 228-234, 2009.

Ke, C. L., Deng, F. S., Chuang, C. Y., Lin, C. H. Antimicrobial actions and applications of chitosan. Polymers, 13(6), 904, 2021.

Koc, B., Akyuz, L., Cakmak, Y. S., Sargin, I., Salaberria, A. M., Labidi, J., Kaya, M. Production and characterization of chitosan-fungal extract films. Food Bioscience, 35, 10054, 2020.

Kong, M., Chen, X. G., Xing, K., Park, H. J. Antimicrobial properties of chitosan and mode of action: a state of the art review. International Journal of Food Microbiology, 144(1), 51-63, 2010.

Leceta, I., Guerrero, P., Ibarburu, I., Dueñas, M. T., De la Caba, K. Characterization and antimicrobial analysis of chitosan-based films. Journal of Food Engineering, 116(4), 889-899, 2013.

Li, X., Wasila, H., Liu, L., Yuan, T., Gao, Z., Zhao, B., Ahmad, I., Physicochemical characteristics, polyphenol compositions and antioxidant potential of pomegranate juices from 10 Chinese cultivars and the environmental factors analysis, Food Chemistry, 175, 575-584, 2015.

Macáková, K., Opletal, L., Polášek, M., Samková, V., & Jahodář, L. Free-radical scavenging activity of some European Boletales. Natural Product Communications, 4(2), 261-264, 2009.

Mahcene, Z., Khelil, A., Hasni, S., Akman, P. K., Bozkurt, F., Birech, K., Tornuk, F., Development and characterization of sodium alginate based active edible films incorporated with essential oils of some medicinal plants. International Journal of Biological Macromolecules, 145, 124-132, 2021.

Martins, J. T., Cerqueira, M. A., Vicente, A. A., Influence of α-tocopherol on physicochemical properties of chitosan-based films. Food Hydrocolloids, 27(1), 220-227, 2012.

Mau, J. L., Lin, H. C., Chen, C. C. Antioxidant properties of several medicinal mushrooms. Journal of Agricultural and Food Chemistry, 50(21), 6072-6077, 2002.

Mokhtari-Hosseini, Z. B., Hatamian-Zarmi, A., Mohammadnejad, J., Ebrahimi-Hosseinzadeh, B. Chitin and chitosan biopolymer production from the Iranian medicinal fungus *Ganoderma lucidum*: Optimization and characterization. Preparative Biochemistry and Biotechnology, 48(7), 662-670, 2018.

Naeem, M. Y., Ozgen, S., Sumayya, R. A. N. İ. Emerging role of edible mushrooms in food industry and its nutritional and medicinal consequences. Eurasian Journal of Food Science and Technology, 4(1), 6-23, 2020.

Neville, P., Poumarat, S., Rebaudengo, E., Fungi Europaei, Volume 9 - Amanita, Limacella & Torrendia, Publisher: Edizioni Candusso, 2004.

Noshirvani, N., Ghanbarzadeh, B., Gardrat, C., Rezaei, M. R., Hashemi, M., Le Coz, C., Coma, V., Cinnamon and ginger essential oils to improve antifungal, physical and mechanical properties of chitosan-carboxymethyl cellulose films. Food Hydrocolloids, 70, 36-45, 2017.

Pérez-Gago, M. B., Nadaud, P., Krochta, J. M., Water vapor permeability, solubility, and tensile properties of heat-denatured versus native whey protein films. Journal of Food Science, 64(6), 1034-1037, 1999.

Priyadarshi, R., Kumar, B., Deeba, F., Kulshreshtha, A., Negi, Y. S. Chitosan films incorporated with apricot (*Prunus armeniaca*) kernel essential oil as active food packaging material. Food Hydrocolloids, 85, 158-166, 2018.

Puttaraju, N. G., Venkateshaiah, S. U., Dharmesh, S. M., Urs, S. M. N., Somasundaram, R. Antioxidant activity of indigenous edible mushrooms. Journal of Agricultural and Food Chemistry, 54(26), 9764-9772, 2006.

Raafat, D., Sahl, H. G. Chitosan and its antimicrobial potential–A critical literature survey. Microbial Biotechnology, 2(2), 186-201, 2009.

Rabea, E. I., Badawy, M. E. T., Stevens, C. V., Smagghe, G., Steurbaut, W. Chitosan as antimicrobial agent: applications and mode of action. Biomacromolecules, 4(6), 1457-1465, 2003.

Ramírez-Anguiano, A. C., Santoyo, S., Reglero, G., Soler-Rivas, C. Radical scavenging activities, endogenous oxidative enzymes and total phenols in edible mushrooms commonly consumed in Europe. Journal of the Science of Food and Agriculture, 87(12), 2272-2278, 2007.

Rice-Evans, C., Miller, N., Paganpa, G., Antioxidant properties of phenolic compounds, Trends in Plant Science, 2(4), 152-159, 1997.

Sady, S., Błaszczyk, A., Kozak, W., Boryło, P., Szindler, M., Quality assessment of innovative chitosan-based biopolymers for edible food packaging applications. Food Packaging and Shelf Life, 30, 100756, 2021.

Sathiyaseelan, A., Shajahan, A., Kalaichelvan, P. T., Kaviyarasan, V. Fungal chitosan based nanocomposites sponges-An alternative medicine for wound dressing. International journal of biological macromolecules, 104, 1905-1915, 2017.

Savin, S., Craciunescu, O., Oancea, A., Ilie, D., Ciucan, T., Antohi, L. S., Oancea, F. Antioxidant, cytotoxic and antimicrobial activity of chitosan preparations extracted from *Ganoderma lucidum* mushroom. Chemistry & Biodiversity, 17(7), e2000175, 2020.

Sesli, E., Denchev, C. M. Checklists of the myxomycetes, larger ascomycetes, and larger basidiomycetes in Turkey. Mycotaxon, 106(2008), 65, 2014.

Silva-Rodrigues, H. C., Silveira, M. P., Helm, C. V., de Matos Jorge, L. M., Jorge, R. M., Gluten free edible film based on rice flour reinforced by guabiroba (*Campomanesia xanthocarpa*) pulp. Journal of Applied Polymer Science, 137(41), 49254, 2020.

Thaipong, K., Boonprakob, U., Crosby, K., Cisneros-Zevallos, L., Byrne, D. H., Comparison of ABTS, DPPH, FRAP, and ORAC assays for estimating antioxidant activity from guava fruit extracts, Journal of Food Composition and Analysis, 19, 669-675, 2006.

Sharma, S. K., Gautam, N. Chemical, bioactive, and antioxidant potential of twenty wild culinary mushroom species. BioMed Research International, 2015, 1-12 2015.

Silva-Rodrigues, H. C., Silveira, M. P., Helm, C. V., de Matos Jorge, L. M., Jorge, R. M., Gluten free edible film based on rice flour reinforced by guabiroba (*Campomanesia xanthocarpa*) pulp. Journal of Applied Polymer Science, 137(41), 49254, 2020.

Siripatrawan, U., Harte, B. R. Physical properties and antioxidant activity of an active film from chitosan incorporated with green tea extract. Food Hydrocolloids, 24(8), 770-775, 2010.

Smolskaitė, L., Venskutonis, P. R., Talou, T. Comprehensive evaluation of antioxidant and antimicrobial properties of different mushroom species. LWT-Food Science and Technology, 60(1), 462-471, 2015.

Stacewicz-Sapuntzakis, M., Bowen, P., Hussain, E., Damayanti-Wood, B., Farnsworth, N., Chemical composition and potential health effects of prunes: A Functional Food?, Critical Reviews in Food Science and Nutrition, 41(4), 251-286, 2001.

Sun, T., Zhou, D., Xie, J., Mao, F. Preparation of chitosan oligomers and their antioxidant activity. European Food Research and Technology, 225(3), 451-456, 2007.

Szydłowska-Czerniaka, A., Dianoczkib, C., Recseg, K., Determination of antioxidant capacities of vegetable oils by ferric-ion spectrophotometric methods. Talanta, 76, 899–905, 2008.

Xie, W., Xu, P., Liu, Q. Antioxidant activity of water-soluble chitosan derivatives. Bioorganic & Medicinal Chemistry Letters, 11(13), 1699-1701, 2001.

Yang, J. H., Lin, H. C., Mau, J. L. Antioxidant properties of several commercial mushrooms. Food chemistry, 77(2), 229-235, 2002.

Yasrebi, N., Zarmi, A. H., Larypoor, M., Zeynali, M., Ebrahimi-Hosseinzadeh, B., Mokhtari-Hosseini, Z. B., Alvandi, H. In vivo and in vitro evaluation of the wound healing properties of chitosan extracted from *Trametes versicolor*. Journal of Polymer Research, 28(10), 1-11, 2021.

Yen, M. T., Yang, J. H., Mau, J. L. Antioxidant properties of chitosan from crab shells. Carbohydrate polymers, 74(4), 840-844, 2008.

Zhang, L., Liu, Z., Sun, Y., Wang, X., Li, L., Effect of α-tocopherol antioxidant on rheological and physicochemical properties of chitosan/zein edible films. LWT-Food Science and Technology, 118, 108799, 2020.

https://boletales.com/genera/boletus/b-reticulatus/ Erişim tarihi: 27.06.2022

Bölüm 2

Laurus nobilis Ekstraktı Kullanılarak Yeşil Sentez Yöntemiyle Üretilen ZnO Nanopartiküllerin Karakterize Edilmesi ve Nanogübre Özellikleri

Nazmi Sedefoğlu [1]

Kağan Veryer[2]

Oğuzhan Ateş[3]

Yusuf Zalaoğlu[4]

Fuat Bozok[5]

Özet

Bu çalışmada Osmaniye ili Fakıuşağı bölgesinde toplanan *Laurus nobilis* bitki yapraklarının özütleri kullanılarak yeşil sentez yoluyla ZnO nanoparçacıkları sentezlenmiş ve farklı konsantrasyonlarda hazırlanarak (0, 62.5, 125, 250 ve 500 ppm) *in vitro* nano gübre kullanım olanakları çeşitli bitki (*Zea mays* (mısır), *Triticum aestivum* (buğday) ve *Vicia sativa* (fiğ)) tohumlarının gelişimleri üzerine etkileri araştırılmıştır. Öğütülmüş *Laurus nobilis* yaprağından 25 g alınıp 500ml dH_2O içerisine konularak 1 saat boyunca 100 ^oC'de sürekli karıştırılmıştır. Süzülerek elde edilen bitki özütünden 50 ml alınarak üzerine 5 g $(CH_3COO)_2Zn$ 0.2 H_2O ilave edilerek buharlaşıncaya kadar sürekli karıştırılarak bekletilmiştir. Pelet kısmı kül fırınında 400, 600 ve 800 ^oC'lerde ayrı ayrı yakılarak ZnO nanopartikülleri elde edilmiştir. Elde edilen tozlar XRD ve UV-Vis kullanılarak karakterize edilmiştir. Sterile edilen tohumlar içlerinde 2 katlı Whatman No:1 filtre kâğıdı bulunan 9 cm'lik petri kaplarına

1 Dr. Öğr. Üyesi, Osmaniye Korkut Ata Üniversitesi, nazmisedefoglu@osmaniye.edu.tr, 0000-0001-5364-7375

2 Arş. Gör. Osmaniye Korkut Ata Üniversitesi, kaganveryer@osmaniye.edu.tr, 0000-0002-0227-1619

3 Doktora Öğrencisi, Osmaniye Korkut Ata Üniversitesi, oguzhan_ates@hotmail.com, 0000-0001-5729-5872

4 Doç. Dr., Osmaniye Korkut Ata Üniversitesi, yzalaoglu@osmaniye.edu.tr, 0000-0003-2191-8112

5 Doç. Dr., Osmaniye Korkut Ata Üniversitesi, fbozok@osmaniye.edu.tr, 0000-0002-9370-7712

https://doi.org/10.58830/ozgur.pub252.c1213

alınarak üzerlerine farklı konsantrasyonlarda ZnO NP'ler ilave edilerek hazırlanan çözeltilerden 10 ml konulup parafilmle kapatılmıştır. Daha sonra petri kapları 8 gün boyunca oda sıcaklığında (25 °C, 12 saat karanlık, 12 saat aydınlık) bekletilmiştir. *L. nobilis* özütü kullanılarak yeşil sentez yöntemiyle elde edilen ZnO nanopartiküllerinin en düşük konsantrasyonlarda (62.5 ve 125 ppm) daha etkili olduğu tespit edilmiştir.

1. Giriş

Küreselleşen dünya ve artan nüfusa bağlı olarak teknoloji tüm insanlar için vazgeçilmezdir. Ayrıca zaman geçtikçe teknolojinin insanların yaşam standartlarını iyileştirme yönünde hızla ilerlediği görülmektedir. Özellikle son yıllarda nano ölçekte (1 ile 100 nm arası) yapılan çalışmalarla ilgilenen ve multidisipliner bir alan olan nanoteknoloji popüler hale gelmiştir (Bhatia vd., 2016; Miller vd., 2004). Ancak nano ölçekli yapılar, yüksek yüzey/hacim oranları, küçük boyutlar, yüksek yüzey enerjileri, kuantum etkisi ve azaltılmış kusurlar gibi özelliklerinden dolayı makro ölçekli yapılara göre daha fazla ilgi görmektedir (Narayanan vd., 2011; Liveri 2006). Özellikle nanoparçacıklar, nano-çubuklar, nano-kristaller, nano-tüpler, nano-teller gibi malzemeler nano ölçekli yapılar arasındadır (Mao vd., 2016). Nanoteknoloji alanındaki araştırmaların hızla artmasıyla boyutları, şekilleri ve morfolojileri nedeniyle mükemmel kimyasal, fiziksel, optik ve mekanik özelliklere sahip nanoparçacıklar elde edilebilmektedir. Ayrıca üstün özelliklere sahip nanoparçacıkların biyomedikal, tıp, gıda, elektronik, kozmetik, tekstil, tarım, sağlık, otomobil endüstrisi, inşaat vb. gibi ekonominin birçok sektöründe uygulamaları bulunmaktadır (Shah vd., 2015; Asmatulu vd., 2013; Kumar vd., 2008; Espitia vd., 2012; Kathirvelu vd., 2009; Li vd., 2005; Ko vd., 2007; Frey vd., 2009; Nair vd., 2010; Pardeike vd., 2009; Prow vd., 2011; Chaloupka vd., 2010]. Bu durum, nanoparçacıkların birçok sektörde daha fazla kullanılması gerekliliğini ortaya koymuştur. Aynı zamanda nanoparçacıkların birçok alanda artan kullanımı ile üretim aşamalarının biyolojik ve çevresel güvenlik açısından dikkatle gözden geçirilmesi kaçınılmaz bir gerçektir. Bilindiği gibi nanoparçacık sentezi için genellikle karmaşık yapıya sahip, maliyetli ve çevreye zarar verme potansiyeli olan kimyasal ve fiziksel yaklaşımlar kullanılmaktadır (Iqbal vd., 2017). Günümüzde bu iki sentez işlemine ek olarak hem çevre dostu hem de toksik kimyasalların kullanımını ortadan kaldıran yeşil sentez yöntemi ile büyük ölçekli nanoparçacık üretimi yapılabilmektedir (Jadoun vd., 2021; Patil vd., 2017; Kumar vd., 2018; El-Borady vd., 2020). Diğer bir deyişle yeşil sentez yöntemi hem biyolojik materyallerin hem de inorganik materyallerin kullanıldığı nanoparçacık sentez süreci olarak tanımlanabilir (Korbekandi vd., 2009; Ishak vd., 2019; Chatterjee vd., 2020; Kharissova

vd., 2013). Bu sentez işleminde bakteri, mantar, alg, maya, küf, virüs gibi canlı mikroorganizmalar ve çoğunlukla bitkiler kullanılmaktadır (Shukla ve Iravani 2017). Bitki ve canlı mikroorganizmaların ekstraktlarında bulunan aminler, fenolik bileşikler, enzimler, proteinler ve pigmentler gibi moleküllerin, indirgeyici etkileri ile metal tuzlarını indirgeyerek metal iyonlarını metal nanoparçacıklara dönüştürdükleri ortaya çıkmaktadır (Gour ve Jain 2019; Velusamy vd., 2016; Boroumand vd., 2015). Ayrıca, yüksek verim ve düşük maliyete sahip olması, tek adımda basit bir işlem olması, daha çevre dostu olması, daha kararlı nanopartiküller elde etmek ve büyük ölçekli sentez için uygun olması gibi temel avantajları açısından yeşil sentez yöntemiyle nanoparçacık elde etme sürecinde bitki ekstraktının kullanımını üstün kılmaktadır (Sastry vd., 2013; Vijayaraghavan vd., 2017).

Daha önceki çalışmalara bakıldığında, farklı bitkiler ve bazı mantar türlerinin özütleri kullanılarak yeşil sentez yöntemiyle çeşitli metal oksitler sentezlenmiştir. (Abbasifar vd., 2020; Rafique vd., 2022; Sharma vd., 2022; Sedefoğlu vd., 2022). Yeşil sentezlenmiş metal oksit nanopartiküller arasında, ZnO NP'ler, fotokatalitik, antibiyofilm, antidiyabetik, antibakteriyel, antifungal, hemolitik ve katalitik aktiviteler gibi üstün özelliklerinden dolayı birçok araştırmacı tarafından sıklıkla araştırılmaktadır (Dulta vd., 2022; Çolak vd., 2017; Mane vd., 2021; Rahimi vd., 2020; Meydan vd., 2022; Kurian vd., 2021; Metwally vd., 2022).

Bu çalışmanın amaçları; (i) Laurus nobilis özütü ile yeşil sentezlenen ZnO NP'leri üretmek, (ii) Üretilen bu naopartiküllerin karakterizasyonunu yapmak ve (iii) ZnO NP'lerin üç farklı bitkinin büyümesi ve gelişimi üzerine etkisini araştırmak şeklinde sıralanabilir.

2. MATERYAL VE YÖNTEM

2.1 Materyal

2.1.1 Bitki Materyali

Bu araştırma kapsamında kullanılan bitki örnekleri Osmaniye ili Fakıuşağı bölgesinden toplanmış ve toplanan örneklerin gerekli morfolojik özellikleri ile GPS koordinatları ve deniz seviyesinden yükseklikleri kaydedilmiştir. Toplanıp preslenerek kurutulan bitki örnekleri herbaryum materyali olarak Osmaniye Korkut Ata Üniversitesi Biyoloji Bölümü'nde saklanmaktadır. "Flora of Turkey and the East Aegean Island" adlı eser kullanılarak bitkiler teşhis edilmiştir (Davis, 1982). Bitki örneğinin lokalitesi ve özellikleri aşağıda verilmiştir.

Laurus nobilis L., Osmaniye Korkut Ata Üniversitesi Yerleşkesi, 37°02'313" K, 36°13'206" D, 154 m, 06.01.2022 (Şekil 1). Aromatik, 2-15 m ye kadar boylanabilen herdem yeşil ağaç ya da çalı formunda çift evcikli (dioik, erkek ve dişi çiçekler ayrı ayrı bitkilerde bulunması durumu) bitkiler. Yapraklar 3-10(11) x 2-4(5) cm boyutunda, dar bir şekilde oval-mızraksıdan geniş yumurtamsıya kadar şekillenmekte. Erkek çiçekler 8-12 stamenli, filamentler tabana yakın kısımlarda armutsu salgı tüylerine sahip. Dişi çiçekler steril 4 stamenli. Meyve 10-12(20) mm, küresel, elips şekilli, siyah renkte. Makilik alanlarda, kayalık yamaçlarda vb. yerlerde 1-1200 m ye kadar yüksekliklerde yayılış göstermektedirler (Davis, 1982).

Şekil 1 Laurus nobilis bitkisinin genel görüntüsü

2.2 Yöntem

2.2.1 Özütleme

Toplanan bitki örnekleri laboratuvara getirilerek gölgede 7 gün boyunca kurutulmuştur. Kurutulan bitki örnekleri bir öğütücü yardımıyla iyice öğütülmüştür. Öğütülen bitki örneğinden 25 g alınıp 500 ml dH_2O içerisine konulduktan sonra 1 saat boyunca 100 ^oC'de sürekli karıştırılmıştır. Daha sonra oda sıcaklığına gelince kadar soğumaya bırakılmış ve çözelti Whatman No:1 kâğıdı ile süzülmüştür. Elde edilen sıvı özüt analizlerde kullanılıncaya kadar +4^oC'de buzdolabında saklanmıştır.

2.2.2 ZnO Nanopartikül Sentezi ve Karakterizasyonu

Elde edilen her bir bitki özütünden 50 ml alınıp üzerine 5 g $(CH_3COO)_2Zn$ 0.2 H_2O (ACS, CAS# 5970–45–6, Merck) ilave edilerek buharlaşıncaya kadar 100 ^oC'de sürekli karıştırılarak bekletilmiştir. Daha sonra geriye kalan pellet kısmı kül fırınında 400, 600 ve 800 ^oC'lerde ayrı ayrı yakılarak ZnO nanopartikülleri elde edilmiştir. Elde edilen tozların karakterizasyonunu yapmak için XRD ve UV-Vis analizleri hizmet alımı şeklinde yapılmıştır.

2.2.3 ZnO Nanopartikülünün *In vitro* Çimlenme Üzerine Etkisi

Farklı sıcaklıklarda yakılarak elde edilen ZnO nanopartiküllerinin farklı konsantrasyonları (0, 62.5, 125, 250 ve 500 ppm) *Zea mays* (mısır), *Triticum aestivum* (buğday) ve *Vicia sativa* (fiğ) tohumlarının çimlenmesi üzerine etkileri araştırılmıştır. Ticari olarak satılan tohumlar Osmaniye ilinde yerel bir satıcıdan temin edilmiştir. Temin edilen tohumların yüzey sterilizasyonu 30 dk boyunca %15'lik sodyum hipoklorit çözeltisinde bekletilerek yapılmıştır. Yüzey sterilizasyonu yapılan tohumlar içlerinde 2 katlı Whatman No:1 filtre kâğıdı bulunan 9 cm'lik petri kaplarına alınarak üzerlerine farklı konsantrasyonlarda ZnO nanopartikülleri ilave edilerek hazırlanan çözeltilerden 10 ml konulup parafilm ile iyice hava almayacak şekilde kapatılmıştır. Daha sonra petri kapları 8 gün boyunca oda sıcaklığında (25 ^oC, 12 saat karanlık, 12 saat aydınlık) bekletilmiştir. 8. günün sonunda petri kaplarında çıkarılan fidelerin kök ve gövde uzunlukları ölçülerek not edilmiştir. Yaş ağırlıkları tartılıp not edildikten sonra kuru ağırlıklarını belirlemek için fideler sabit tartıma gelinceye kadar (yaklaşık 48 saat) fırında 50 ^oC'de bekletilmiştir. Fırından çıkarılan örneklerin tartımı yapılmış ve kuru ağırlıkları belirlenmiştir.

2.2.4 İstatistiksel Analiz

Yeşil sentez yöntemiyle üretilen ZnO NP'lerin test edilen bitkilerin büyüme ve gelişmesini değerlendirmek için SPPS paket programı (Versiyon 18.0, IBM İstatistik, ABD) kullanılmıştır. Sonuçlar tek yönlü varyans analizi (ANOVA) ile Duncan testi uygulanarak yapılmıştır (değerler %95 güven aralığında sunulmuştur).

3. Bulgular ve Tartışma

3.1 XRD

X-ışını difraktometresi metodu kristal olan ya da amorf malzemelerin yapısal ve kristalografik yapısı hakkında detaylı bilgi sağlamak için kullanılan en yaygın yöntemdir. Bitki ekstraktları ile hazırlanan toz ZnO örneklerin x ışını toz kırınım analizleri Rigaku Miniflex XRD ile yapılmış ve bu XRD Cu Kα ışınımı ve $\lambda = 1{,}5418$ Å dalga boyuna sahip bir lazerle donatılmıştır ayrıca bu ölçümler normal koşullarda tarama açısı $2\theta = 20^{o} – 70^{o}$ aralığında, adım aralığı olan $0{,}02^{o}$ ile alınmıştır.

Şekil 2'de grafikte XRD pikleri görülmektedir. Numunelerin XRD sonuçları, P63mc uzay grubuna ait hekzagonal vurtzit ZnO yapısında kristalleştiği göstermektedir (PDF 36-1451 ya da ICSD 76641). XRD grafiğinde bütün örneklerin vurtzit yapıda olan (101), (002), (101), (102), (110), (103), (200), (112) ve (201) düzlemlerine atfedilen piklere sahip olduğu görülmüş ve bunların haricinde herhangi bir ikincil faz gözlenmemiştir. Bu sonuçlar üretilen malzemelerin saf fazlı ZnO olduğunu göstermektedir (Kisi ve Elcombe 1989).

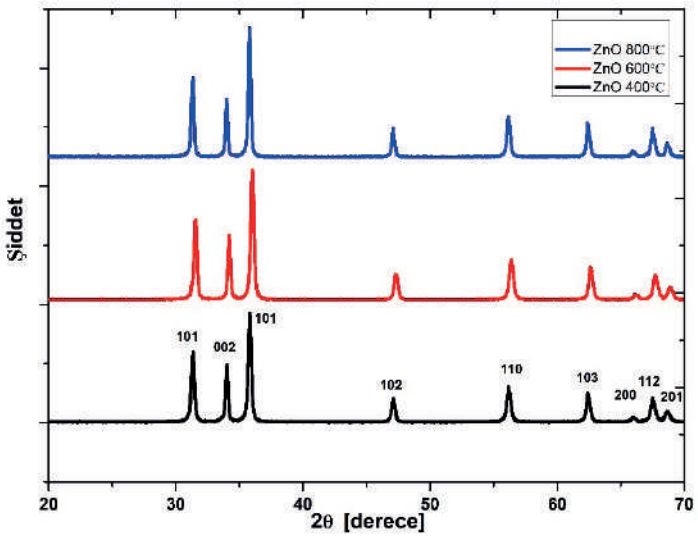

Şekil 2. Laurus nobilis ekstraktı ile farklı kalsinasyon sıcaklığında sentezlenen ZnO'ların 2θ = 20º – 70º XRD desenleri

Ayrıca kalsinasyon sıcaklığının artması ile numunelerin XRD'lerinde piklerin şiddetinde artma olduğunu kristalliğinin arttığını göstermektedir. Bunun ile birlikte bütün numunelerde 101 pikinin en şiddetli yönelim olduğu görülmüştür ve bu literatür ile uyum içerisindedir (Sadananda kumar ve ark 2013).

3.2 UV-Vis

Örneklerin optik özellikleri Shimadzu UV-3600 Plus UV-vis spektrometresi ile belirlenmiştir. Dalgaboyuna karşı yüzde yansıma verileri alınan bu ölçümler Şekil 3'te verilmiştir. Örneklerin ölçümleri toz halinde alınmıştır.

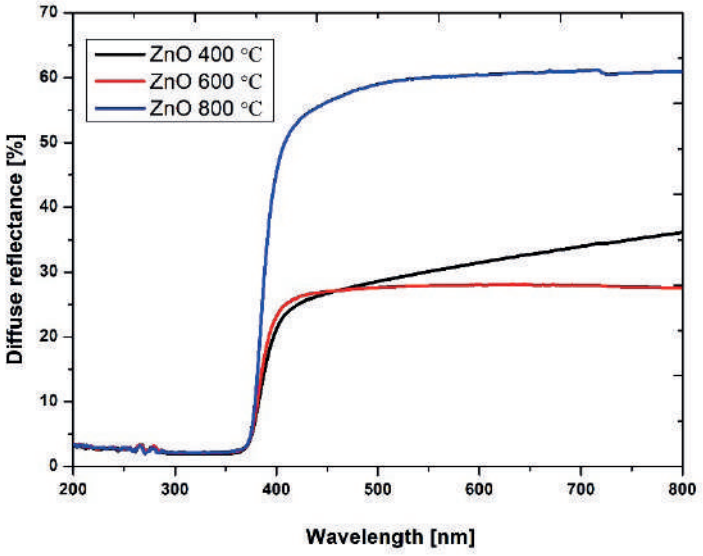

Şekil 3 Laurus nobilis ekstraktı ile farklı kalsinasyon sıcaklığında sentezlenen ZnO tozlarının UV-VIS spektrometre ölçümlerinin dalga boyuna karşı % Yayılma Yansıma grafikleri

Örneklerin yansımaları 500 nm dalga boyunu geçen değerler için %50'nin üzerinde olduğu görünmekte ve bu değerler literatür değerleri ile uyum içerisindedir. Ayrıca kalsinasyon sıcaklığının azalması ile birlikte yansıma değerinde azalma olduğu gözlemlendi. Bunun yanı sıra bütün kalsinasyon sıcaklıklarında *Laurus nobilis* (Defne) ekstraktı ile hazırlanan örneklerin yansımalarının yüksek olduğu görülmektedir. Bütün örnekler içinde soğurma 370-380 nm civarında başlamıştır. Bu değerler yaklaşık olarak benzer çalışmalarda aynıdır (Tan ve ark 2005, Sedefoglu, 2016).

4.3 SEM Analizi

Örneklerin morfolojik yapısı Zeiss Sigma 300 taramalı elektron mikroskobu (SEM) ile yapılmıştır. Şekil 4'te nano malzemelerin 10000X ile yakınlaştırılan SEM görüntüleri bulunmaktadır.

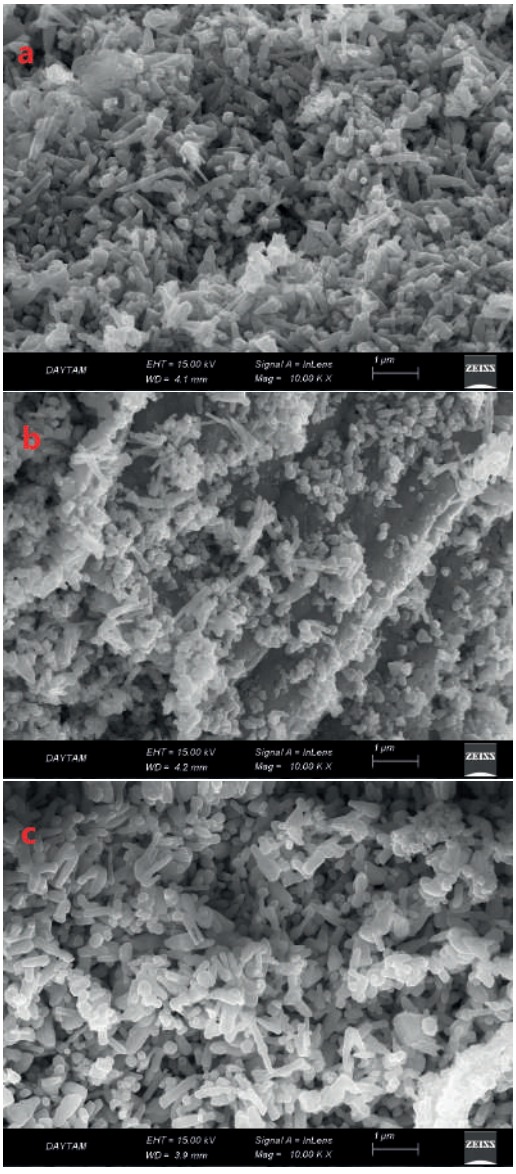

Şekil 4 Laurus nobilis ekstraktı ile farklı kalsinasyon sıcaklığında sentezlenen ZnO tozlarının SEM görüntüleri (a: 400 ºC, b: 600 ºC, c: 800 ºC)

Nanoparçacıkların görüntülerinde homojen olmayan şekilde dağılan granüller görülmektedir. Bu granüllerin geometrileri bitki ekstraktı ve kalsinasyon sıcaklığı ile değişmiştir. Şekil 4 incelendiğinde küçük partiküllerin bir araya gelerek büyük partiküller meydana getirdiği gözlemlenmiştir. SEM görüntülerinde yaklaşık 1 μm boyutunda oluşan topaklanmalar ile 1

μm altında büyüklüklerde homojen olmayan bir şekilde üretilen parçacıklar gözlemlenmiştir. Granüllerin yüzeylerinde farklı yönelimler, açı farklılıkları görülmektedir. Sentezlenen nano malzemelerin kalın çubuklar, küçük parçacıklar ve hekzagonal geometriler şeklinde olduğu görülmektedir.

3.4 Tohum Çimlenmesi

Bu araştırma ile *Laurus nobilis* (Defne) bitkisinin özütü elde edilmiş ve elde edilen özütle yeşil sentez yöntemiyle ZnO nanopartikülleri (NP) üretilmiştir. Üretilen nanopartiküllerin farklı konsantrasyonları hazırlanarak (0, 62.5, 125, 250 ve 500 ppm) *in vitro* nano gübre kullanım olanakları çeşitli bitki (*Zea mays* (mısır), *Triticum aestivum* (buğday) ve *Vicia sativa* (fiğ)) tohumlarının gelişimleri üzerine etkileri araştırılmıştır. Her iki bitkinin özütü kullanılarak yeşil sentez yöntemiyle elde edilen ZnO nanopartiküllerinin en düşük konsantrasyonlarda (62.5 ve 125 ppm) daha etkili olduğu tespit edilmiştir (Şekil 5-8).

Defne bitkisi özütü kullanılarak ve farklı sıcaklıklarda fırında kalsine edilen ZnO NP'lerin genellikle en düşük konsantrasyonda (62.5 ppm) kontrole göre daha fazla kök uzamasını etkilediği görülmektedir. Bununla birlikte daha yüksek konsantrasyonlarda (125, 250 ve 500 ppm) uygulandığında ise kök uzamasını engelleyici etkiye sahip olduğu tespit edilmiştir. 400, 600 ve 800 ^{o}C'lerde ayrı ayrı kalsine edilen ZnO NP'lerin en düşük konsantrasyonda (62.5 ppm) uygulanmasıyla mısır fidelerinin kök uzunluklarını kontrole göre sırasıyla %18, %16 ve %5 oranlarında, gövde uzunluklarını ise %15, %11 ve %6 oranlarında artırdığı belirlenmiştir. 400 ve 600 ^{o}C'de kalsinasyonla elde edilen ZnO NP'ler buğday fidelerinin kök uzunluklarını kontrole göre 62.5 ppm konsantrasyonda %13 ve %2 oranlarında artırırken, 800 ^{o}C'de kalsine edilen ZnO nanopartikülleri ise %18 oranında azaltmış ve buğday fidelerinin gövde uzunlukları ise %17, %8 ve %12 oranlarında artmıştır. Benzer şekilde, 400 ve 600 ^{o}C'lerde kalsinasyonla elde edilen ZnO NP'lerin fiğ fidelerinin kök uzunluklarını %9 ve %7 oranlarında artırırken, 800 ^{o}C'de kalsine edilen ZnO NP'nin yaklaşık %25 oranında azalttığı tespit edilmiştir. Bununla birlikte, fiğ fidelerinin gövde uzunlukları ise test edilen bütün konsantrasyonlarda kontrole göre azalmıştır. Yaş ağırlıklara bakıldığında, mısırda 600 ve 800 ^{o}C'de, buğdayda 400 ve 600 ^{o}C'de fiğ bitkisinde ise 400 ve 800 ^{o}C'de kontrole göre bir artış gözlenmiştir. Mısır ve buğday bitkilerinin kuru ağırlıkları 800 ^{o}C'de kalsine edilen 62.5, 125 ve 250 ppm konsantrasyonlarda kontrole göre artarken, fiğ bitkisinin ise 62.5 ve 125 ppm konsantrasyonlarda artma gözlenmesine rağmen, 250 ppm ve üzeri konsantrasyonlarda azalmıştır.

Bu sonuçlardan yola çıkarak elde edilen ZnO NP'lerin bazı bitkilerin kök uzamalarına etki ederken, bazılarının ise gövde uzamalarına daha çok etki ettiği söylenebilir. Bununla birlikte ileride yapılacak çalışmalarda, elde edilen nanopartiküllerin arazi şartlarında kullanılması, etki mekanizmalarının araştırılması önerilmektedir. Aynı zamanda, ileriki çalışmalarda elde edilecek toz halindeki NP'lerin püskürtme yoluyla saksılarda yetiştirilecek olan çeşitli bitkilerin yapraklarına uygulanması da düşünülmektedir.

Daha önceki yapılan çalışmalarda, bu çalışma ile benzer sonuçlar elde edenlerle birlikte farklı sonuçlar elde eden araştırmacılarda bulunmaktadır. Ewais vd., (2017) yaptıkları çalışmada, *Ocimum tenuiflorum* özütü kullanılarak yeşil sentez yöntemiyle elde ettikleri ZnO nanopartiküllerin farklı konsantrasyonlarının (25, 50, 100 ve 200 ppm) *Phaseolus vulgaris* bitkisinin büyüme ve gelişimi üzerine etkilerini araştırmışlar ve araştırma sonunda, en iyi sonucun 50 ppm Zn+100 ppm ZnO NP'lerin yapraktan püskürtme yoluyla olduğunu tespit etmişlerdir. Rafique vd, (2022) tarafından yapılan çalışmada, *Syzygium cumini* yapraklarının özütü kullanılarak ZnO NP elde edilmiş ve elde edilen bu partikülün *Pennisetum glaucum*'un tohum gelişimi üzerine etkileri araştırılmıştır. Sonuç olarak, kontrol ile kıyaslandığında elde edilen ZnO NP'lerin, *P. glaucum*'un tohum gelişimini %60 oranında artırdığı belirlenmiştir. Sharma vd., (2022) tarafından yapılan çalışmada, *Eucalyptus lanceolata* yaprak özütü kullanılarak yeşil sentez yöntemiyle ZnO NP elde etmişler ve elde edilen bu nanopartiküllerin farklı konsantrasyonlarının mısır tohumun gelişimi üzerine etkilerini araştırmışlardır. Araştırma sonunda mısır gelişimi için en iyi sonuç 200 ppm konsantrasyonda alınmış ve bu konsantrasyondan daha yüksek konsantrasyonda (400 ppm) bitki gelişimi için negatif etki gösterdiği sonucuna varılmıştır.

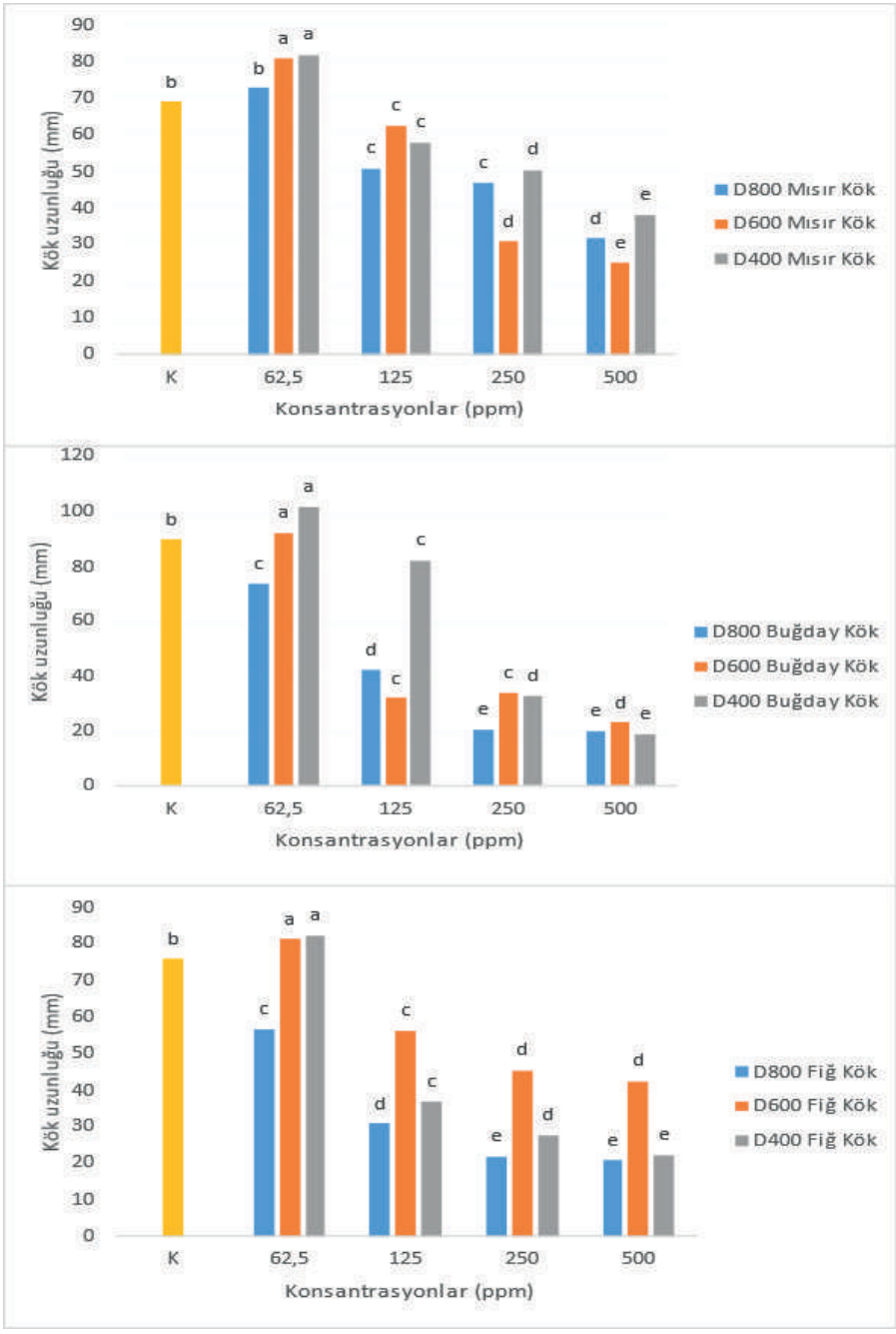

Şekil 5. Laurus nobilis özütü kullanılarak elde edilen ZnO nanopartiküllerinin test edilen bitkilerin kök uzunluğuna etkisi

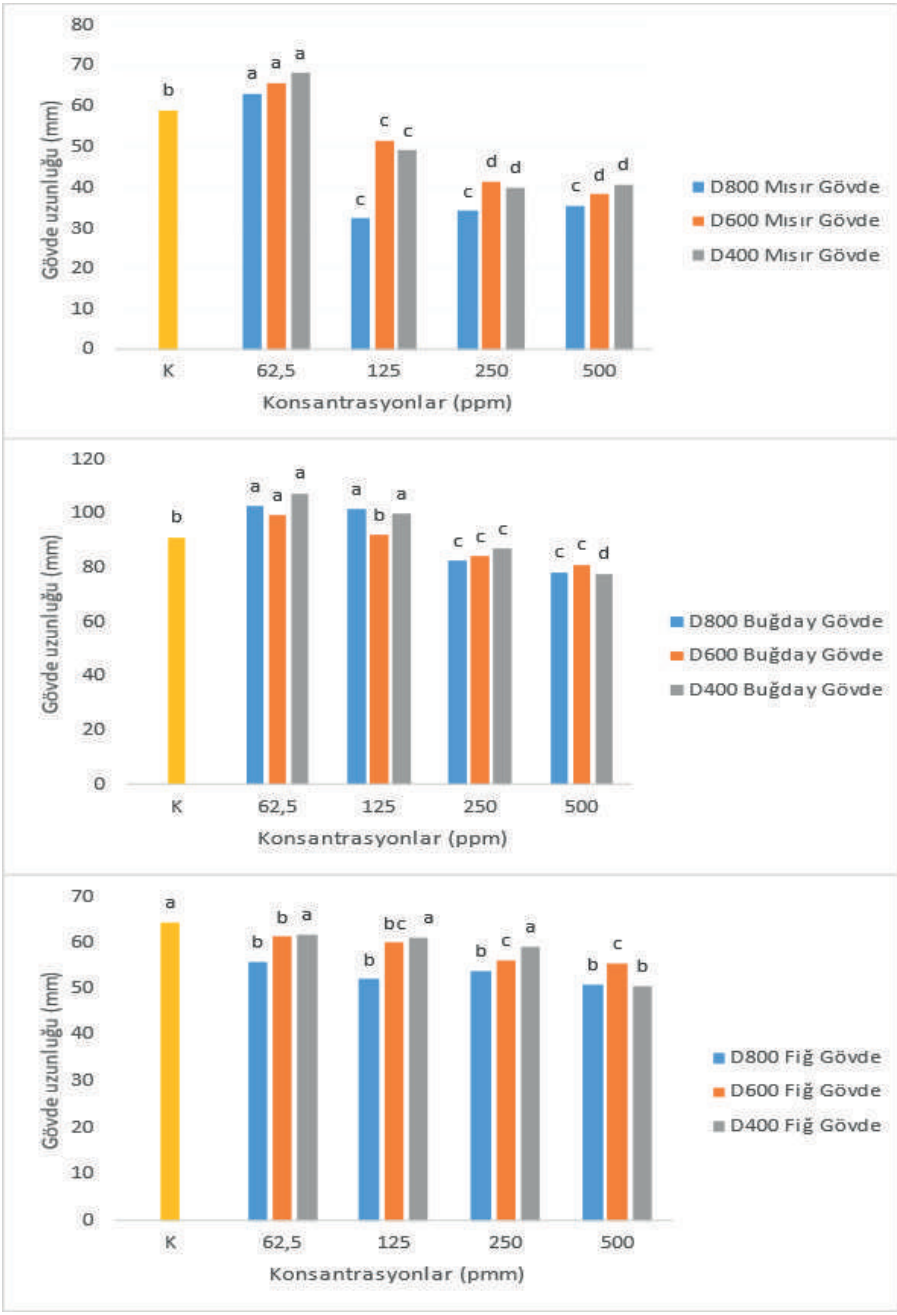

Şekil 6 Laurus nobilis özütü kullanılarak elde edilen ZnO nanopartiküllerinin test edilen bitkilerin gövde uzunluğuna etkisi

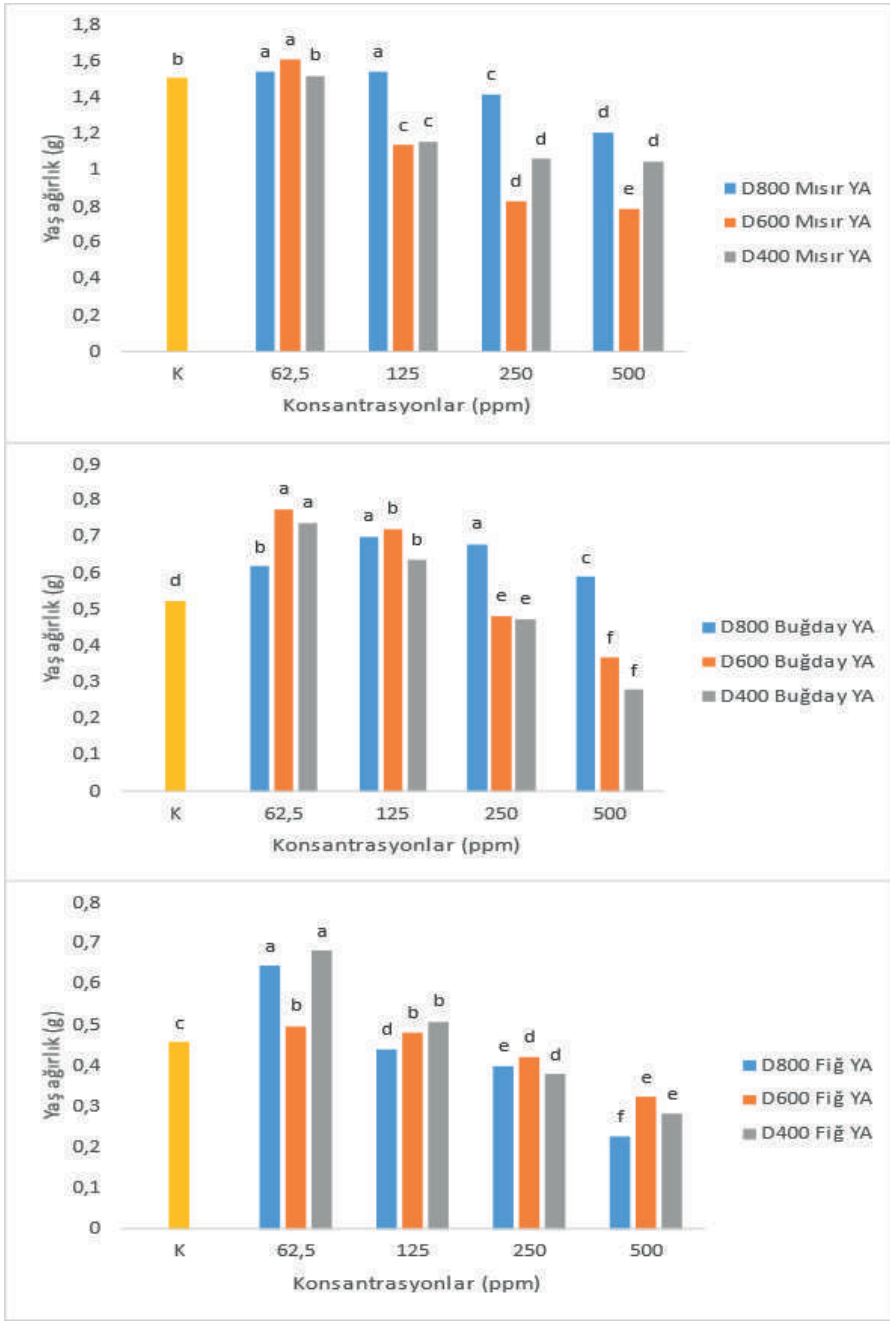

Şekil 7 Laurus nobilis özütü kullanılarak elde edilen ZnO nanopartiküllerinin test edilen bitkilerin yaş ağırlıkları üzerine etkisi

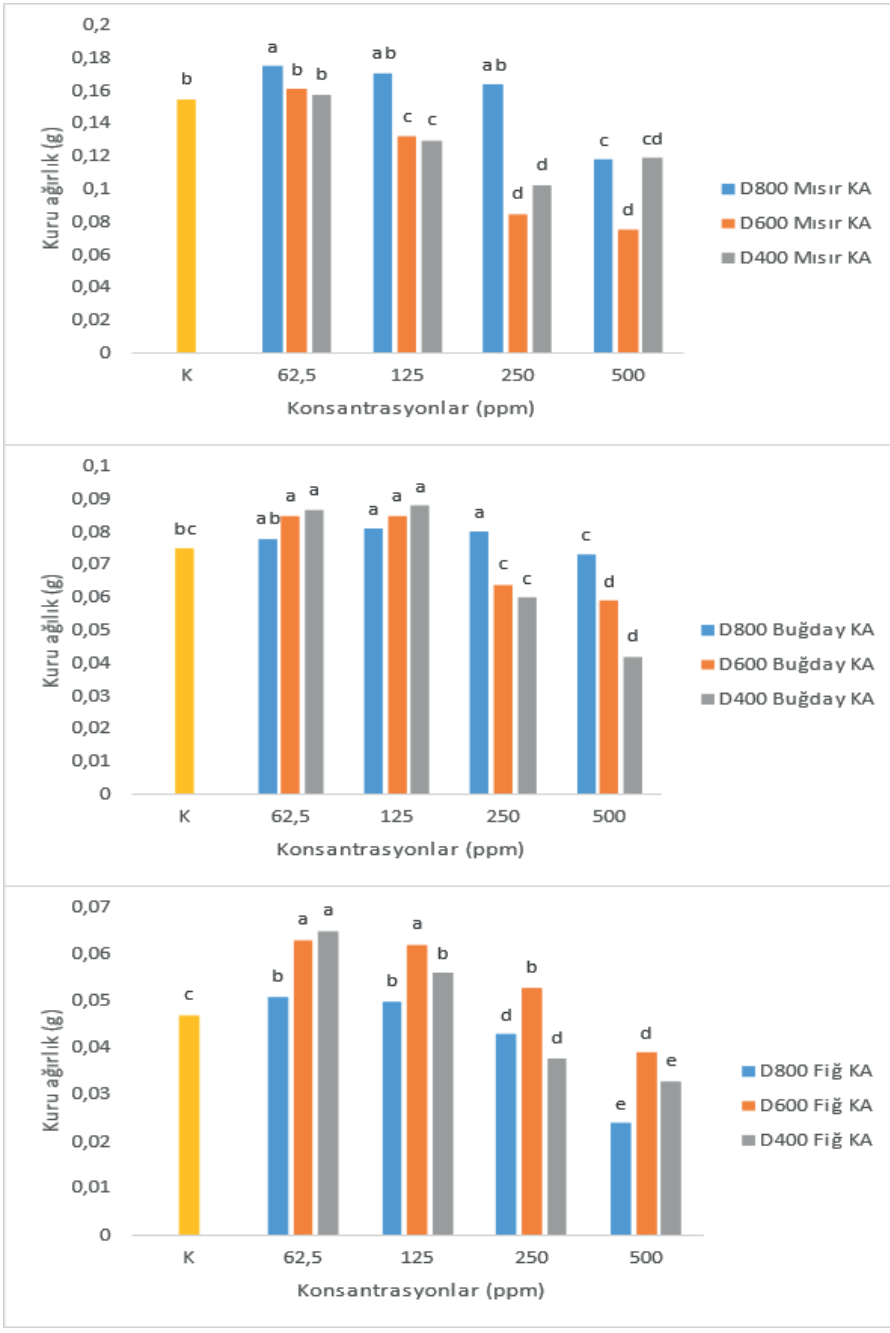

Şekil 8 Laurus nobilis özütü kullanılarak elde edilen ZnO nanopartiküllerinin test edilen bitkilerin kuru ağırlıkları üzerine etkisi

5. Sonuçlar ve Öneriler

Bu çalışma ile *Laurus nobilis* bitkisinin özütü kullanılarak yeşil sentez yöntemiyle ZnO nanopartikülleri elde edilmiştir. Elde edilen bu nanopartiküllerin XRD, UV-Vis ve SEM analizleri yapılmıştır. Bununla birlikte yeşil sentez yöntemiyle üretilen nanopartiküllerin nanogübre özellikleri in vitro olarak farklı tohumlar (*Triticum aestivum*, *Zea mays* ve *Vicia sativa*) üzerinde test edilmiştir.

Bu çalışmada, ZnO nano malzemelerin elde edilmesi sürecinde örneklerin optiksel, yapısal ve yüzey morfolojilerinin kimyasal sentezleme yöntemi ile üretilen numuneler ile uyumlu olduğu gösterilmiştir. Örneklerle yapılan XRD çalışmalarında örneklerin saf hekzagonal vurtzit yapıda ZnO olduğu bulunmuştur. Örneklerin dağınımlı yansıma sonuçlarında 375 nm civarında soğurma gerçekleştiği bulunmuştur. SEM görüntüleri, üretim koşullarının değişmesi ile parçacık morfolojisinin değiştiğini açıkça ortaya koymuştur.

Mısır, buğday ve fiğ bitkilerinin kök, gövde uzunluklarını ve yaş ve kuru ağırlıklarını en düşük konsantrasyonda (62.5 ppm) uygulanan ZnO NP'ler kontrole göre belirli bir oranda artırmıştır. Daha yüksek konsantrasyonlarda ise konsantrasyon artışına bağlı olarak inhibe ettiği tespit edilmiştir. Böylelikle, test edilen her üç bitkinin de büyüme ve gelişmesi artmıştır. Ancak, farklı bitki özütleri kullanılarak yeşil sentez yöntemiyle elde edilen çeşitli nanopartiküllerin sadece in vitro koşullarda değil aynı zamanda arazi koşullarında da hem köklere hem de püskürtmek suretiyle yapraklara uygulanarak test edilmesi ve ayrıca bu nanopartiküllerin etki mekanizmalarının da araştırılması önerilmektedir.

Teşekkür

Bu çalışma Osmaniye Korkut Ata Üniversitesi Bilimsel Araştırma Projeleri Birimi tarafından (Proje No: OKÜBAP-2022-PT2-016) desteklenmiş ve "Farklı bitki ekstraktları kullanarak yeşil sentez yöntemiyle ZnO nanoparçacık üretimi ve nanogübre olarak kullanım olanaklarının araştırılması" (Tez no:791920) başlıklı Yüksek Lisans tez çalışmasından üretilmiştir.

6. Kaynaklar

Abbasifar, A., Shahrabadi, F., ValizadehKaji, B., Effects of green synthesized zinc and copper nano-fertilizers on the morphological and biochemical attributes of basil plant. Journal of Plant Nutrition, 43(8), 1104-1118, 2020.

Asmatulu, R., Nguyen, P., Asmatulu, E., Nanotechnology Safety in the Automotive Industry, in: R. Asmatulu (Ed.) Nanotechnology Safety, Elsevier, Amsterdam, 57–72, 2013.

Bhatia, S., Nanoparticles types, classification, characterization, fabrication methods and drug delivery applications, In: natural polymer drug delivery systems, 33–93, Springer, Cham, 2016.

Boroumand, M.A., Namvar, F., Moniri, M., Tahir, P., Aziz, S., Mohamad, R., Nanoparticles biosynthesized by fungi and yeast: a review of their preparation, properties, and medical applications. Molecules, 20 (9), 16540–16565, 2015.

Chaloupka, K., Malam, Y., Seifalian, A. M., Nanosilver as a new generation of nanoproduct in biomedical applications. Trends Biotechnology, 28(11), 580–588, 2010.

Chatterjee, A., Kwatra, N., Abraham, J. Nanoparticles fabrication by plant extracts. Phytonanotechnology, 143–157, 2020.

Çolak, H., Karaköse, E., Duman, F., High optoelectronic and antimicrobial performances of green synthesized ZnO nanoparticles using *Aesculus hippocastanum*. Environmenthal Chemistry Letters, 15, 547–552, 2017.

Davis, P.H. Flora of Turkey and The East Aegean Islands, The University Press, 1982.

Dulta, K., Koşarsoy Ağçeli, G., Chauhan, P., Jasrotia, R., Chauhan, P. K., Ecofriendly synthesis of zinc oxide nanoparticles by carica papaya leaf extract and their applications. Journal of Cluster Science, 33, 603–617, 2022.

El-Borady, O.M., Ayat, M. S., Shabrawy, M. A., Millet, P., Green synthesis of gold nanoparticles using Parsley leaves extract and their applications as an alternative catalytic, antioxidant, anticancer, and antibacterial agents. Advanced Powder Technology, 31(10), 4390–4400, 2020.

Espitia, P. J. P., Soares, N. D. F. F., Coimbra, J. S. D. R., de Andrade, N. J., Cruz, R.S., Medeiros, E. A. A., Zinc oxide nanoparticles: synthesis, antimicrobial activity and food packaging applications, food and bioprocess technology, 5, 1447–1464, 2012.

Ewais, E. A., Ismail, M. A., Badawy, A. Vegetative growth, photosynthetic pigments and yield of Phaseolus vulgaris (L.) plants in response to the application of biologically-synthesized zinc oxide nanoparticles and zinc sülfate. Al Azhar Bulletin of Science, 9, 33-46, 2017.

Frey, N. A., Peng, S., Cheng, K., Sun, S., Magnetic nanoparticles: synthesis, functionalization, and applications in bioimaging and magnetic energy storage. Chemical Society Reviews, 38 (9), 2532–2542, 2009.

Gour, A., Jain, N. K., Advances in green synthesis of nanoparticles, Artificial Cells Nanomedicine Biotechnology, 47(1), 844–851, 2019.

Iqbal, T., Tufail, S., Ghazal S., Synthesis of silver, chromium, manganese, tin and iron nano particles by different techniques. International Journal of Nanoscience and Nanotechnology, 13 (1), 19–52, 2017.

Ishak, N. M., Kamarudin, S. K., Timmiati, S. N. Green synthesis of metal and metal oxide nanoparticles via plant extracts: an overview. Materials Research Express, 6 (11) 112004, 2019.

Jadoun, S., Arif, R., Jangid, N. K., Meena, R. K., Green synthesis of nanoparticles using plant extracts: a review, Environmental Chemistry Letters, 19(1), 355–374, 2021.

Karaköse, E., Çolak, H. and Duman, F. Green synthesis and antimicrobial activity of ZnO nanostructures Punica granatum shell extract, Green Processing Synthesis, 6(3), 317–323, 2017.

Kathirvelu, S., D'souza, L., Dhurai, B., UV protection finishing of textiles using ZnO nanoparticles, Indian Journal of Fibre and Textile Research, 34(3), 267-273, 2009.

Kharissova, O. V., Dias, H. V. R., Kharisov, B. I., Pérez, B. O., Pérez, V. M. J., The greener synthesis of nanoparticles, Trends Biotechnol. 31 (2013) 240–248.

Kisi, E. H., Elcombe, M. M., parameters for the wurtzite structure of ZnS and ZnO using powder neutron diffraction. Acta Crystallographica Section C, 45(12), 1867-1870, 1989.

Ko, S. H., Pan, H., Grigoropoulos, C. P., Luscombe, C. K., Fréchet, J. M. J., Poulikakos, D., All-inkjet-printed flexible electronics fabrication on a polymer substrate by low- temperature high-resolution selective laser sintering of metal nanoparticles. Nanotechnology, 18 (34), 345202, 2007.

Korbekandi, H., Iravani, S., Abbasi, S., Production of nanoparticles using organisms. Critical Reviews in Biotechnology, 29(4), 279–306, 2009.

Kumar, A., Vemula, P. K., Ajayan, P. M., John, G., Silver-nanoparticle-embedded antimicrobial paints based on vegetable oil. Nature Materials, 7(3), 236–241, 2008.

Kumar, M., Mehta, A., Mishra, A., Singh, J., Rawat, M., Basu, S., Biosynthesis of tin oxide nanoparticles using *Psidium guajava* leave extract for photocatalytic dye degradation under sunlight. Materials Letters, 215, 121–124, 2018.

Kurian, A., Elumalai, P., Study on the impacts of chemical and green synthesized (Leucas aspera and oxy-cyclodextrin complex) dietary zinc oxide na-

noparticles in Nile tilapia (*Oreochromis niloticus*), Environmental Science and Pollution Research, 28(16), 20344–20361, 2021.

Li, Y., Wu, Y., Ong, B. S., Facile synthesis of silver nanoparticles useful for fabrication of high-conductivity elements for printed electronics. Journal of the American Chemical Society, 127(10), 3266–3267, 2005.

Liveri, V. T., Controlled synthesis of nanoparticles in microheterogeneous systems. Springer Science and Business Media, Palermo, 2006.

Mane, P., Shinde, B., Mundada, P., Karale, B., Burungale, A., Biogenic synthesis of ZnO nanoparticles from *Parthenium histerophorus* extract and its catalytic activity for building bioactive polyhydroquinolines. Research on Chemical Intermediates, 47, 1743–1758, 2021.

Mao, B. H., Tsai, J. C., Chen, C. W., Yan, S. J., Wang, Y. J., Mechanisms of silver nanoparticle-induced toxicity and important role of autophagy. Nanotoxicology, 10(8), 1021–1040, 2016.

Metwally, A. A., Abdel-Hady, A., Haridy, M. A. M., Ebnalwaled, K., Saied, A. A., Soliman, A. S., Wound healing properties of green (using *Lawsonia inermis* leaf extract) and chemically synthesized ZnO nanoparticles in albino rats. Environmental Science and Pollution Research, 29(16), 23975–23987, 2022.

Meydan, I., Burhan, H., Gür, T., Seçkin, H., Tanhaei, B., Sen, F., Characterization of *Rheum ribes* with ZnO nanoparticle and its antidiabetic, antibacterial, DNA damage prevention and lipid peroxidation prevention activity of *in vitro*. Environmental Research, 204, 112363, 2022.

Miller, J. C., Serrato, R., Represas-Cardenas, J. M., Kundahl, G., The Handbook of Nanotechnology: Business, Policy, and Intellectual Property Law, John Wiley and Sons, New Jersey, 2004.

Nair, R., Varghese, S. H., Nair, B. G., Maekawa, T., Yoshida, Y., Kumar, D. S., Nanoparticulate material delivery to plants. Plant Science, 179(3), 154–163, 2010.

Narayanan, K. B., Sakthivel, N., Green synthesis of biogenic metal nanoparticles by terrestrial and aquatic phototrophic and heterotrophic eukaryotes and biocompatible agents, Advances in colloid and interface science, 169(2), 59–79, 2011.

Pardeike, J., Hommoss, A., Müller, R. H., Lipid nanoparticles (SLN, NLC) in cosmetic and pharmaceutical dermal products, International Journal of Pharmaceutics, 366(1-2), 170–184, 2009.

Patil, M. P., Kim, G. D., Eco-friendly approach for nanoparticles synthesis and mechanism behind antibacterial activity of silver and anticancer activity of gold nanoparticles, Applied microbiology and biotechnology, 101(1), 79–92, 2017.

Prow, T. W., Grice, J. E., Lin, L. L., Faye, R., Butler, M., Becker, W., Wurm, E. M. T., Yoong, C., Robertson, T. A., Soyer, H. P., Roberts, M. S., Nanoparticles and microparticles for skin drug delivery. Advanced Drug Delivery Reviews, 63(6), 470–491, 2011.

Rafique, M., Tahir, R., Gillani, S. S. A., Tahir, M. B., Shakil, M., Iqbal, T., Abdellahi, M. O., Plant-mediated green synthesis of zinc oxide nanoparticles from *Syzygium cumini* for seed germination and wastewater purification. International Journal of Environmental Analytical Chemistry, 102(1), 23-38, 2022.

Rahimi, K. S. M. G., Karimi, E., Oskoueian, E., Homayouni-Tabrizi, M., Anticancer properties of green-synthesised zinc oxide nanoparticles using Hyssopus officinalis extract on prostate carcinoma cells and its effects on testicular damage and spermatogenesis in Balb/C mice. Andrologia, 52 (1), e13450, 2020.

Sadananda kumar N., Bangera K. V., Shivakumar G. K. Effect of annealing on the properties of zinc oxide nanofiber thin films grown by spray pyrolysis technique. Applied Nanoscience, 4(2), 209-216, 2013.

Sastry, A. B. S., Karthik Aamanchi, R.B., Prasad, S. R. L., Murty, B. S., Large-scale green synthesis of Cu nanoparticles, Environmental chemistry letters, 11(2), 183-187, 2013.

Sedefoglu, N. Metal katkılı yarıiletken çinko oksit (ZnO) malzemelerin üretimi ve karakterizasyonu. Çukurova Üniversitesi Fen Bilimleri Enstitüsü, Doktora Tezi, Adana, 129 s, 2016.

Sedefoglu, N., Zalaoglu, Y., Bozok, F., Green synthesized ZnO nanoparticles using Ganoderma lucidum: Characterization and In Vitro Nanofertilizer Effects. Journal of Alloys and Compounds, 918, 165695, 2022.

Shah, M., Fawcett, D., Sharma, S., Tripathy, S. K., Poinern, G. E. J., Green synthesis of metallic nanoparticles via biological entities. Materials, 8 (11) 7278–7308, 2015.

Sharma, P., Urfan M., Anand, R., Sangral, M., Hakla, H. R., Sharma, S., Das, R., Pal, S., Bhagat M., Green synthesis of zinc oxide nanoparticles using *Eucalyptus lanceolata* leaf litter: characterization, antimicrobial and agricultural efficacy in maize. Physiology and Molecular Biology of Plants, 28(2), 363-381, 2022.

Shukla, A.K., Iravani, S., Metallic nanoparticles: green synthesis and spectroscopic characterization, Environmental Chemistry Letters, 15(2), 223-231, 2017.

Tan, S. T., Chen, B. J., Sun, X. W., Fan, W. J., Kwok, H. S., Zhang, X. H., Chua S. J., Blueshift of optical band gap in ZnO thin films grown by metal-organic chemical-vapor deposition. Journal of Applied Physics, 98(1), 013505, 2005.

Velusamy, P., Kumar, G. V., Jeyanthi, V., Das, J., Pachaiappan, R., Bio-inspired green nanoparticles: synthesis, mechanism, and antibacterial application, Toxicological research, 32(2), 95-102, 2016.

Vijayaraghavan, K., Ashokkumar, T., Plant-mediated biosynthesis of metallic nanoparticles: A review of literature, factors affecting synthesis, characterization techniques and applications, Journal of Environmental Chemical Engineering, 5(5), 4866-4883, 2017.

Chapter 3

Quantum Calculus Approach to the Dual Number Sequences

Faik Babadağ[1]

Abstract

In recent years, many researchers have focused on the chaotic dynamics of quantum calculus, which arises in a variety of areas including the study of fractals, multi-fractal measures, combinatorics and special functions.

In this paper, owing to some useful q-calculus notations, we consider the sequence of q-Fibonacci dual number and q-Lucas dual number with a different perspective and we present some formulas, facts, and properties about these number sequences. After that, some fundamental identities are given, such as D' ocagnes, Cassini, Catalan, and Binet formulas and relations of the q-dual number sequences, and defined the new dual polynomial and function called q-dual Fibonacci polynomial and function sequences. Then, we provide some properties for these sequences.

1. Introduction

W. K. Clifford (1845-1879) introduced the algebra of dual numbers as a tool for his geometrical investigations, and Kotelnikov gave the first applications (Kotelnikov, 1985). Eduard Study gave line geometry and kinematics using dual numbers and dual vectors (Study, 2022). He showed that the points of the dual unit sphere in $\mathbb{D}^3$ have a one-to-one relationship. Dual numbers have modern applications in computer modeling of rigid bodies, mechanism design, kinematics, human body modeling, and dynamics (Guggenheimer, 2012; Fischer,1998; Nurkan, 2015; Angeles, 1998).

1 Dr. Öğr. Üyesi, Kırıkkale Üniversitesi, Mühendislik ve Doğa Bilimleri Fakültesi
Orcid: 0000 0001 9098 838X, faik.babadag@kku.edu.tr

https://doi.org/10.58830/ozgur.pub252.c1214

A dual number is defined by the form $a_0 + \varepsilon a_1$, where a_0 and a_1 are real numbers and ε is the dual unit taken to satisfy $\varepsilon^2=0$ with $\varepsilon \neq 0$.

The addition and multiplication of any dual numbers $\mathbb{A}$ and $\mathbb{B}$ are defined, respectively, as follows:

$$\mathbb{A} + \mathbb{B} = (a_0 + b_0) + \varepsilon(a_1 + b_1)$$

and

$$\mathbb{A}\mathbb{B} = a_0 b_0 + \varepsilon(a_0 b_1 + a_1 b_0)$$

In the literature, the Fibonacci and the Lucas numbers play an important role in various areas such as mathematics and related fields. For positive integer n, the linear sequences F_n and L_n are defined by $\mathrm{F}_{n+2}=\mathrm{F}_{n+1} + \mathrm{F}_n$ and $\mathrm{L}_{n+2}=\mathrm{L}_{n+1} + \mathrm{L}_n$. Here, the initial conditions are $\mathrm{F}_0=0$, $\mathrm{F}_1=1$, $\mathrm{L}_0=2$, and $\mathrm{L}_1=1$, respectively. The Binet formulas of these numbers are

$$\mathrm{F}_n = \frac{\alpha^n - \beta^n}{\alpha - \beta}$$

and

$$\mathrm{L}_n = \alpha^n + \beta^n$$

The properties, relations, results between Fibonacci and Lucas numbers can be found in (Horadam, 1963; Koshy, 2018, 2019; Maynez, 2016; Nalli, 2009; Oduol, 2020; Vorobiov, 1974). Quantum calculus is important in both physics and mathematics. In recent years, many researchers have become interested in quantum calculus, which occurs in a variety of mathematical fields of combinatorics and special functions. For understanding of this paper, we demonstrate definitions and facts from the quantum calculus. The q-integer (Kac, 2002; Kome, 2022; Stum, 2013; Akkus, 2019) is shwon by

$$[n]_q = \frac{1 - q^n}{1 - q} = 1 + q + \cdots + q^{n-1} \qquad (1)$$

of two variables n and q. For positive integer m and n, we obtain

$$\begin{cases} [m+n]_q = [m]_q + q^m[n]_q \\ [mn]_q = [m]_q + [n]_{q^m} \end{cases} \tag{2}$$

In this paper, some basic concepts of dual number sequences are given using q-dual Fibonacci number sequences and q-dual Lucas number sequences. Moreover, we obtain the main identities and define quantum dual Polynomials and functions.

2. q -Dual Fibonacci and Lucas Number Sequences

In this section, we give dual number sequences with components including quantum integers, which are called q-dual Fibonacci number sequences and q-dual Lucas number sequences. Moreover, we obtain the main identities.

Definition 2.1. Dual number sequences can be given in the forms:

$$\mathcal{F}_n = \frac{\alpha^n(1-q^n)}{\alpha-\alpha q} + \varepsilon\frac{\alpha^{n+1}(1-q^{n+1})}{\alpha-\alpha q} \tag{3}$$

or equivalent

$$\mathcal{F}_n = \alpha^{n-1}[n]_q + \varepsilon\alpha^n[n+1]_q \tag{4}$$

are called the n^{th} q-dual Fibonacci number sequences and

$$\mathcal{L}_n = \frac{\alpha^n(1-q^{2n})}{1-q^n} + \varepsilon\frac{\alpha^{n+1}(1-q^{2n+2})}{1-q^{n+1}} \tag{5}$$

or equivalent

$$\mathcal{L}_n = \frac{\alpha^n[2n]_q}{[n]_q} + \varepsilon\frac{\alpha^{n+1}[2n+2]_q}{[n+1]_q} \tag{6}$$

are called as the n^{th} q-dual Lucas number sequences, where ε is the dual unit and $\varepsilon^2 = 0$.

Theorem 2.2. (Binet's formula) For $n \geq 0$, the Binet formulas for dual number sequences are

$$\begin{cases} \mathcal{F}_n = \alpha^{n-1}[n]_q\underline{\alpha} + (\alpha q)^n\underline{\beta} \\ \mathcal{L}_n = \dfrac{\alpha^n[2n]_q}{[n]_q}\underline{\gamma} + \alpha^{n+1}(1-q)\underline{\beta} \end{cases} \tag{7}$$

Moreover, these dual number sequences are shown another expression of the form

$$\begin{cases} \mathcal{F}_n = \dfrac{\alpha^n\underline{\alpha} - (\alpha q)^n\underline{\gamma}}{\alpha - \alpha q} \\ \mathcal{L}_n = \alpha^n\underline{\alpha} + (\alpha q)^n\underline{\gamma} \end{cases} \tag{8}$$

where

$$\begin{cases} \underline{\alpha} = 1 + \alpha\varepsilon \\ \underline{\beta} = \varepsilon \\ \underline{\gamma} = 1 + (\alpha q)\varepsilon \end{cases} \tag{9}$$

Proof. By taking Equalities 1, 2, 4 and 9, we have

$$\begin{aligned} \mathcal{F}_n &= \alpha^{n-1}[n]_q + \varepsilon\alpha^n[n+1]_q \\ &= \alpha^{n-1}[n]_q + \varepsilon\alpha^n\left([n]_q + q^n\right) \\ &= \alpha^{n-1}[n]_q(1 + \alpha\varepsilon) + \varepsilon\alpha^n q^n \\ &= \alpha^{n-1}[n]_q\underline{\alpha} + (\alpha q)^n\underline{\beta} \end{aligned}$$

Calculate the Binet formula for the q-dual Lucas number sequences $\mathcal{L}_n$ in other form

$$\begin{aligned} \mathcal{L}_n &= \frac{\alpha^n(1-q^{2n})}{1-q^n} + \varepsilon\frac{\alpha^{n+1}(1-q^{2n+2})}{1-q^{n+1}} \\ &= \alpha^n(1+q^n) + \varepsilon\alpha^{n+1}(1+q^{n+1}) \\ &= \alpha^n(1+\alpha\varepsilon) + (\alpha q)^n(1+\alpha q\varepsilon) \\ &= \alpha^n\underline{\alpha} + (\alpha q)^n\underline{\gamma} \end{aligned}$$

Theorem 2.3. (Catalan's identity) For $n > r,\ r \geq 1$

$$\mathcal{F}_{n+r}\mathcal{F}_{n-r} - \mathcal{F}_n^2 = \frac{\alpha^{2n-2}q^n}{1-q}\left([-r]_q + [r]_q\right)\left(1 + [2]_q\varepsilon\right)$$

Proof. By using Equalities 1, 2, 8, and 9, after some calculations. We have

$$\begin{aligned}
&\mathcal{F}_{n+r}\mathcal{F}_{n-r} - \mathcal{F}_n^2 \\
&= \frac{\alpha^{n+r}\underline{\alpha} - (\alpha q)^{n+r}\underline{\gamma}}{\alpha - \alpha q}\ \frac{\alpha^{n-r}\underline{\alpha} - (\alpha q)^{n-r}\underline{\gamma}}{\alpha - \alpha q} - \left(\frac{\alpha^n\underline{\alpha} - (\alpha q)^n\underline{\gamma}}{\alpha - \alpha q}\right)^2 \\
&= \frac{\alpha^{2n-2}q^n\,(2 - q^{-r} - q^r)}{(1-q)^2}\,\underline{\alpha}\,\underline{\gamma} \\
&= \frac{\alpha^{2n-2}q^n\,(1 + 1 - q^{-r} - q^r)}{(1-q)^2}\left(1 + [2]_q\varepsilon\right) \\
&= \frac{\alpha^{2n-2}q^n}{1-q}\left([-r]_q + [r]_q\right)\left(1 + [2]_q\varepsilon\right)
\end{aligned}$$

This completes the proof.

Remember that in the case $r = 1$ in Theorem 2.3, it reduces to Cassini's identity of the q-dual Fibonacci number sequences.

Corollary 2.4. (Cassini identity) For $n \geq 1$, we will have

$$\mathcal{F}_{n+1}\mathcal{F}_{n-1} - \mathcal{F}_n^2 = \frac{\alpha^{2n-2}q^n}{1-q}\left([-1]_q + [1]_q\right)\left(1 + [2]_q\varepsilon\right)$$

Theorem 2.5. (d' Ocagne's identity) For any integer m and n, we have

$$\mathcal{F}_m\mathcal{F}_{n+1} - \mathcal{F}_n\mathcal{F}_{m+1} = \alpha^{m+n+1}\left([m]_q - [n]_q\right)\underline{\alpha}^2\left(1 + \underline{\beta}\right)$$

Proof. Using Equalities 2, 3, 7 and 9, we get

$$\begin{aligned}
&\mathcal{F}_m\mathcal{F}_{n+1} - \mathcal{F}_n\mathcal{F}_{m+1} \\
&= \alpha^{m-1}\left([m]_q\,\underline{\alpha} + (\alpha q)^m\underline{\beta}\right)\left(\alpha^n[n]_q\,\underline{\alpha} + (\alpha q)^{n+1}\underline{\beta}\right) \\
&\quad -\alpha^{n-1}\left([n]_q\,\underline{\alpha} + (\alpha q)^n\underline{\beta}\right)\left(\alpha^m[m]_q\,\underline{\alpha} + (\alpha q)^{m+1}\underline{\beta}\right) \\
&= \alpha^{m+n-1}\left(\frac{q^n - q^m}{1-q}\right)\underline{\alpha}^2 + \alpha^{m+n}(q^m - q^n)\underline{\alpha}\underline{\beta} \\
&= \frac{\alpha^{m+n}}{\alpha}\left([m]_q - [n]_q\right)\underline{\alpha}^2 + \alpha^{m+n}\left([n]_q - [m]_q\right)\underline{\alpha}\underline{\beta} \\
&= \frac{\alpha^{m+n}}{\alpha}\left([m]_q - [n]_q\right)\underline{\alpha}^2\left(1 - \underline{\beta}\right)
\end{aligned}$$

Theorem 2.6. For positive integers m, r and s with $m \geq r$ and

$m \geq s$, then the following holds between the q-dual Fibonacci number sequences and the q-dual Lucas number sequences

$$\mathcal{L}_{m+r}\mathcal{F}_{m+s} - \mathcal{L}_{m+s}\mathcal{F}_{m+r} = 2q^m\alpha^{2m+r+s-1}\left([s]_q - [r]_q\right)\left(1 + [2]_q\varepsilon\right)$$

Proof. By using Equalities 2, 3, 7 and 9, also doing necessary calculations, we will have

$$\begin{aligned}
&\mathcal{L}_{m+r}\mathcal{F}_{m+s} - \mathcal{L}_{m+s}\mathcal{F}_{m+r} \\
&= \left(\frac{\alpha^{m+r}[2m+2r]_q}{[m+r]_q}\underline{\gamma} + \alpha^{m+r+1}(1-q)\underline{\beta}\right)\left(\alpha^{m+s-1}[m+s]_q\,\underline{\alpha} + (\alpha q)^{m+s}\underline{\beta}\right) \\
&\qquad - \left(\frac{\alpha^{m+s}[2m+2s]_q}{[m+s]_q}\underline{\gamma} + \alpha^{m+s+1}(1-q)\underline{\beta}\right) \\
&= 2q^m\alpha^{2m+r+s-1}\left(\frac{q^r - q^s}{1-q}\right)\underline{\alpha}\,\underline{\gamma} \\
&= 2q^m\alpha^{2m+r+s-1}\left(\frac{q^r - 1 + 1 - q^s}{1-q}\right)\underline{\alpha}\,\underline{\gamma} \\
&= 2q^m\alpha^{2m+r+s-1}\left([s]_q - [r]_q\right)\left(1 + [2]_q\varepsilon\right)
\end{aligned}$$

3. q- Dual Fibonacci and Lucas Polynomial Sequences

In this section, we define q-dual polynomial sequences which generalizes q-polynomial sequences $\mathrm{F}_n(t)$ and $\mathrm{L}_n(t)$. We obtain the Binet formulas for q-dual polynomial sequences. Moreover, we give some properties and identities for these quantum dual polynomial sequences

Definition 3.1. For $p(t)$ and $r(t)$ dual component polynomials, the q-polynomial sequences $\mathrm{F}_n(t)$ and $\mathrm{L}_n(t)$ are provided as follows:

$$\begin{cases} \mathrm{F}_{n+2}(t) = p(t)\mathrm{F}_{n+1}(t) - r(t)\mathrm{F}_n(t) \\ \mathrm{L}_{n+2}(t) = p(t)\mathrm{L}_{n+1}(t) - r(t)\mathrm{L}_n(t) \end{cases} \qquad (10)$$

Here, the initial conditions are $\mathrm{F}_0(t)=0$, $\mathrm{F}_1(t)=1$, $\mathrm{L}_0(t)=2$, and $\mathrm{L}_0(t)=p(t)$, respectively.

Clssify the q-dual polynomial squences $\mathrm{F}_n(t)$ and $\mathrm{L}_n(t)$
acording to the given the polynomials $p(t)$ and $r(t)$ values,
repectively.

1. Assume that $p(t) = aq + 1$ and $r(t) = a^2 q$ are constant polynomials, we obtain as follows:

$$\begin{cases} \mathrm{F}_{n+2}(t) = (aq+1)\mathrm{F}_{n+1}(t) - a^2 q\, \mathrm{F}_n(t) \\ \mathrm{L}_{n+2}(t) = (aq+1)\mathrm{L}_{n+1}(t) - a^2 q \mathrm{L}_n(t) \end{cases}$$

2. Assume that $p(t) = \lambda(s)$ and $r(t) = -1$ are not constant polynomials, then we have

$$\mathrm{F}_{n+2}(t) = \lambda(s)\mathrm{F}_{n+1}(t) + \mathrm{F}_n(t)$$

wth the initial conditions $\mathrm{F}_0(t) = 0$, $\mathrm{F}_1(t) = 1$. From Equality 10, roots of $x^2 - p(t)x + r(t) = 0$ are

$$\alpha(x) = \frac{p(t) + \sqrt{p^2(t) - 4r(t)}}{2}$$

ad

$$\beta(x) = \frac{p(t) - \sqrt{p^2(t) - 4r(t)}}{2}$$

Then, the Binet formulas for q-polynomials $\mathrm{F}_n(t)$ and $\mathrm{L}_n(t)$ are

$$\mathrm{F}_n(t) = \frac{\alpha^n(x) - \beta^n(x)}{\alpha(x) - \beta(x)}$$

and

$$\mathrm{L}_n(t) = \alpha^n(x) + \beta^n(x)$$

Defintion 3.2. Let $\mathcal{F}_n(t)$ and $\mathcal{L}_n(t)$ be dual polynomial sequences Then, the folowing recurrence relations are obtained

$$\mathcal{F}_n = \mathrm{F}_n(t) + \varepsilon \mathrm{F}_{n+1}(t) \qquad (11)$$

and

$$\mathcal{L}_n(t) = \mathrm{L}_n(t) + \varepsilon \mathrm{L}_{n+1}(t) \qquad (12)$$

FromEquality 11, the initial conditions of the q-dual Fibonacci polynomial sequences are

$$\mathcal{F}_0 = \mathrm{F}_0(t) + \varepsilon \mathrm{F}_1(t) = \varepsilon$$

and

$$\mathcal{F}_1 = \mathrm{F}_1(t) + \varepsilon \mathrm{F}_2(t) = 1 + p(t)$$

From Euality 12, the initial conditions of the q-dual Lucas polynomial sequeces are

$$\mathcal{L}_0(t) = \mathrm{L}_0(t) + \varepsilon \mathrm{L}_1(t) = 2 + \varepsilon p(t)$$

and

$$\mathcal{L}_1(t) = \mathrm{L}_1(t) + \varepsilon \mathrm{L}_2(t)$$

$$= p(t) + \varepsilon\left(p^2(t) - r(t)\right)$$

where ε is dual unit.

Theoem 3.3. The Binet formula of the q-dual polynomials $\mathcal{F}_n(t)$ and $\mathcal{L}_n(t)$ are

$$\mathcal{F}_n(t) = \frac{\alpha^n(x)\underline{\alpha}(x) - \beta^n(x)\underline{\beta}(x)}{\alpha(x) - \beta(x)}$$

and

$$\mathcal{L}_n(t) = \alpha^n(x)\underline{\alpha}(x) + \beta^n(x)\underline{\beta}(x)$$

Here,

$$\underline{\alpha}(x) = 1 + \alpha(x)\varepsilon$$

and

$$\underline{\beta}(x) = 1 + \beta(x)\varepsilon$$

Proof. For the q-dual polynomials $\mathcal{F}_n(t)$ and $\mathcal{L}_n(t)$, the proof is calculated similarly to the theorem 2.2.

By doing some calculations, the following relations can be obtained

$$\mathcal{F}_1(t) - \alpha(x)\mathcal{F}_0(t) = \underline{\beta}(x)$$

$$\mathcal{F}_1(t) - \beta(x)\mathcal{F}_0(t) = \underline{\alpha}(x)$$

$$\mathcal{L}_1(t) - \alpha(x)\mathcal{L}_0(t) = (\beta(x) - \alpha(x))\underline{\beta}(x)$$

$$\mathcal{L}_1(t) - \beta(x)\mathcal{L}_0(t) = (\alpha(x) - \beta(x))\underline{\alpha}(x)$$

4. q-Dual Fibonacci and Lucas Function Sequences

In this section, we define quantum dual function sequences or briefly q-dual function sequences in the quantum calculus.

Definition 4.1. Assume that $p(t)$ is an arbitrary function. Its q-derivative operator is shown by

$d_q p(t) = p(qt) - p(t)$ (Kac, 2002).

Note that in particular $d_q(t) = (q-1)t$,

$$\lim_{q\to 1} D_q p(t) = \lim_{q\to 1} \frac{p(qt)-p(t)}{(q-1)t} = \frac{d_q(t)}{dt} \qquad (13)$$

were $q \neq 1$. The n^{th} q-dual Fibonacci function sequences is given by $\mathcal{F}_n(t) = \mathrm{F}_n(t) + \mathrm{F}_{n+1}(t)\varepsilon$, where $\mathrm{F}_n(t)$ is the n^{th} q-Fibonacci function sequences and ε is dual unit. Then, q-derivative is

$$\begin{cases} D_q\mathcal{F}_n(t) = D_q(\mathrm{F}_n(t) + \mathrm{F}_{n+1}(t)\varepsilon) \\ \qquad\qquad = D_q\mathrm{F}_n(t) + D_q\mathrm{F}_{n+1}(t)\varepsilon \end{cases} \qquad (14)$$

Here $D_q\mathrm{F}_n(t)$ demonstrate the derivative of $\mathrm{F}_n(t)$

Proposition 4.2. For the integer $n > 0$, if $\mathrm{F}_n(t) = (t-\mu)_q^n$ is selected, q-derivative of the function sequences $\mathrm{F}_n(t)$ can be given in the form

$D_q\mathrm{F}_n(t) = [n]_q\mathrm{F}_{n-1}(t)$,

where μ is constant.

Proof. From Equalities 13 and 14, we compute q-derivative of the function sequences $\mathrm{F}_n(t)$, we obtain

$$\begin{aligned} D_q\mathrm{F}_n(t) &= \frac{\big(q(t-\mu)\big)^n - (t-\mu)^n}{(q-1)(t-\mu)} \\ &= \frac{(q^n-1)(t-\mu)^{n-1}}{(q-1)} \\ &= [n]_q\mathrm{F}_{n-1}(t) \end{aligned}$$

and the derivative of the n^{th} q-dual Fibonacci function sequences is

$$\begin{aligned} D_q\mathcal{F}_n(t) &= [n]_q\mathrm{F}_{n-1}(t) + [n+1]_q\mathrm{F}_n(t)\varepsilon \\ &= [n]_q\mathrm{F}_{n-1}(t) + q^n[1]_q\,\varepsilon \end{aligned}$$

Example 4.3. For the integer $n < 0$, consider the function $\mathrm{F}_{-n}(t) = (t - \mu)_q^{-n}$, we calculate the q-derivative of $\mathrm{F}_n(t)$ and $\mathcal{F}_n(t)$.

Proof. By using Definition 3.1 and Equality 13, we can write

$$D_q \mathrm{F}_{-n}(t) = \frac{\big(q(t-\mu)\big)^{-n} - (t-\mu)^{-n}}{(q-1)(t-\mu)}$$

$$= \frac{(q^{-n}-1)(t-\mu)^{-n-1}}{(q-1)}$$

$$= [-n]_q \mathrm{F}_{-(n+1)}(t)$$

$$= -\frac{[n]_q}{q^n} \mathrm{F}_{-(n+1)}(t)$$

and doing necessary calculations, $D_q \mathcal{F}_{-n}(t)$, we get

$$D_q \mathcal{F}_{-n}(t) = -\frac{[n]_q}{q^n} \mathrm{F}_{-(n+1)}(t) - \frac{[n+1]_q}{q^{n+1}} \mathrm{F}_{-(n+2)}(t)\varepsilon$$

5. Conclusion

In the present paper, the q-dual number sequences have been introduced by using the notations from quantum calculus. First of all the recurrence relation for these numbers have been obtained. Then, some fundamental identities are obtained such as the Binet formulas, the Cassini, the Catalan, and the d'Ocagne identities. Furthermore, the new polynomials and functions which are called q-dual Fibonacci and q-dual Lucas polynomial and function sequences. Also, we have presented some properties and identities for these polynomial and function sequences.

References

[1] Kotelnikov, A. P. (1895). Screw Calculus and Some Applications to Geometry and Mechanics. Kazan, Russia: Annals of the Imperial University of Kazan.

[2] Study, E. (2022). Geometry der Dynamen. German edition, Legare Street Press, Berlin, Germany.

[3] Guggenheimer, H. W. (2012). Differential Geometry. Dover Publications, New York.

[4] Fischer, I. (1998). Dual Number Methods in Kinematics, Statics and Dynamics. New York, USA: CRC Press,.

[5] Nurkan, S. K., & Guven. I. A. (2015). Dual Fibonacci Quaternions, Advances in Applied Clifford Algebras, 25, 403–414.

[6] Angeles, J. (1998). The Application of Dual Algebra to Kinematic Analysis. Computational Methods in Mechanical Systems: Mechanism Analysis, Synthesis, and Optimization, NATO ASI Series, Springer Berlin Heidelberg, 161, 3–32.

[7] Horadam, A. F. (1961). A generalized Fibonacci sequence. The American Mathematical Monthly, 68(5), 455-459.

[8] Horadam, A. F. (1963). Complex Fibonacci numbers and Fibonacci quaternions. The American Mathematical Monthly, 70(3), 289–291.

[9] Koshy, T. (2018). Fibonacci and Lucas Numbers with Applications. 1, John Wiley Sons.

[10] Koshy, T. (2019). Fibonacci and Lucas Numbers with Applications, Volume 2, John Wiley Sons.

[11] Maynez, A. G., & Acosta A. P. (2016). A Method to Construct Generalized Fibonacci Sequences, Journal of Applied Mathematics, 2016, ID 4971594, http://dx.doi.org/10.1155/2016/4971594.

[12] Nalli, A., & Haukkanen, P. (2009). On Generalized Fibonacci and Lucas Polynomials, Chaos Solitons Fractals, 42, 3179-3186.

[13] Oduol, F., & Okoth, I. O. (2020). On generalized Fibonacci numbers. Communications in Advanced Mathematical Sciences, 3(4), 186–202.

[14] Vorobiov, N. (1974). Numeros De Fibonacci, Editorial MIR, Moscu, URSS.

[15] Kac, V., & Cheung, P. (2002). Quantum Calculus, Springer.

[16] Kome, S., Kome, C. & Catarino, P. (2022). Quantum Calculus Approach to the Dual Bicomplex Fibonacci and Lucas Numbers. Journal of Mathematical Extension, 6(2), 1-17.

[17] Stum, B., & Quiros, A. (2013). On Quantum Integers and Rationals, Hal Open Science 649/13022, 107-130.

[18] Akkus, I. & Kızılaslan, G. (2019). Quaternions: Quantum Calculus Approach with Applications, Kuwait Journal of Science 46(4), 1-13.

Chapter 4

Some Remarks on the 14th Sustainable Development Goal in Türkiye

Nurcihan Hacıoğlu Doğru[1]

Abstract

Marine and oceans are important resources that provide numerous services such as sustaining life, food supply, clean energy, and transportation. However, these valuable resources, along with the habitats they support, are subjected to various anthropogenic pressures, including climate change, population growth, and industrial intensity. In order to create social, economic, and ecological value, sustainable utilization of the sea and its resources can only be achieved through the development and implementation of management strategies based on marine sciences. Recognizing the significance of marine and ocean conservation, the United Nations adopted a framework consisting of 17 Sustainable Development Goals (SDGs) in 2015, which includes the enhancement of sustainable use and conservation of seas and oceans as a priority goal. Effective strategies to combat overfishing, ocean acidification and worsening coastal eutrophication have been emphasized. Türkiye, being a country surrounded by three seas and rich in water resources, is also highly affected by water pollution. Industrial activities, agricultural use, urbanization, population growth, and hydrological conditions contribute to water pollution, making it a significant environmental issue in the country. In this context, the aim of this study is to examine the issues related to seas and marine resources in Türkiye in line with the 2030 Sustainable Development Goals and provide a fresh perspective on what has been done and what needs to be done in the context of Goal 14. The objective is to develop science-based strategies, intensify research capacity, and provide information on the necessary actions to be taken.

1 Prof. Dr., Çanakkale Onsekiz Mart University, Faculty of Sciences, Department of Biology, Çanakkale, Türkiye, nurcihan.n@gmail.com ,ORCID: 0000-0002-5812-9398

https://doi.org/10.58830/ozgur.pub252.c1215

1. Introduction

The emergence of contemporary environmental movements in the 1960s and 1970s necessitated the examination of the concepts of development and environment together (Scoones, 2007). This situation was further advanced in the report known as the Brundtland Report, also referred to as "Our Common Future" (Brundtland, 1987), which introduced the concept of sustainable development to a new level. In this report, sustainable development, defined as meeting the needs of the present without compromising the ability of future generations to meet their own needs, emerged as a concept that encompasses various disciplines in today's world (Thiele, 2016). Today, sustainability and sustainable development have become indispensable concepts for modern societies, and they have become the guiding principles in the actions and decisions of governments, communities, organizations, and individuals in the modern world (Caradonna, 2014).

Sustainable development is an approach to development that aims to achieve social and economic progress in harmony with environmental sustainability. This approach involves using resources efficiently and effectively to meet the needs of current generations while considering the needs of future generations. Sustainable development is addressed in three fundamental dimensions: economic, social, and environmental. In the economic dimension, sustainable development seeks to promote economic growth while reducing inequalities, eradicating poverty, and ensuring the equitable distribution of resources. In the social dimension, the focus is on improving human well-being and safeguarding basic human rights such as education, health, equality, and gender justice. In the environmental dimension, the objectives include sustainable management of natural resources, conservation of biodiversity, combating climate change, and reducing environmental impacts. What sets sustainable development apart from traditional environmental conservation approaches is its proactive and holistic focus on long-term evolving dynamic processes (Portney, 2015; Bozoğlu and Ciğerim, 2022). It considers the interconnections between economic, social, and environmental aspects and seeks to promote a balanced and integrated approach for a sustainable future.

After sustainable development came to the agenda of countries, the question of how countries would achieve this development emerged. How countries will make a plan and program, how they will organize their investments and what should be done for sustainability has become an important topic of discussion. At this point, various targets have emerged and it has been stated that countries can achieve sustainable development

by realizing these goals (Yıldırım and Yıldırım, 2020). The latest goals for the countries of the world to reach sustainable development are in the form of "2030 Sustainable Development Goals". The "2030 Sustainable Development Goals", which contain 17 basic goals and were adopted in 2015, are seen as a historical global achievement.

Oceans and seas, which hold a significant place in our daily lives, serve as the locomotive of the blue economy and blue growth, encompassing global climate regulation, maritime transportation, marine tourism, health, and fisheries. Therefore, the oceans, seas, and underwater life should be on the agenda of all countries aiming for sustainable world goals. This priority is particularly crucial for countries with coastlines. This priority has led to the inclusion of the oceans and seas in the "2030 Sustainable Development Goals" and their identification with Goal 14 (Global Sustainable Development Report, 2023). SDG 14 focuses on the sustainable use and conservation of oceans and seas, addressing issues such as overfishing, ocean acidification, and coastal eutrophication. It aims to protect marine and ocean biodiversity and encourages countries to support research financing in this field. It is a crucial goal within the Sustainable Development Goals framework, aiming to combat the negative impacts of overfishing, ocean acidification, and coastal eutrophication, and to promote the preservation of marine and ocean biodiversity.

Türkiye is a country surrounded by seas on three sides and connected to oceans through straits. It has four different sea systems: the Sea of Marmara, the Mediterranean Sea, the Black Sea, and the Aegean Sea. The diverse ecological characteristics of its seas and inland waters have resulted in high biodiversity. This situation highlights the importance of preserving, developing, and sustainably managing water resources, especially marine resources, for the country. Türkiye's rich marine and inland water resources play a vital role in various aspects of the country's economy and society. They support sectors such as fisheries, maritime transportation, tourism, energy, and provide important ecological services. However, the sustainable use and effective management of these resources are essential to ensure their long-term viability and to avoid overexploitation or degradation. Efforts are made to protect and conserve marine and inland water ecosystems in Türkiye, including the establishment of marine protected areas, the implementation of sustainable fishing practices, and the promotion of responsible tourism. Furthermore, water resource management plans and regulations are developed to ensure the sustainable utilization of these valuable resources while considering ecological, economic, and social factors. The sustainable management of marine and inland water resources in Türkiye is not only

important for the country's own well-being but also contributes to the global efforts for the conservation and sustainable use of these vital ecosystems.

The aim of this study is to project the current situation in Türkiye's seas, as well as provide information on the progress made so far and the necessary actions and recommendations to be taken in line with the Sustainable Development Goals (SDGs). It focuses on the development of strategies, planning, and regulations in pursuit of sustainable development.

2. Physical Structure of the Country's Seas

Türkiye, surrounded by the Mediterranean, Black, and Aegean Seas, has a coastline of 8,333 kilometers (including islands), making it one of the countries with the longest coastal strip in Europe. The distribution of this coastline is approximately 33.66% in the Aegean Sea, 20.34% in the Black Sea, 20.07% in the Mediterranean, and 11.20% in the Sea of Marmara. Approximately 65% of the country's population is settled along the coast (Dölgen et al., 2006).

The Black Sea, with a surface area of 496,064 km², has an average depth of 1,197 meters and its deepest point reaches 2,245 meters. The continental shelf along the Turkish coastline of the Black Sea is narrow, with a coastal length of 1,795 kilometers. The salinity of the Black Sea is 18 parts per thousand, and it is known for having the world's largest hydrogen sulfide reserves. Therefore, there is no life below depths ranging from 150 to 200 meters. More than half of the fish caught in Türkiye come from this sea, making it economically significant for the country. The Black Sea also holds importance in terms of maritime transportation due to its coastal ports (Akengin et al., 2016).

The Sea of Marmara, with a surface area of 11,350 km², is the smallest sea in Türkiye. It separates the Asian and European parts of Türkiye and has the characteristic of being an inland sea. The deepest point of the Sea of Marmara is 1,238 meters. It has a wide continental shelf. It is connected to the Black Sea through the Istanbul Strait and to the Aegean Sea through the Çanakkale Strait. The coastline of the Sea of Marmara is 1,275 kilometers long. It holds importance due to fishing and port activities. The Turkish Straits System (Bosphorus and Çanakkale) are significant in terms of upper and lower currents. The Black Sea, which receives heavy rainfall and is the outlet for numerous rivers, is 40 cm higher in elevation compared to the Sea of Marmara. The excess water flows from the Istanbul Strait to the Sea of Marmara and then through the Çanakkale Strait to the Aegean Sea. The salinity of the Aegean Sea is higher compared to the Marmara and Black

Seas. The denser waters flow as bottom currents through the straits towards the Black Sea.

The Istanbul Strait, which connects the Sea of Marmara to the Black Sea, is the narrowest and one of the busiest waterways in the world. The widest part of the Istanbul Strait is 3,600 meters, located in the north between the Anadolu Lighthouse and Turkeli Lighthouse. The narrowest part is 698 meters, between the Anadolu Fortress and the Rumeli Fortress. The depth of the Istanbul Strait varies between 30 and 110 meters. This strait holds significant strategic importance and enhances Türkiye's geopolitical position. Istanbul Port serves as a gateway for Türkiye's exports and imports, connecting it to the rest of the world.

The Çanakkale Strait, which connects the Sea of Marmara to the Aegean Sea, has its widest point at the southern boundary, measuring 3,600 meters, and its narrowest point is between Çanakkale and Kilitbahir, with a width of 1,200 meters. The depth of the strait varies between 50 and 140 meters. The Çanakkale Strait holds strategic importance as it connects the Marmara and Aegean seas. Similar to the Istanbul Strait, it is also a busy waterway. Both the Istanbul and Çanakkale straits are significant for fishing activities as well (Taşlıgil, 2004).

The Mediterranean, which is the largest sea surrounding Türkiye, covers an area of 2,500,000 km^2. It is connected to the Atlantic Ocean through the Strait of Gibraltar and to the Indian Ocean through the Suez Canal. The average depth of the Mediterranean is 1,400 meters, with the deepest point reaching 4,400 meters. Apart from the İskenderun and Mersin Gulfs, the continental shelf of the Mediterranean is quite narrow. The salinity level is 36 parts per thousand. Along the Turkish coastline, temperatures in the Mediterranean range from 14°C to 34°C. The length of the Turkish coastline along the Mediterranean is approximately 1,577 km. The Mediterranean Sea holds significant importance, particularly in terms of marine tourism. It also plays a crucial role in port activities and maritime transportation (Atalay, 2011).

The Aegean Sea, located between Türkiye and Greece, has a total area of 214,000 km^2 including the islands. There are approximately 3,000 islands in the Aegean Sea. It is the sea with the longest coastline for Türkiye. The length of the Turkish coastline along the Aegean Sea is 2,805 km, accounting for approximately one-third of the total length of our coasts. The Aegean region has numerous bays, gulfs, and peninsulas due to its indented coastline. The salinity level in the Aegean Sea is 25 parts per thousand. It holds significant importance in terms of fishing and port activities. It also contributes significantly to the Turkish economy through marine tourism (Başeren, 2006).

Our seas, besides their impact on our country's climate and strategic importance, are also significant economic resources. They hold great potential in terms of harvested seafood, maritime transportation, and natural resources on the seabed. This potential carries significant importance for the future of our country.

3. Sustainable Blue Economy for Marine Ecosystems

The concept of blue economy was first introduced by Pauli (2010), emphasizing that the blue economy creates wealth in terms of sustainability and therefore, the balance between environmental and economic goals needs to be achieved.

The blue economy conceptualizes the oceans as "development areas" that integrate conservation, sustainable use, oil and mineral extraction, bio-research, sustainable energy production, and marine transportation (United Nations, 2019). The blue economy is seen as a comprehensive development approach that promotes growth by emphasizing the efficient and optimal use of marine resources without compromising sustainability elements (Mohanty, 2019). At the core of the global blue economy concept lies the provision of healthy oceans to serve future generations while ensuring economic growth derived from the oceans (Atakpa, 2018). Table 1 further elucidates the concept of the blue economy and provides a detailed overview of its components (World Bank, 2016; Toplu-Yılmaz, 2021).

Table 1. The scope of the blue economy (abbreviated from Toplu-Yılmaz, 2021)

Type of activity (nature of business)	**Activities within Subcategories**
Collection and trade of marine resources	Seafood harvesting
	Utilization of marine organisms for pharmaceutical and chemical applications
Extraction and utilization of non-renewable resources from the sea	Mining of minerals
	Energy resource extraction
	Freshwater production
The use of renewable natural resources (wave, wind, tidal energy)	Renewable energy generation offshore
Trade within and across oceans	Transportation and trade
	Coastal development
	Tourism and recreation
Indirect impact on the economy and the environment	Carbon capture
	Coastal protection
	Waste management and industrial infrastructure
	Presence of biodiversity

As can be seen in the table, the blue economy encompasses numerous activities such as tourism in the seas and coastal regions, fishing, extraction of marine resources for cosmetics and medicines, maritime transport, production of shipbuilding and maritime equipment, extraction of oil and minerals, carbon sequestration and coastal recreation (Toplu-Yılmaz, 2021).

The evaluation of our seas in terms of the blue economy involves the sustainable and efficient utilization and management of marine resources. The blue economy is an approach that aims to maximize the economic potential of marine and ocean resources while also targeting environmental sustainability and the conservation of ecosystems. Türkiye has significant potential for a thriving blue economy due to its surrounding seas and extensive coastline. Various sectors such as fisheries, marine tourism, maritime transportation, energy resources, marine mining, water sports, and underwater resources form the key components of the blue economy in our seas.

Fisheries and aquaculture sectors are significant sources of income derived from the rich fish and seafood resources in Türkiye's seas. They provide employment opportunities and contribute to exports.

Marine tourism also holds great economic value for Türkiye. Our beautiful beaches, bays, and islands attract tourists who prefer sea, sun, and beach vacations. These tourism activities contribute to increased tourism revenue and the development of local economies.

Maritime transportation plays an important role due to Türkiye's strategic location. Waterways such as the Istanbul and Çanakkale Strait serve as vital transit points for maritime trade and heavy ship traffic. Our ports are the lifelines of foreign trade and the logistics sector.

Furthermore, our seas also hold potential for energy resources, particularly wind and solar energy. Projects related to offshore wind and solar energy contribute to clean energy production and energy security.

Marine mining also plays a significant role within the blue economy of our seas. Resources such as minerals, oil, and natural gas found in the seabed can be economically evaluated and contribute to the country's economy.

The evaluation of Türkiye's seas in terms of the blue economy requires the sustainable utilization of this potential and the preservation of marine resources. Measures such as sustainable fishing practices, conservation of marine ecosystems, management of environmental impacts, and marine spatial planning can ensure the successful management of the blue economy.

Goal 14 of the Sustainable Development Agenda 2030 aims to promote sustainable blue economy and its objectives include (TCCSBB, 2019);

14.1 By 2025, prevent and significantly reduce all forms of marine pollution, including marine debris and nutrient pollution, particularly from land-based activities.

14.2 By 2020, sustainably manage and protect marine and coastal ecosystems, taking actions to restore and enhance their resilience, in order to achieve healthy and productive oceans, addressing the adverse impacts on these ecosystems.

14.3 By 2030, minimize and address the impacts of ocean acidification, including through enhanced scientific cooperation at all levels.

14.4 By 2020, effectively regulate harvesting and end overfishing, illegal, unreported, and unregulated (IUU) fishing, and destructive fishing practices, and implement science-based management plans, in order to restore fish stocks in the shortest time feasible, at least to levels that can produce maximum sustainable yield as determined by their biological characteristics.

14.a Enhance the conservation and sustainable use of oceans and their resources by implementing international law as reflected in the United Nations Convention on the Law of the Sea (UNCLOS), which provides the legal framework for the conservation and sustainable use of oceans and their resources, in accordance with the Intergovernmental Oceanographic Commission Criteria and Guidelines on the Transfer of Marine Technology, in order to increase scientific knowledge, develop research capacity, and transfer marine technology to developing countries, particularly Small Island Developing States (SIDS) and Least Developed Countries (LDCs), and promote the contribution of marine biodiversity to their development.

14.b Provide access for small-scale artisanal fishers to marine resources and markets.

14.c Enhance the conservation and sustainable use of oceans and their resources, as reflected in UNCLOS, which sets out the legal framework for the conservation and sustainable use of oceans and their resources, as stated in paragraph 158 of the document "The Future We Want."

In our country, the most important and highest revenue-generating component of the blue economy is fishing activities, which fall under the category of harvesting and trade of marine resources. According to the Turkish Statistical Institute (TÜİK) data for 2022, the production of aquatic products increased by 6.2% compared to the previous year, reaching

849,808 tons. Of this production, 30% consists of marine fish obtained through fishing, 5.6% consists of other marine products obtained through fishing, 3.9% consists of inland fish obtained through fishing, and 60.6% consists of aquaculture products (Figure 1).

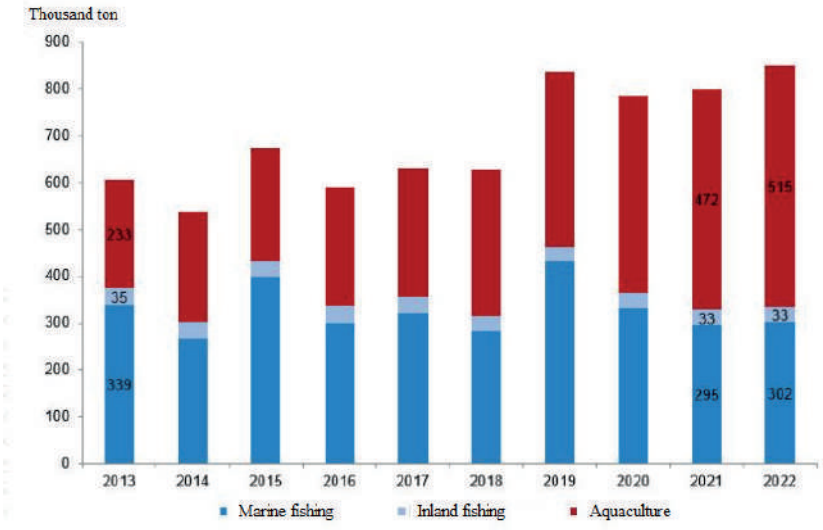

Figure 1: Aquaculture production, 2013-2022 (TÜİK, 2022)

In 2022, the production of fishery products increased by 2.1%, with a total production of 335,003 tons through fishing activities. Aquaculture production reached 514,805 tons, while marine fisheries increased by 2.3% compared to the previous year, and inland fisheries increased by 0.4%. The quantity of harvested marine fish reached 254,535 tons, with the most commonly caught species being anchovy (125,980 tons), bonito (49,892 tons), and sardine (16,729 tons). Aquaculture production increased by 9.1% in 2022 compared to the previous year. Of the total aquaculture production, 368,742 tons were from marine aquaculture, and 146,063 tons were from inland aquaculture. The most important fish species cultivated were trout with 145,649 tons in inland aquaculture, and sea bass with 156,602 tons and sea bream with 152,469 tons in marine aquaculture (TÜİK, 2022).

In addition to fishing activities, there is a need for the development of all the activity areas mentioned in Table 1 in our country's seas. However, we believe that special emphasis should be placed on marine biotechnology. Marine biotechnology is undergoing rapid development worldwide and

has reached an exciting stage in areas such as aquaculture, biochemistry, genetics, genomics, health, cosmetics, environment, bioenergy, and more. Genomic and proteomic methods provide valuable information for the sustainability of marine ecosystems and the exploration and utilization of marine biodiversity. Although marine biotechnology has a wide range of applications, from biomedical to environmental fields, its importance is just starting to be recognized in our country (TÜDAV, 2017).

In order to successfully implement the blue economy and make significant contributions to the country's economy, it is important to pay attention to issues such as food security, marine pollution, and overfishing in fishing activities. To achieve this, the following measures can be taken:

Food security: Emphasis should be placed on the production of healthy and reliable food in fishing activities. Good agricultural practices, hygiene standards, and traceability measures should be implemented. Fishermen should handle and store their catch properly.

Marine pollution: Environmental protection measures should be implemented to prevent marine pollution. Discharge of industrial waste into the sea should be controlled, and wastewater treatment facilities should be used to keep our seas clean. Additionally, recycling and awareness campaigns are important for reducing plastic and other waste in the oceans.

Overfishing: Preventing overfishing is essential for the sustainability of fish stocks. Fishing activities should be carried out using sustainable fishing methods that allow for the reproduction of fish populations. Regulations such as laws, quotas, and fishing seasons can help control overfishing.

In this field, plans and strategies focused on blue growth should be developed by following the incentives provided by the European Union and similar institutions.

Priority should be given to marine biotechnology studies, and various institutions should be supported through universities to promote research and development in this area.

These measures will ensure the sound management of the blue economy and the sustainable use of marine resources. This will lead to both economic development and the preservation of the ecosystems in our seas.

4. Pollution Problem in Turkish Seas

Marine systems, whose economic and ecological importance is increasingly due to their high nutrient, mineral and energy content, are threatened by a

variety of pollutants that reach through the atmosphere, coastlines, lakes and rivers (Doğan-Sağlamtimur and Subaşı, 2018). In particular, maritime transport, accidents, industrial activities, tourism, urbanization and high waste discharge cause a decrease in the amount of oxygen in sea water and have become an important threat to the life of marine organisms (İncaz et al., 2005; Ecel, 2007). Marine pollution occurs when the capacity to dispose of pollutants accumulated in water is exceeded (Artüz, 1992; Nauke and Holland, 1992; Aras, 2001; Clark, 2001; Güven and Öztürk, 2005; İncaz et al., 2005; Butt, 2007; Zuin et al., 2009).

4.1. Marine pollution from ships

Ship-source pollution is a significant source of marine pollution. The waste, spills, and emissions generated during ship operations can pollute the oceans. This pollution can occur in various forms:

Oil pollution: It occurs when oil contaminates the seas due to fuel transfers, maritime accidents, or leaks from oil tankers. Oil pollution can cause serious harm to marine life and disrupt ecosystems.

Chemical pollution: During the transportation of chemicals on ships, leaks or the discharge of chemical waste into the sea can result in chemical pollution. This type of pollution can directly impact marine life and cause damage to aquatic ecosystems.

Wastewater pollution: Discharging wastewater from ships, including waste from toilets, sinks, and kitchens, can lead to wastewater pollution. The pollutants contained in this waste can degrade water quality and affect marine life.

Air pollution: Ship engines emit harmful gases and particles into the atmosphere. These emissions can contribute to air pollution and environmental impacts in coastal areas near the seas.

In Türkiye, as well as globally, marine pollution and issues related to coastlines are prominent concerns. The Black Sea, Aegean Sea, and Mediterranean Sea are heavily polluted. Maritime transportation, accidents, the widespread production and use of oil and its derivatives, and discharges play a significant role in the industrial pollution of the seas (Doğan-Sağlamtimur and Subaşı, 2018).

According to data from the Turkish Statistical Institute (DİE), more than 20,000 ships visit ports in Türkiye each year, including multiple visits by the same ship within a year (Environmental Inspection Report, 2002). Hazardous substances carried by ships consist of approximately 70% (94.8

million tons) crude oil, 26% (34.2 million tons) petroleum products, and the remaining 4% (6 million tons) liquefied gases and chemical products (Orhon et al., 2008).

Pollution caused by ships is a comprehensive and complex issue. Initially, maritime pollution is not limited to oil alone. Apart from oil, wastewater, garbage, and other types of waste discharged or discarded from ships can also contribute to marine pollution. The cargo responsible for pollution resulting from maritime accidents is not solely limited to oil or petroleum derivatives. However, when we mention pollution caused by ships, the first thing that comes to mind is typically oil pollution caused by ships. There are two main reasons for oil pollution caused by ships. The first reason is the operation of tankers carrying oil cargo as well as other ships, and the second reason is oil pollution resulting from maritime accidents involving both oil tankers and occasionally non-tanker ships.

Intentional or operational oil pollution, resulting from the deliberate discharge of oil by ships during their operations, constitutes a major component of oil pollution in the seas. Intentional oil pollution, arising primarily from the normal activities of non-tanker ships and especially oil tankers, is based on two main causes. The first cause is the discharge of oil pollution resulting from the emptying of ballast water in tankers, and the second cause is oil pollution arising from the washing of cargo and sometimes fuel tanks. Accidental oil pollution, on the other hand, is actually the type of pollution that attracts the most attention from the international community. In today's world, where tanker capacities have reached unimaginable sizes, maritime accidents resulting from navigation errors, mistakes made by individuals responsible for ship management, and occasionally force majeure events have caused and continue to cause major disasters to the marine environment. The scale of marine pollution in general and, specifically, oil pollution caused by ships has reached alarming levels in recent times, making it a matter of great concern for both coastal states and the international community in terms of pollution prevention (Abdullahzade, 2009).

In the Mediterranean, the increase in the amount of domestic waste based on seasonal population growth due to tourism, industry, and agricultural activities, as well as waste from yacht tourism and petroleum derivatives resulting from maritime transportation, are significant causes of pollution. The Mediterranean accounts for 28% of global oil transportation, and around 20,000 tons of oil per year seep into the Mediterranean due to accidents or negligence from the 60 oil refineries located in its vicinity (Doğan-Sağlamtimur and Subaşı, 2018).

In the Aegean Sea, pollutants primarily reach through residential and industrial waste, wastewater discharges, runoff from precipitation, agricultural and port activities, maritime traffic, and rivers flowing into the sea. With the addition of wastewater discharges from the Turkish coast to the Aegean Sea and the influence of the Çanakkale Strait, the sea is exposed to a pollution load equivalent to a population of nearly 20 million (Doğan-Sağlamtimur and Subaşı, 2018).

The Sea of Marmara is an inland sea that connects the Black Sea to the Aegean and Mediterranean Seas through the Istanbul and Çanakkale Straits, respectively (Dölgen et al., 2006). In terms of size and capacity as a recipient environment for waste materials, the Sea of Marmara has about 100 times less capacity compared to the Mediterranean Sea and 1,000 times less compared to the Black Sea (Akkaya, 2004). The increasing maritime traffic in the Sea of Marmara, along with pollution triggered by the bilge and ballast waters of marine vessels, results in a significant pollution load spreading over a wide area (Doğan-Sağlamtimur and Subaşı, 2018).

The Black Sea in our country receives pollutant loads from various rivers, primarily including the Sakarya, Yeşilırmak, and Kızılırmak, as well as the Danube River, which carries the pollutant load of almost all of Europe. The pollution of the Black Sea is not limited to the sea and rivers; the region is also threatened by environmental pollution (Talınlı & Sarıöz, 2002). Annually, 548 km3 of water flows from the Black Sea to the Sea of Marmara, while only 249 km3 of water flows from the Sea of Marmara to the Black Sea through the bottom current. This indicates that pollution occurring in the Black Sea will have approximately twice the impact on the Sea of Marmara compared to the influence of the Sea of Marmara on the Black Sea (Doğan-Sağlamtimur & Subaşı, 2018).

Marine pollution in the Turkish Straits, which connect the Black Sea and the Mediterranean Sea, is primarily caused by maritime transportation through the Çanakkale and Istanbul Straits. The contribution of pollution from maritime traffic in the Istanbul Strait to the total pollution has been determined to be approximately 10% (Orhon et al., 2008). Records show that a total of 162 significant marine accidents have occurred in Türkiye until today. Out of these accidents, 105 took place in the Istanbul Strait, 35 in the Çanakkale Strait, and 22 in the Sea of Marmara. Among these incidents, 4% were fires, 30% were groundings, 52% were collisions between two vessels, 72% were collisions with docks or waterfront mansions, and 10% occurred due to other reasons. It has been noted that there are six accidents per 1 million miles of passage through the Istanbul Strait, which is twice the

number of accidents that occur in the Suez Canal (Doğan-Sağlamtimur and Subaşı, 2018).

To prevent and reduce ship-source pollution, various measures have been implemented. International maritime organizations have established standards and guidelines to control ship emissions, regulate waste management, and prevent marine pollution. These measures include the proper management of ship waste, promotion of recycling, use of wastewater treatment systems, and monitoring of ship operations.

International cooperation is crucial in combating ship-source pollution. Collaboration and awareness-raising activities should be conducted among the maritime sector, shipowners, port operators, governments, and non-governmental organizations. Additionally, innovations such as the development of ship technologies and the use of eco-friendly fuels can be effective in addressing marine pollution.

4.2. Domestic Waste and Land-Based Marine Pollution

Domestic waste and land-based marine pollution occur when waste from land areas and coastal settlements reaches the sea. This type of pollution can result from various factors and can cause significant harm to marine ecosystems. Here are some examples of domestic waste and land-based marine pollution:

Sewage discharge: Urban areas have sewage systems that collect domestic waste and used water and discharge it into the sea. However, in cases where sewage systems are inadequate or faulty, waste can directly reach the sea or coastlines. This can lead to water pollution and harm to aquatic life.

Beach and coastal pollution: Touristic areas or coastal settlements can experience pollution due to litter, plastic waste, and other land-based debris left by visitors or the local population. Beach and coastal pollution disrupts marine ecosystems, damages the food sources of marine organisms, and leads to the degradation of coastal ecosystems.

Agricultural pollution: During agricultural activities, fertilizers, agricultural chemicals, and irrigation water can reach the sea through rivers. Agricultural pollution can result in the excessive accumulation of nutrients like nitrates and phosphates in aquatic ecosystems. This impairs water quality, reduces oxygen levels in the seawater, and negatively affects marine life.

Industrial pollution: Wastewater from industrial facilities, factory discharges, and industrial waste can reach the sea. These wastes may contain chemicals, heavy metals, toxic compounds, and other pollutants. Industrial

pollution can lead to water pollution, harm to aquatic life, and disrupt the balance of ecosystems.

To combat domestic waste and land-based marine pollution, measures such as the establishment of wastewater treatment plants, improvement of sewage systems, implementation of environmental conservation policies, and public awareness campaigns are taken. Additionally, there are various international agreements and regulations in place to control marine pollution on a global scale.

Land-based pollution is particularly evident in the Sea of Marmara. As a relatively small sea, it is essential for all coastal municipalities to invest in wastewater treatment to minimize the impact of pollution on the Sea of Marmara. Additionally, monitoring the pollution in the Sea of Marmara from a public health perspective and providing transparent and easily accessible information to the public entering the sea is important.

Since the Sea of Marmara is replenished with oxygenated waters from the North Aegean and the Çanakkale, special attention should be given to preventing pollution in the Northern Aegean and the Çanakkale. Monitoring the pollutants carried by the surface currents from the Black Sea is also of great importance. This way, the pollution budgets of the Marmara and Black Seas can be updated.

4.3. Eutrophication and Heavy Metal Pollution

Eutrophication is a type of pollution that occurs in water systems due to the accumulation of excessive nutrients. It is often caused by sources such as agricultural activities, sewage discharge, and industrial waste, which introduce high levels of nitrogen and phosphorus compounds into water systems. These nutrients promote rapid algae growth in aquatic ecosystems, leading to excessive proliferation of aquatic plants and a decrease in oxygen levels in the water. As a result, the balance of aquatic life is disrupted, leading to fish deaths and a decline in water quality.

Heavy metal pollution, on the other hand, occurs when heavy metals are released into water systems. Industrial activities, mining, energy production, and waste disposal are common sources of heavy metal contamination in water. Metals such as lead, mercury, cadmium, and arsenic can accumulate in aquatic environments, posing a serious threat to aquatic organisms and ecosystems. The long-term accumulation of these metals can impact the health and reproductive abilities of aquatic organisms and affect population dynamics. Furthermore, heavy metals can have significant effects on human

health and can be transmitted to humans through contaminated water sources.

Several measures are taken to combat these types of pollution. To control eutrophication, it is important to regulate fertilizer use in agricultural areas, treat sewage water, and improve industrial waste management. Preventing heavy metal pollution involves using wastewater treatment systems in industrial facilities, ensuring safe waste disposal practices, and being cautious with products containing heavy metals.

Regular monitoring of aquatic ecosystems, determination of pollution levels, and the development of effective conservation strategies are also crucial. These efforts are vital for the protection of water resources, the sustainability of aquatic life, and the preservation of human health.

There is limited data available on eutrophication-related pollution in Turkish seas. However, in recent times, the use of phosphate-free cleaning products has helped reduce the ecological damage caused by their release into the marine environment. It is important to comply with the standards set by EU countries in this regard and promote the use of phosphate-free cleaning products. The use of phosphate compounds increases the phosphate content in water, leading to a process known as eutrophication, which results in decreased oxygen levels and negatively affects marine organisms. The increased phosphate levels lead to rapid algae growth, organic matter accumulation at the bottom, insufficient oxygen levels, and fish deaths. Changes in parameters such as odor, taste, and color can be observed in seawater. The choice of raw materials used is important not only for the preservation of our seas and the environment but also for water conservation. Protecting our seas from pollution is crucial. Particularly along the Mediterranean coasts, there have been observed retreats in endemic seagrass meadows known as Posidonia oceanica due to pollution from domestic sources. These seagrass meadows are considered the lungs of the Mediterranean due to their oxygen production, and although they are under protection, they are still threatened by various factors.

There are numerous studies on heavy metals in Turkish waters. It is known that heavy metals can also transfer to humans through marine organisms. However, so far, specific fish species that are harmful to human health have not been identified. Nevertheless, monitoring studies need to continue in order to assess the situation. (TÜDAV, 2017).

Excessive plankton growth, particularly during the spring months, is a common manifestation of eutrophication and can be observed in widespread

areas. Many seas in Türkiye, especially the Sea of Marmara, experience excessive plankton growth, also known as plankton blooms. This phenomenon typically begins in the spring season and ends around June. However, in the past decade, the frequency of these blooms has increased fivefold, primarily due to the excessive input of nutrient salts. This nutrient input leads to the overgrowth of single-celled organisms called phytoplankton, which can be seen on the water surface as red or sometimes white patches. These blooms, which primarily contribute to oxygen depletion in seawater, can also result in fish mortality if they persist for a long time. It is recommended to regularly monitor the dynamics of the phytoplankton and coccolithophores responsible for these occurrences, particularly in the Turkish Straits System. Furthermore, the occurrence frequency of phenomena such as "mucilage" and "sea snot," which are indicators of pollution, has also increased in recent years, especially in the Marmara and Northern Aegean waters, particularly during the spring season.

Marine mucilage, also known as sea snot, is a dense and highly viscous substance composed of polymers derived from various marine organisms, including excretions and secretions of different sizes and species such as viruses, bacteria, phytoplankton, and even zooplankton. It consists of dissolved and polymeric organic matter, rich in extracellular polysaccharides, and exhibits hydrogel-like properties. The jelly-like and adhesive characteristics of marine mucilage enable it to encapsulate a wide range of marine organisms.

The mucilage problem has been frequently observed in the Adriatic Sea since the 1870s. In the Aegean Sea, it was documented between 1990 and 2010, while in the Sea of Marmara , it was first observed between 2007 and 2010, and most recently in June 2021, with severe intensity (Danovaro et al., 2009).

The recent intense mucilage formation in the Sea of Marmara, which has high human activity, is considered to be a result of environmental pollutants and pressures such as climate change affecting the Sea of Marmara ecosystem. The prominent presence of polysaccharides and carbohydrates in mucilage structure indicates that it originates from phytoplankton-derived materials. The transition from a mild winter to spring and hot summer months leads to calm sea currents and reduced wave activity, creating stagnant conditions in the water column. These conditions promote the development of anoxic conditions, delayed decomposition of humic compounds, and accelerated production of mucilage. Some studies have reported that a high N/P ratio and low levels of certain nutrient elements can accelerate mucilage production (Mecozzi et al., 2001).

The Marmara Basin is home to numerous Organized Industrial Zones and industrial establishments. Additionally, agricultural and livestock activities take place within the basin. Residential areas and industrial facilities within the Marmara Basin contribute pollutants to the air and water from areas where solid waste is disposed of. Agriculture and livestock activities result in the influx of significant amounts of N, P, and pesticides into the basin. Airborne pollutants such as polycyclic aromatic hydrocarbons (PAHs), polychlorinated biphenyls (PCBs), and polybrominated diphenyl ethers (PBDEs) are released into the atmosphere from domestic and industrial activities. In addition to C, N, and P pollution in water, metals, PAHs, PCBs, PBDEs, pharmaceuticals, and microplastics are transported to the Sea of Marmara through discharges, rainfall, and dry and wet deposition from the atmosphere (Aydın, 2021).

4.4. Plastic Waste Pollution in Marine Systems

Plastic waste pollution in our seas is an environmental issue that occurs as a result of plastic materials being discarded or transported into marine environments. Plastic waste can enter the seas from various sources, such as the dumping of waste in coastal areas, garbage disposed of from marine vessels or ships, litter carried from coastlines, and plastics transported through rivers. The majority of plastic waste in the oceans remains in marine ecosystems for a long time, causing various negative effects. Plastics can take years to degrade, during which they can be ingested by marine organisms or entangle fish and marine mammals in fishing nets, leading to suffocation. Additionally, plastics that are fragmented by sunlight and wave action can become microplastics, which can be consumed by marine organisms. This situation can progress through the food chain, reaching organisms at the top trophic levels and ultimately impacting humans as well.

Plastic waste pollution not only harms marine ecosystems and biodiversity but also creates visual pollution and negatively affects the tourism sector. Furthermore, the release of chemical substances contained in plastics can have adverse effects on water quality and the health of marine ecosystems. Several measures are being taken to address this issue. Firstly, waste management and recycling systems need to be strengthened to prevent plastic waste from reaching the seas. Steps can be taken to reduce plastic consumption, ban or limit single-use plastics, and replace plastic packaging with recyclable materials. In addition, raising public awareness and conducting educational campaigns are crucial. It is important for individuals to understand the impact of plastic waste on nature and the oceans and to raise awareness about proper waste management practices.

Internationally, there are agreements and initiatives aimed at combating plastic waste pollution. For example, the "Marine Plastic Pollution" program led by the United Nations Environment Programme (UNEP) contributes to collaboration and the development of strategies among countries. Combating plastic waste pollution is an important step towards preserving marine ecosystems and achieving a sustainable environment. It requires the responsibility and adherence to proper waste management practices by every individual and institution.

More than 40% of plastic waste consists of single-use products, and over half of plastic items become waste within three years (Lebreton and Andrady, 2019; Tortell, 2020). If current plastic consumption and waste management systems continue, it is estimated that by 2025, the oceans will receive 6.4 million tons of plastic waste every day (Jambeck et al., 2015). An Australian study cited in WWF's report titled "No Plastic in Nature" revealed that humans ingest 5 grams of plastic per week, equivalent to consuming a credit card's worth of plastic. The ingestion of plastics into the human body occurs primarily through water consumption. According to WWF, the Mediterranean Sea receives 0.57 million tons of plastic waste annually, and this amount is expected to increase further (WWF, 2019). WWF's report titled "Out of the Plastic Trap: Saving the Mediterranean from Plastic Pollution" indicated that Türkiye is the third-highest contributor of plastic waste to the Mediterranean Sea, following Egypt and Italy (Boucher and Bilard, 2020).

Türkiye is surrounded by various seas where economic activities such as industry, fishing, shipping, and tourism take place. The coastal areas of the Mediterranean and Aegean Seas are particularly important for tourism. The success of combating plastic pollution in these areas will not only affect the diversity of marine life and ecosystems but also tourism revenues and the quality of tourists' experiences. In the Black Sea, shipping, fishing activities, and tourism are both sources and sectors affected by plastic pollution. Food and packaging waste, plastic bottles, and cigarette butts are the most commonly found plastic waste in nature, accounting for 70% of plastic waste according to WWF Australia's report titled "Plastic Revolution to Reality." Unfortunately, these wastes are frequently observed along all coastlines of Türkiye. The prevalence of polystyrene and polyethylene plastics in marine environments supports this data, as these materials are commonly used in packaging (UNDP, 2021). As of 2018, the average plastic packaging recycling rate in the EU was 41.5%. In Türkiye, 9.6 million tons of plastic are produced annually, with 2.2 million tons of plastics being released into the market as packaging, and only half a million tons of this packaging being

recycled. According to a study conducted in 2015, Türkiye ranks 14th in the world in terms of mismanaged plastic waste. The low rates of waste collection and deficiencies in waste management further exacerbate the environmental impact of plastic waste. According to a WWF report published in 2018, 144 tons of plastic waste from Türkiye enters the Mediterranean Sea every day. Similar studies have identified significant amounts of plastics reaching the sea in other regions as well (Alessi et al., 2018; Baysal et al., 2020).

Plastics enter the seas through direct or indirect pathways. Direct input is caused by litter left on beaches or plastic products discarded into the sea during fishing or transportation activities. Indirect input, on the other hand, refers to the transportation of plastic waste to the seas through various pathways such as wind or river currents, originating from land-based activities and inadequately managed plastic waste (including littering, pesticide packaging, greenhouse covers, etc.). Research on plastic pollution has found that 80% of plastic waste in the seas is land-based, while only 20% is generated from marine activities (Akdoğan and Güven, 2019). One of the main sources of land-based plastic pollution in Türkiye is the deficiencies in waste management practices. There are still four municipalities in Türkiye that do not provide waste services. In municipalities where waste services are provided, the proportion of the population receiving waste services in those municipalities is 98.8% of the total population. Of the collected waste, 67.2% is subjected to controlled landfilling, 20.2% is disposed of in open dumpsites, and only 12.3% is sent to recycling facilities (TÜİK, 2018). Due to the lack of effective recycling and recovery infrastructure, plastic waste can easily end up in the environment, bypassing the waste management system. Although efforts are being made to prevent uncontrolled dumping and transform open dumpsites into controlled landfill sites, the disposal of waste in open dumpsites (in a manner not compliant with the EU Landfill Directive) continues. Coastal areas, river basins, and hillsides are used as open dumpsites. Some of the plastic waste disposed of in controlled landfill sites also mixes with the environment through rainfall, soil movements, and wind. To prevent this situation, land conditions and prevailing wind directions should be taken into account when selecting sites for controlled landfill areas. Additionally, storage cells opened in controlled landfill sites should be covered with soil daily to prevent potential leaks of plastic waste. Source separation of household waste will both reduce the amount of plastic entering the environment and promote resource and energy conservation. Dual collection systems are in place in EU countries, and steps in this direction are also regulated in Türkiye through the Zero Waste Regulation, Packaging Waste Regulation, and the Environment Agency Law related to

deposit systems. Municipalities need to establish infrastructure for separate waste collection through waste collection centers. However, the deficiencies of municipalities in the separate collection or sorting of packaging waste lead to the leakage of plastic waste into the environment. Moreover, delays in the implementation of the deposit system contribute to the increase in plastic pollution stemming from beverage packaging. Improper disposal of waste in terrestrial areas and coastal regions is one of the most significant factors in the release of plastic waste into the environment. Intentionally leaving, dropping, or wind-blown litter from open waste bins are among the causes of terrestrial pollution. The amount of plastic entering the environment in this way is not yet known in Türkiye, and national-scale studies should be conducted. The increase in plastic consumption along with the increase in consumption overall, combined with weaknesses in waste management system monitoring and implementation, leads to single-use plastic packaging and other disposable products becoming the most common sources of pollution in the seas. Plastic waste is the most commonly encountered waste in coastal areas and beaches in terms of volume (Gönülal et al., 2016; Ertaş, 2021).

This situation applies to both the Mediterranean and the Black Sea, although the sources and types of waste may vary. Along Türkiye's Mediterranean coast, packaging waste, small plastic particles, and single-use products are more prevalent compared to other types of plastic waste (Öztekin et al., 2019). In the Black Sea, packaging waste is predominantly observed, while cigarette butts tend to increase during the summer season. One important problem in our seas is ghost nets. Particularly in the Black Sea, there are large amounts of nets and plastics on the seabed. Globally, ghost nets account for 10% of plastic waste in the seas and are the most lethal type of plastic waste for marine organisms (WWF, 2020). Fishing nets and gear used in fishing and monitoring activities contain a significant amount of plastic, and after they reach the end of their lifespan, fishermen may discard them into the sea. These abandoned nets continue to capture fish and other marine organisms and, being made of plastic, persist in the marine environment for decades without decomposing. According to WWF data, 28% of the plastic waste entering the Mediterranean is derived from fishing (both capture and aquaculture) and shipping activities. Unmanaged plastics harm marine life, the predators that consume them, and ultimately humans. Additionally, plastics dumped into the seas also damage the fishing and tourism sectors. The estimated cost of the damage caused, including the cost of cleaning up such waste, is $13 billion for these industries. Microplastics, which are not visible to the naked eye (less than 5 mm in size), also infiltrate

the environment in large quantities, similar to macroplastics. This infiltration occurs through various pathways such as the use of cosmetic products, improper storage of raw materials, and the wear of vehicle tires and large plastics. These invisible particles harm marine life and smaller organisms that create the conditions necessary for the survival of larger organisms (Baysal et al., 2020). With China's ban on plastic waste imports in 2018, Türkiye's volume of plastic waste imports has been increasing (Tremblay, 2019).

Türkiye is a country that imports a significant amount of plastic waste, especially from Europe. Despite restrictions on the import of unsorted plastics and a reduction in the import quota for packaging waste imposed by the European Union, Türkiye still remains a country that imports waste from abroad. One serious problem that arises is that a portion of the imported packaging waste is not recyclable and is illegally incinerated. According to a report by Greenpeace in 2019, Türkiye's monthly plastic waste imports increased from 4,000 tons in the first quarter of 2016 to 33,000 tons per month in the first quarter of 2018. A large portion of this import came from the United Kingdom (Greenpeace, 2019). According to data compiled from the UN Comtrade platform, this amount reached 225,376 tons in 2019. The Ministry of Environment and Urbanization decided that companies could meet 80% of their plastic waste processing capacity through imported waste from 2019 and the beginning of 2020, and then reduced this percentage to 50%. However, despite this decision, Türkiye's plastic waste imports continue. The Ministry of Environment and Urbanization banned the import of polyethylene, which constitutes a significant portion of plastic waste imports, as of July 2, 2021, with a regulation published in the Official Gazette numbered 31485 on May 18, 2021. However, another regulation published in the Official Gazette numbered 31537 on July 10, 2021, lifted the ban on the import of waste polyethylene.

4.5. Global Climate Change Effects on Marine Systems

Türkiye is a country with rich biodiversity and a strategic location, surrounded by seas such as the Aegean Sea, Mediterranean Sea, Black Sea, and Sea of Marmara . However, these seas are significantly affected by the impacts of climate change. Climate change has various negative effects on the seas. The increase in sea water temperatures has significant impacts on marine ecosystems. Warm water can disrupt food chains and habitats that are vital for marine organisms. Additionally, the increase in ocean acidification can harm coral reefs and weaken the calcium shells of marine organisms.

Climate change also leads to rising sea levels. Increased sea levels can result in coastal erosion, salinization, and flooding in coastal areas (Cheung et al., 2009). Coastal ecosystems are threatened as a result of the rising sea levels. The effects of climate change can be observed in various ways in Türkiye's seas. For example, the temperature rise and sea level increase in the Mediterranean Sea affect agriculture, tourism, and natural life in coastal regions. In the Black Sea, changes in sea water temperature have impacts on fishing and marine ecosystems. Türkiye is taking various steps to combat climate change and protect its seas. These steps include promoting the use of renewable energy sources, establishing marine protected areas, implementing measures to combat coastal erosion, and implementing programs to tackle marine pollution. However, more work and international cooperation are needed in the areas of climate change and the protection of seas. Ensuring the healthy preservation of seas and adapting to the impacts of climate change is of great importance for Türkiye's future sustainability and ecosystem health (TUDAV, 2017).

5. Conclusions and Recommendations

Türkiye, in its journey of development from the past to the future, prioritizes the protection and improvement of the environment in line with its global responsibilities while advancing its country economically and socially. In this context, our country emphasizes its readiness to contribute to a sustainable world since the adoption of the 2030 Agenda for Sustainable Development. Türkiye adopts the approach of integrating Sustainable Development Goals (SDGs) into its Development Plans and sectoral strategies, and implementing and monitoring them in a comprehensive manner. Türkiye, surrounded by seas on three sides, is a country with high biological diversity due to the influence of its diverse ecological characteristics in its seas and inland waters. Therefore, the conservation, development, sustainable use, and effective management of water resources, especially marine resources, are important. In addition to the strategic plans of public institutions related to Development Plans, key policy documents for Sustainable Development Goals (SDGs) include the National Climate Change Strategy Document, Climate Change Adaptation Strategy and Action Plan, Biodiversity Strategy and Action Plan, National Wetlands Strategy, and Türkiye National Marine Research Strategy Document SKA 14.

The components of the main policy framework that overlaps with SKA 14 are as follows:

- Conservation of water quality in coastal and transitional waters

• Expansion of marine and coastal protected areas, strengthening of the conservation system, and effective management

• Ensuring effective stock management through identification, monitoring, and control of fish stocks

• Support for sustainable aquaculture production

• Development of aquaculture practices

• Conservation of genetic resources in aquatic organisms and establishment of gene banks

• Support for research and technology development activities in the field of aquaculture

• Facilitation of market access for producer organizations

• Implementation of science-based and effective resource management in fisheries and strengthening of administrative capacity

• Enhancement of product diversity and branding in aquaculture, considering environmental sustainability, to increase competitiveness in international markets.

Our legislation includes regulations for the protection and prevention of pollution in coastal and marine ecosystems. The Environmental Law and relevant legislation establish principles for preventing the entry of waste originating from land-based and maritime activities into our seas. Principles for the discharge of wastewater and the prevention of water pollution, as well as the monitoring and control procedures for these purposes, are also regulated. In the event of pollution, regulations are in place to ensure maritime safety, protect the sea and its surroundings, and prevent harm to life and property. To conserve fish stocks and economically benefit from fishery resources, our legislation addresses matters related to their acquisition, trade, and utilization. Türkiye evaluates SKA 14 within two main thematic focuses:

i. Prevention of marine pollution and ecosystem conservation, and

ii. Sustainable production of aquatic products and stock management.

Based on the consideration of TÜİK (Turkish Statistical Institute) data, Türkiye's National Voluntary Reviews of the Sustainable Development Goals, and studies on marine pollution, the following activities are recommended:

• In the context of preventing marine pollution and conserving ecosystems, an ecosystem-based integrated management approach should

be adopted, considering both the quality and quantity of water resources. Important steps should be taken in pollution monitoring and prevention, as well as in the identification and conservation of biodiversity.

• In the context of sustainable production of aquatic products and stock management, activities should focus on monitoring stocks, protecting endangered species, and enhancing stocks through restocking efforts. Additionally, important steps such as utilizing information and communication technologies in the aquaculture sector, certifying and monitoring aquaculture facilities, should be taken.

• Maximizing the utilization of aquatic resources from our seas and inland waters, while ensuring a balance between conservation and use based on the principle of sustainability.

• Increasing the contribution of seafood consumption to meeting people's protein needs.

• Enhancing the effectiveness of producer organizations in seafood production and marketing.

• Establishing well-equipped fishing harbors and logistics centers for the benefit of fishermen and aquaculture farmers.

• Ensuring the recording of seafood products obtained from seas and inland waters at the points of landing to facilitate access to accurate, reliable, and up-to-date data.

• Improving the legal framework for the conservation of fish stocks and the development of aquaculture.

• Conducting research in various fields such as Pharmacology and Biomedical Sciences, Marine Bioproducts, Marine Bioenergy, Marine Microbiology, Algal Biotechnology, Biomaterials and Nanobiotechnology, Functionality/Sustainability of Marine Ecosystems, and similar topics in Türkiye's seas. In this regard, activities in marine biotechnology should be encouraged.

References

Abdullahzade, C. (2009). Gemilerden kaynaklanan petrol kirliliği: Türk hukukundaki son gelişmelerin değerlendirilmesi. *Ankara Üniversitesi Hukuk Fakültesi Dergisi*, *58*(4), 694–710.

Akdoğan, Z., Güven, B. (2019). Microplastics in the environment: A critical review of current understanding and identification of future research needs. *Environmental Pollution*, *254*, 1–24.

Akengin, H., Dölek, İ., Özdemir, Y. (2016). *Türkiye'nin Denizleri ve Kıyıları*. In book: Türkiye`nin Fiziki Coğrafyası. 287-310.

Alessi, E., Giuseppe, C. (2018). *Out of the plastic trap: saving the Mediterranean from plastic pollution*. WWF Mediterranean Marine Initiative, Rome, Italy.

Aras, O. N. (2001). *Petrol üretiminin deniz kirliliğine etkisi ve kontrolü*. İnsan ve Felaketler Uluslararası Konferansı, Bakü, Azerbaycan.

Artüz, İ. (1992). *Deniz kirlenmesi*. İstanbul, Türkiye, Ofset Baskı Atölyesi.

Atakpa, D. (2018). Blue economy in a nutshell. Retrieved from https://www.researchgate.net/publication/327550968_BLUE_ECONOMY_IN_A_NUTSHELL_Capt_N N_SD_Atakpa.

Atalay, İ. (2011) Türkiye Coğrafyası ve Jeopolitiği. Meta Basım Matbaacılık. Bornova/İzmir.

Aydın, M. E. (2021). *Marmara denizinde müsilaj oluşumu muhtemel sebepleri ve öneriler*, Marmara Deniz Ekolojisi; Deniz Salyası Oluşumu, Etkileşimleri ve Çözüm Önerileri, Türkiye Bilimler Akademisi.

Başeren, S. H. (2006) *Ege Sorunları*, Tüdav Yayınları No: 25, ISBN: 9758825143 Ankara

Baysal, A., Saygın, H., Ustabaşı, G. Ş. (2020). Microplastic occurrences in sediments collected from Sea of Marmara -Istanbul Türkiye. *Bulletin of Environmental Contamination and Toxicology*, *105*, 522–529.

Brundtland, G. H. (1987). *Brundtland report. Our common future*. Comissão Mundial, *4*(1), 17-25.

Boucher, J., Bilard, G. (2020). *The Mediterranean: Mare plasticum*. Gland, Switzerland: IUCN.

Bozoğlu, O. Ciğerim, E. (2022). Sürdürülebilirlik, Sürdürülebilir Kalkınma ve Sürdürülebilir Üniversiteler. *Socrates Journal of Interdisciplinary Social Studies*, *8*(18), 146–158.

Butt, N. (2007).The impact of cruise ship generated waste on home ports and ports of call: A study of Southampton. *Marine Policy*, *31*(5), 591–598.

Caradonna, J. L. (2014). *Sustainability: A history*. Oxford University Press.

Cheung, W. W. L., Lam, V. W. Y., Sarmiento, J. L., Kearney K., Watson, R., Pauly, D. (2009). Projecting global marine biodiversity impacts under climate change scenarios. *Fish and Fisheries*, *10*(3): 235–251.

Clark, R. B. (2001). *Marine Pollution*. New York, USA, Oxford University Press.

Dalberg Advisors, WWF Mediterranean Marine Initiative (2019). *Stop the Flood of Plastic: How Mediterranean countries can save their sea*.

Danovaro, R., Fonda Umani, S., Pusceddu, A. (2009). Climate change and the potential spreading of marine mucilage and microbial pathogens in the Mediterranean Sea. *PLoS ONE, 4*(9): e7006. doi:10.1371/journal.pone.0007006.

Doğan-Sağlamtimur, N., Subaşı, E. (2018). Ship generated marine pollution and waste reception facilities from the World and Türkiye: General perspective, management and suggestions. *Pamukkale Univ Muh Bilim Derg*, *24*(3), 481–493.

Dölgen, D., Alpaslan, N., Sarptaş, H. (2006). *Kıyı yerleşimlerine uygun sıvı ve katı atık yönetim stratejileri üzerine görüşler*. Türkiye'nin Kıyı ve Deniz Alanları VI. Ulusal Konferansı, Muğla, Türkiye, 7-11 Kasım 2006.

Ecel, M. (2007). *Çevre ve Boğazların Güvenliği, Karadeniz Petrol ve Gaz Zirvesi*. T.C. Çevre ve Orman Bakanlığı Çevre Yönetimi Genel Müdürlüğü Deniz ve Kıyı Yönetimi Dairesi Başkanlığı, Ankara, Türkiye.

Environmental Inspection Report. (2002). *Gemilerin denizleri ve limanları kirletmesini önleme ve kirlilikle mücadele*. *Sayıştay Dergisi*, *44-45*, 107–120.

Ertaş, A. (2021). Assessment of origin and abundance of beach litter in Homa Lagoon coast, West Mediterranean Sea of Türkiye. Estuarine. *Coastal and Shelf Science*, *249*, 107–114.

Global Sustainable Development Report, (2023). https://sdgs.un.org/gsdr/gsdr2023

Gönülal O., Öz İ., Güreşen S.O., Öztürk B. (2016). Abundance and composition of marine litter around Gökçeada Island (Northern Aegean Sea). Aquatic Ecosystem Health and Management, 19(4), 461–467.

Greenpeace (2019). *Plastik atıkların yeni adresi: Türkiye*. Erişim Tarihi: Mart 2021. Erişim Adresi: https://www.greenpeace.org/Türkiye/haberler/plastik-atiklarin-yeniadresi-turkiye/

Güven, K. C., Öztürk, B. (2005). *Deniz Kirliliği*. İstanbul, Türkiye, TÜDAV Yayınları No: 21.

İncaz, S., Alkan, G. B., Bakırcı, E. (2005). *Uluslararası mevzuatta deniz kirliliği ve Türkiye'deki uygulamaları*. İTÜ Mühendislik Fakültesi, Deniz Ulaştırma İşletme Mühendisliği, İstanbul, Türkiye.

Jambeck, J. R., Andrady, A., Geyer, R., Narayan, R., Perryman, M., Siegler, T., Wilcox, C., Lavender Law, K. (2015). Plastic waste inputs from land into the ocean, *Science*, *347*,768–771.

Lebreton, L., Andrady, A. (2019). *Future scenarios of global plastic waste generation and disposal*. Palgrave Commun. 5, 6.

Mecozzi, M., Acquistucci, R., Noto, V. D., Pietrantonio, E., Amici, M., Cardarilli, D. (2001). Characterization of mucilage aggreagtes in Adriatic and Tyrrhenian Sea: structure similarities between mucilage samples and the insoluble fractions of marine humic substances. *Chemosphere*, *44,* 709–720.

Mohanty S. K., Dush, P., Gupta, A. (2019). Blue Economy Enhancing Growth and Sustainability, Research and Informatio System for Developing Countries. Blue Economy Forum. Retrieved from http://ris.org.in/blueeconomy-enhancing-growth-and-sustainability.

Nauke, M., Holland, G. L. (1992). The role and development of global marine conventions: two case histories. *Marine Pollution Bulletin*, *25*(1–4), 74–79.

Orhon, D., İnce, O., Sözen, S. (2008). Deniz kaynaklı petrol ve petrol türevi atıkların geri kazanılması-çevre korunmasında önemli atılım. *Su ve Çevre*, *23*.

Öztekin, A., Bat, L., Baki, O.G. (2019). Beach Litter Pollution in Sinop Sarikum Lagoon Coast of the Southern Black Sea. *Turkish Journal of Fisheries and Aquatic Sciences*. *20*(3), 197–205.

Pauli, G. (2010). *The Blue Economy: 10 Years, 100 Innovations, 100 Million Jobs*. Taos, US: Paradigm Publications.

Portney, K. E. (2015). *Sustainability*. MIT Press.

Scoones, I. (2007). *Sustainability. Development in Practice*, *17*, 589–596.

Şener, M., Dogruyol, P., Balkaya, N. (2019). Microplastic pollution in the Black Sea coast of the Anatolian side of Istanbul, Türkiye. *Desalination and Water Treatment*, *172*, 351–358.

Talınlı, İ., Sarıöz, K. (2002). *Marmara kıyı alanında petrol dökülmesine bağlı çevresel hasar değerlendirmesi: Volgoneft-248 kazası*. Türkiye'nin Kıyı ve Deniz Alanları IV. Ulusal Konferansı, İzmir, Türkiye, 5-8 Kasım 2002.

Terzi, Y., Erüz C., Özşeker, K. (2020) Marine litter composition and sources on coasts of south-eastern Black Sea: A long-term case study. *Waste Management*, *105*, 139–147.

Thiele, L. P. (2016). *Sustainability*. John Wiley & Sons.

Toplu-Yılmaz, Ö. (2021). Türkiye'de Sürdürülebilir Mavi Ekonomi için Balıkçılık Desteklerinin Değerlendirilmesi. *Ömer Halisdemir Üniversitesi İktisadi ve İdari Bilimler Fakültesi Dergisi*, *14*(3), 906–923.

Tortell P. (ed.) (2020). *Earth 2020: An Insider's Guide to a Rapidly Changing Planet*. Cambridge, UK: Open Book Publishers,

Tremblay, P. (2019). *Türkiye becomes new dump for global plastic waste*. Erişim Tarihi: Nisan 2021. Erişim Adresi: https://www.al-monitor.com/pulse/

originals/2019/06/Türkiye-becomes-the-new-dump-for-global-plastic-waste.html

TÜDAV, (Türk Deniz Araştırmaları Vakfı) (2017). 2017 Yılı Türkiye Denizleri Raporu, Erişim Tarihi: 23.06.2023. file:///C:/Users/Hp/Desktop/TUDAV_2017_Denizler_Raporu_s%20(1).pdf

Türkiye Cumhuriyeti Cumhurbaşkanlığı Strateji ve Bütçe Daire Başkanlığı [TCCSBB], (2019). 7.-11. kalkınmaplanı,www.sbb.gov.tr.

TÜİK, (2022). Su Ürünleri, 2022. Haber Bülteni, Erişim Tarihi: 23.06.2023 https://data.tuik.gov.tr/Bulten/Index?p=Su-Urunleri-2022-49678

TÜİK (2018). Belediye Atık İstatistikleri 2018. TÜİK Haber Bülteni, TS 30666. Erişim Tarihi: Mart 2021 Erişim Adresi: https://tuikweb.tuik.gov.tr/ PreHaberBultenleri.do?id=306663

UNDP Türkiye, (2018). *Plastik Atıklarla Mücadelenin en etkili yolu Geri Dönüşüm Tesisleri Haberi* Erişim Tarihi: Temmuz 2021. Erişim adresi: https://www.tr.undp.org/content/Türkiye/tr/home/presscenter/articles/2018/07/plastik-at_klarlamuecadelenin-en-etkili-yolu-geri-doenueuem-tes0.html

United Nations (2019). *Blue Economy Concept Paper.* Retrieved from https://sustainabledevelopment.un.org/content/documents/2978BEconcept.pdf

WWF (2020). *Stop Ghost Gear: The Most Deadly Form of Marine Plastic Debris*. WWF International.

Yıldırım, S. Yıldırım, D. Ç. (2020). *Achieving Sustainable Development Through a Green Economy Approach. S. Patti ve G. Trizzino (Eds), Advanced Integrated Approaches to Environmental Economics and Policy: Emerging Research and Opportunities* (s. 1- 22), Hershey PA, USA, IGI Global Publication.

World Bank (2016). *Oceans 2030: Financing the blue economy for sustainable development*. Retrieved from https://thedocs.worldbank.org/en/doc/446441473349079060010022016/original/AMCOECCBlueEconomyDevelopmentFramework.pdf

Zuin, S., Belac, E., Marzi, B. (2009). Life cycle assessment of shipgenerated waste management of Luka Koper. *Waste Management*, *29*(12), 3036–3046.

Bölüm 5

N-Heterosiklik Karben Öncülü Benzimidazol Tuzlarının Suzuki-Miyaura Tepkimesine Ligant Etkisi

Ülkü Yılmaz[1]

Özet

Biyoaktivite açısından geniş bir yelpazeye sahip biarillerin sentezinde kullanılan karbon-karbon (C-C) eşleşme tepkimeleri arasında en tercih edilen yöntem Suzuki-Miyaura (SM) tepkimesidir. Toksisitesi düşük reaktiflerin kullanımı ve ılıman şartlarda kolay gerçekleşen bir tepkime türü olması bu yönteme olan ilgiyi artırmaktadır. Tepkime sırasında paladyum katalizörleri tercih edilmektedir. SM tepkimesinde çoğunlukla tercih edilen N-Heterosiklik karben (NHC)-Pd katalitik sistemi diğer sistemler ile kıyaslandığında elektronik yapısının rahatça değiştirilebilmesi, hava ve neme duyarlılığının olmaması avantajlarını içerir. Bu anlamda benzimidazol tuzları NHC lerin hazırlanması için faydalı öncüllerdir. Benzimidazolyum halojenür-Pd$(OAc)_2$ katalitik sistemleri ile katalizlenen *in situ* SM tepkimesi günümüzde seçkin biaril sentez yöntemidir.

1. Giriş

Biaril bileşikleri farmakolojik ve agrokimyasal açısından önemli bileşiklerdir. Biariller günümüzde kullanılan birçok ilacın içeriğinde bulunan fonksiyonel gruplar olup antifungal, anti-inflammatuar, antiromatizmal, antitümöral ve antihipertensif gibi biyoaktivitelere sahiptirler. Bifonazole (antifungal), fenbufen (anti-inflamatuar), valsartan (antihipertensif) ve sonidegib (antineoplastik) ilaçları bifenil türevleridir [1-3]. Bu yüzden biarilerin ve bifenillerin kolay ve ekonomik bir şekilde sentezlenebilmeleri için birçok sentetik metot geliştirilmiştir. Bunlardan Suzuki-Miyaura tepkimesi (SM) en çok tercih edilen biaril sentez yöntemlerinden biridir. SM

1 Prof. Dr., Malatya Turgut Özal Üniversitesi, Mühendislik ve Doğa Bilimleri Fakültesi, Mühendislik Temel Bilimleri Bölümü, ulku.yilmaz@ozal.edu.tr, ORCID ID: 0000-0002-2806-4781

https://doi.org/10.58830/ozgur.pub252.c1216

tepkimesiyle paladyum katalizörü varlığında aril halojenürler ile arilboronik asitler arasında yeni C-C bağı oluşarak bifenil türevlerinin ya da daha geniş anlamıyla biarillerin sentezi gerçekleştirilir [4-6]. SM C-C çapraz eşleşme tepkimesini katalizleyen paladyum katalizörleri farklı ligantlar kullanılarak geliştirilebilmektedirler. Bunlardan en önemli ligant grubu NHC ve NHC öncülü olarak kullanılan benzimidazolyum halojenürlerdir [7-9].

2. Karbon-Karbon (C-C) Eşleşme Tepkimeleri

Birçok uygulama alanına sahip olan yeni reaktiflerin özellikle de biyoaktif moleküllerin sentezi açısından C-C bağı oluşum tepkimeleri organik ve tıbbi kimya çalışmalarında büyük öneme sahiptirler [10]. Karbon-karbon çapraz bağlanma tepkimeleri bir metal katalizör varlığında bir organik elektrofil ile bir organometalik nükleofil arasındaki tepkime olarak tanımlanabilir (Şekil 2.1) [11].

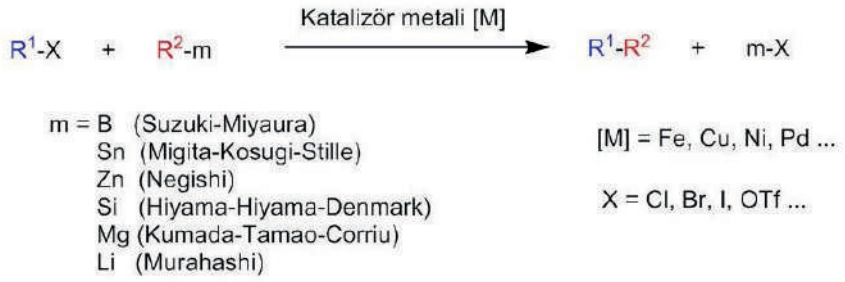

Şekil 2.1. C-C çapraz bağlanma tepkimelerinin genel şeması

Bu tür tepkimelerde Ni ve Pd metalleri indirgenme-yükseltgenme basamağı değişim durumunun kolaylığı nedeniyle diğer metaller ile kıyaslandığında katalitik merkez olarak daha çok tercih edilirler. Bununla birlikte en güçlü katalitik sistemler Pd metali varlığında oluşturulabilmiştir [11-13].

2.1. Suzuki-Miyaura (SM) Tepkimesi

Çapraz C-C bağ oluşumu tepkimelerinin içinde en dikkat çekeni SM tepkimesidir. Keşfedildiğinden bu yana (1979) [14] biaril türevlerinin sentezi için kullanılan en önemli metottur. Genel olarak paladyum içeren bir katalizör sistemi ve baz varlığında aril, vinil, ve alkil halojenürler ile organoboranlardan C-C bağı oluşumuyla biarillerin sentezlenmesi metodudur (Şekil 2.2.1) [4,8,11].

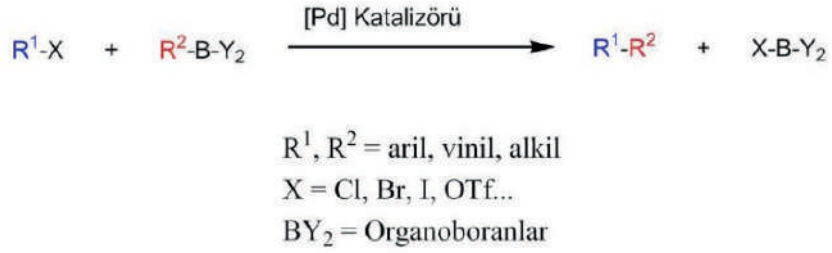

Şekil 2.2.1. Palladyum katalizörlü Suzuki-Miyaura tepkimesinin genel şeması

Suzuki Miyaura tepkimelerinde en temel haliyle üç aşamalı bir katalitik döngü söz konusudur. Birinci aşamada katalizörün organik halojenürle etkileştiği yükseltgeyici katılım söz konusudur. Arkasından metal üzerindeki ligantların yer değişimi ile transmetalasyon adımı gerçekleşir. Son olarak iki bileşik arasında yeni C-C bağının oluşumu ile biaril sentezinin gerçekleştiği indirgeyici ayrılma aşaması (Şekil 2.2.2) ile tepkime sonlanır [4,11,15,16].

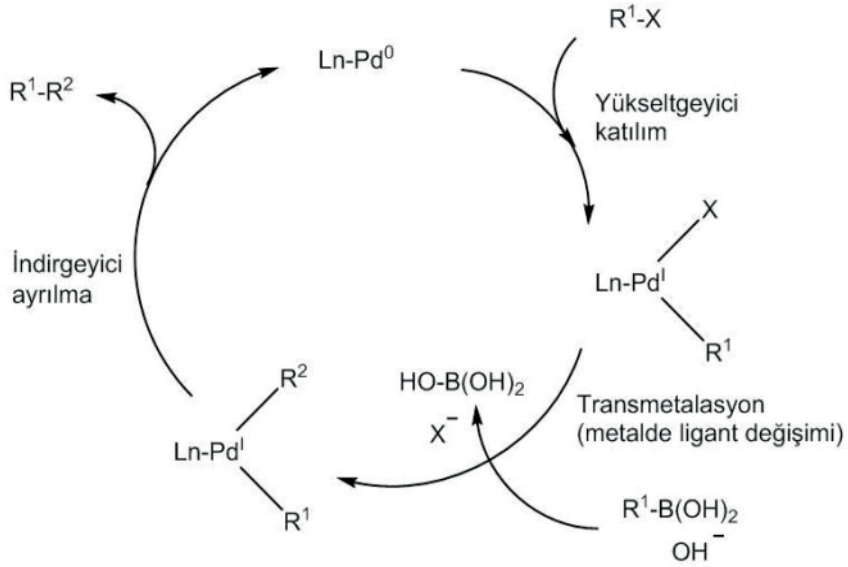

Şekil 2.2.2. Palladyum katalizörlü SM tepkimelerinde genel katalitik döngü

2.2.1. Suzuki-Miyaura Tepkimesinde Kullanılan Ligantlar

Homojen katalizörler ile desteklenen SM tepkimelerinde kullanılan çeşitli ligantlar vardır. Birincisi P-donör ligantlardır ve bu gruba fosfin ile fosfor içeren palladasaykıllar (paladyum içeren halkalar) girmektedir. N-donör ligantlar ise piridinler-iminler, imidatlar, pirimidinler, aminler, orto metalli palladasaykıllar, pincer tip amitler ve hidrazonlar girmektedir [17]. Üçüncü grup ise kullanım açısından diğer ligant gruplarına göre daha avantajlı olan N-heterosiklik karben (NHC) ligantları ya da NHC öncülleridir [18]. NHCler fosfin ligantları ile kıyaslandığında güçlü elektron sağlayıcı olmaları yanı sıra termal kararlılık, havaya ve neme karşı hassasiyetinin azlığı, düşük toksisite ve yüksek performans göstererek daha dikkat çeker hale gelmiştir [19-23]. NHC-palladyum kompleksleri ilk olarak Hermann vd. tarafından [24] hazırlandı. Organ vd. tarafından keşfedilen NHC-Pd-piridin yani PEPPSI (piridinle güçlendirilmiş ön katalizör hazırlama kararlılaştırma ve başlatma) kompleksi ise elektronca daha da zenginleştirilmiş olan bir tür olduğundan SM tepkimelerinde oldukça yüksek verimlere sebep olmuştur [25].

NHC-Pd kompleksleri katalizör öncülleri olarak NHC lerden sentezlenirken inert şartlar gerekmektedir. Bunun yerine NHC öncülü olabilecek azolyum tuzları kullanılarak karşılık gelen NHC *in situ* gelişen deprotonasyon ile elde edilerek Pd metali yanında yerinde kullanılan katalizörlere dönüşebilirler. Böylece havaya neme karşı oldukça kararlı katalitik sistemler elde edilmektedir. Son zamanlarda yapılan çalışmalarda kaydedildiğine göre in situ gelişen katalitik sistemlerin kullanımı ile özellikle imidazolyum tuzlarının Pd ile birlikte kullanımı sonucunda dikkate değer tepkime verimleri kaydedilmiştir [26-28].

2.2.2. İmidazolyum Tuzlarının SM Tepkimelerinde Ligant Etkisi

Yapılan ilgili bir çalışmada geleneksel ısıtma ile aril klorürlerden Pd/1,3-bis(2,6-diizopropilfenil)imidazolyum klorür tuzu katalitik sistemi yanında 6 saatte % 75 tepkime verimiyle bifenil türevi sentezlenirken, başlangıçta ilgili tuz ve palladyumdan sentezlenen kompleks kullanılarak (Şekil 2.2.2.1) katalizör öncülü olarak kullanıldığında aynı tepkime 22 saatte ancak % 68 verim ile gerçekleştirilebilmiştir [29].

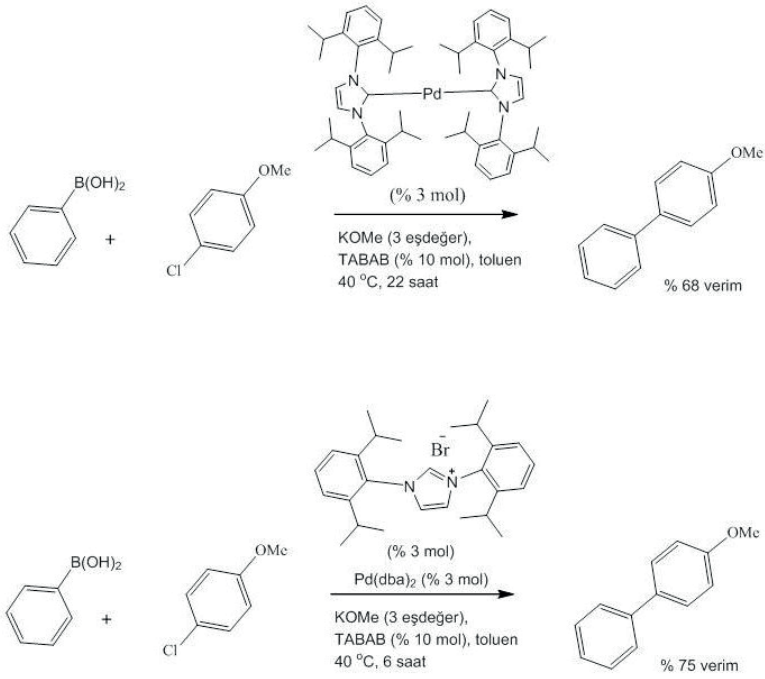

Şekil 2.2.2.1. Pd/imidazolyum tuzu katalitik sisteminin Pd-NHC kompleks katalizör öncülüne üstünlüğü

Kumar vd. tarafından yapılan çalışmada ise benzer şekilde $Pd(OAc)_2$ ve amido-N-imidazolyum tuzlarından oluşturulan katalitik sistem kullanılarak *in situ* gelişen tepkime ile heteroaril bromürler ve klorürlerden % 70 üzerinde tepkime verimleri ile biaril türevleri sentezlenmiştir [30].

2.2.3. Benzimidazolyum Tuzlarının SM Tepkimelerinde Ligant Etkisi

NHC bazlı ligantlar uygun sübstitüentler kullanılarak sterik ve elektrofilik özellikleri açısından iyileştirilebilmektedirler. Bu bağlamda en çok kullanılan NHC öncülü çekirdek benzimidazoldür. Dahası SM tepkimelerinde paladyum yanında ligant olarak kullanılan NHC öncülü benzimidazolyum halojenürler oldukça başarılı dönüşümlere sebep olmuşlardır [23, 31,32]. Örneğin, Chiu vd. yaptıkları çalışmada alkil köprülere sahip bisbenzimidazolyum halojenür/Pd $(OAc)_2$ katalitik sistemlerini baz olarak *t*-BuOH ın kullanıldığı ve aril bromürler ile boronik asitlerden 60 °C

sıcaklıkta 1 saat tepkime süresiyle yaklaşık % 100 e varan verimlerle bifenil türevlerinin sentezi gerçekleştirilmiştir [33]. Wang vd. tarafından sentezlenen ksilil ve piridil köprülü bisbenzimidazol tuzları (Şekil 2.2.3.1) $Pd(OAc)_2$ yanında kullanıldığında deaktif aril klorürlerin eşleşme tepkimelerinde ılıman şartlarda bile yüksek verimler elde edilmiştir [34].

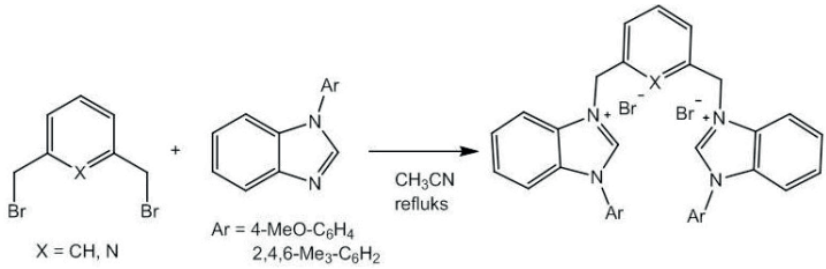

Şekil 2.2.3.1. Ksilil ve piridil köprülü bisbenzimidazolyum dibromürler

Düşünceli vd. tarafından yapılan çalışmada ise kinoksalin köprülü bisbenzimidazol tuzları sentezlenerek (Şekil 2.2.3.2) aril klorürlerin reaktif olarak kullanıldığı bifenil türevlerinin sentezinde ligant öcülü olarak kullanılmış ve Cs_2CO_3 ın baz olarak kullanıldığı 80 °C de gerçekleşen tepkimelerde verim % 91 e kadar ulaşmıştır [35].

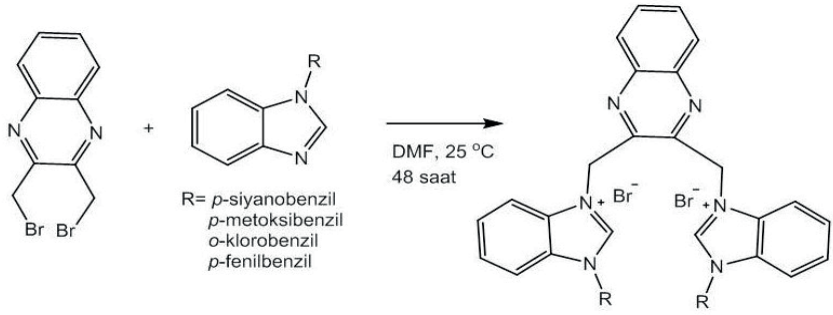

Şekil 2.2.3.2. Kinoksalin köprülü bisbenzimidazolyum dibromürler

Yiğit tarafından yapılan çalışmada perhidrobenzimidazolinyum klorür tuzları (Şekil 2.2.3.3) NHC öncülü olarak kullanılarak $Pd(OAc)_2$ varlığında DMF:H_2O çözücü karışımı içerisinde K_2CO_3 bazı ile 80 °C ve 1 saat tepkime süresinde gerçekleşen SM tepkimelerinde deaktif aril klorür reaktiflerin kullanılmasına rağmen tepkime verimi GC-MS de ölçüldüğü üzere % 74-98 olarak kaydedilmiştir [36].

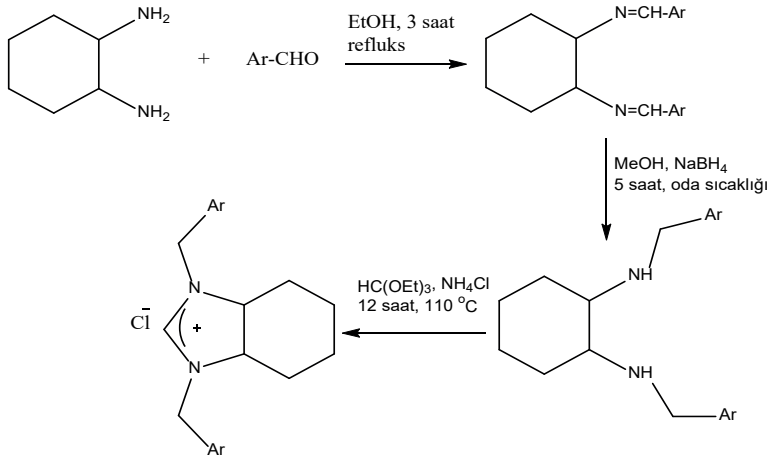

Şekil 2.2.3.3. Perhidrobenzimidazolinyum klorürler

Özdemir vd. tarafından yapılan çalışmada (Şekil 2.2.3.4) alkanil köprüleri ile sentezlenmiş bisbenzimidazol tuzları paladyum katalizör sistemlerinde kullanılarak aril klorürler ve fenilboronik asitlerden bifenil türevleri sentezlenmiştir. SM tepkime verimleri % 54-97 aralığında kaydedilmiştir [37].

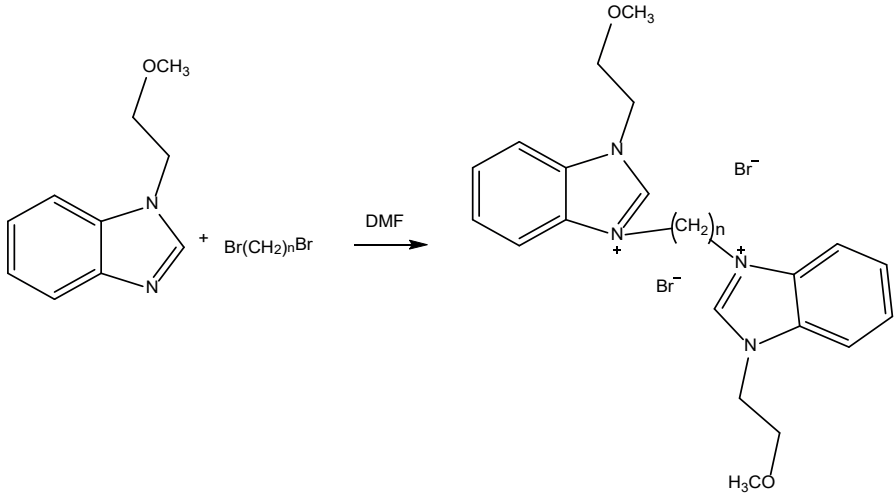

Şekil 2.2.3.4. Alkanil köprülü bisbenzimidazolyum dibromürler

3. Mikrodalga Destekli Tepkimelerde Sentez Kolaylığı

Yaklaşık otuz yıldan bu yana organik sentezlerde mikrodalga radyasyonu ile dielektrik ısıtma kullanılmaktadır. Bu tür ısıtmanın yapılabilmesi

için mikrodalga radyasyonunu alan malzemenin dielektrik katsayısının yüksekliğine göre ısıtma da güçlü olacaktır. Gün geçtikçe sentezde önemini artıran mikrodalga geleneksel ısıtma ile kıyaslandığında mükemmel bir şekilde tepkime süresini kısaltıp seçiciliği artırarak hedef ürünün verimini artırmaktadır [38-40]. İlk defa 1996 yılında mikrodalga desteği SM tepkimelerinde kullanılmış olup [41] şaşırtıcı etkisi nedeniyle sonrasında birçok eşleşme tepkimelerinde destekleyici teknik olarak kullanılmıştır [42,43]. Suzuki-Miyaura tepkimelerinde mikrodalga ısıtma ile geleneksel ısıtma kıyaslandığında tepkime verimleri yakın olduğu halde tepkime süreleri saatlerden dakikalara hatta saniyelere düşmektedir [44-47]. Bu yüzden mikrodalga destekli tepkimelerin ileriki yıllarda sayısının artacağını öngörmek zor değildir.

4. Benzimidazol Tuzlarının Mikrodalga Destekli SM Tepkimelerinde Ligant Olarak Kullanımı

Yılmaz vd. tarafından gerçekleştirilen çalışmada [48] NHC öncülü olarak furfuril ve tiyenil grupları içeren bisbenzimidazol tuzları sentezlenerek (Şekil 4.1) yapıları spektroskopik yöntemlerle (^{1}H, ^{13}C-NMR ve IR) belirlendikten sonra mikrodalga destekli SM tepkimelerinde etkinlikleri belirlenmek üzere bir dizi optimizasyon denemeleri yapılmıştır.

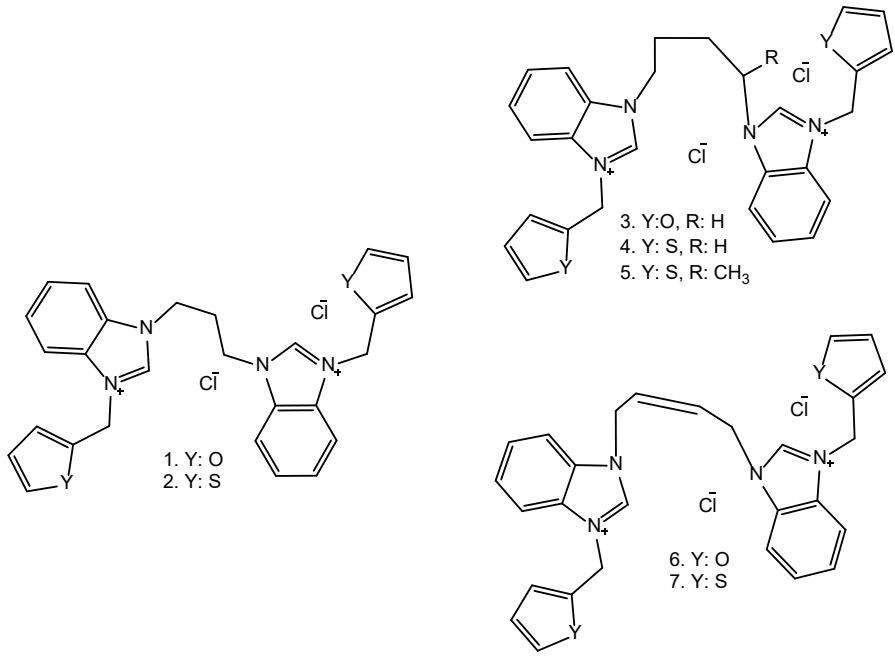

Şekil 4.1. Furfuril ve tiyenil grupları içeren bisbenzimidazol tuzları

Katalitik sistemde bulunan $Pd(OAc)_2$/benzimidazol tuzu oranı, çözücü karışımı, baz türü, geleneksel ısıtma etkisi, mikrodalga gücü vs. belirlenerek en etkin oranlar belirlenmiştir (Şekil 4.2).

Şekil 4.2. Optimizasyon tepkimeleri

Buna göre şartlar en etkin hale getirildiğinde tüm SM tepkimelerinin uygulanması için % 1 mmol $Pd(OAc)_2$, % 1 mmol benzimidazolyum diklorür tuzu (1-7), 1 mmol aril halojenür, 1.2 mmol fenilboronik asit 2 mmol K_2CO_3 ve DMF/H_2O çözücü karışımı kullanılmıştır. Tepkimeler 145 °C de 400 W güçte mikrodalga ısıtma kullanılarak 5 dakikada % 25-99 aralığında verimler ile gerçekleştirilmiştir. (Şekil 4.3)

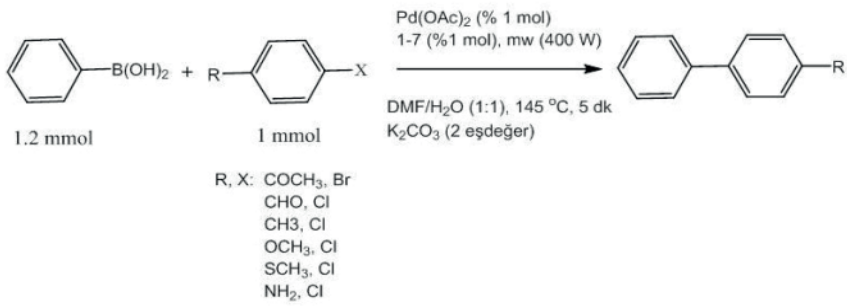

Şekil 4.3. SM Tepkimeleri

SM tepkimeleri için en etkili benzimidazol ligantları bulmaya yönelik yapılan başka bir çalışmada [49] ise trimetilsililmetil grubu içeren bir seri benzimidazol tuzu sentezlenerek mikrodalga destekli tepkimelerde kullanılmıştır. Çalışmada elektron sağlayıcı gruplara sahip tuzlarının katalitik sistemde daha etkili oldukları görülmüştür (Şekil 4.4).

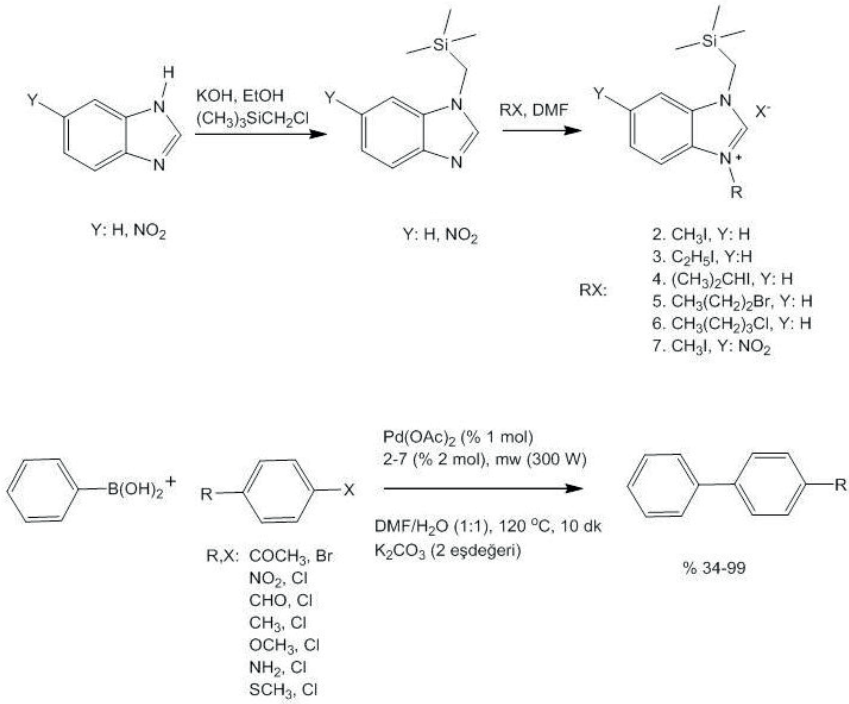

Şekil 4.4. Trimetilsislilmetil içerikli benzimidazol tuzlarının tepkimelere etkisi

Mikrodalga desteki SM tepkimelerine benzimidazol ligantlarının katkısı inert tepkime ortamı gerektirmediğinden oldukça değerlidir. Bir grup silisyum içeren benzimidazol tuzu (Şekil 4.5) ile yapılan C-C bağı oluşum tepkimelerinde yüksek verimler kaydedilmiş ayrıca 4-kloroanisol ile yapılan tepkimelerde ise tepkime verimleri % 50-76 aralığında olup deaktif klorlu halojenürler olamalarına rağmen oldukça iyi sonuçlardır [40].

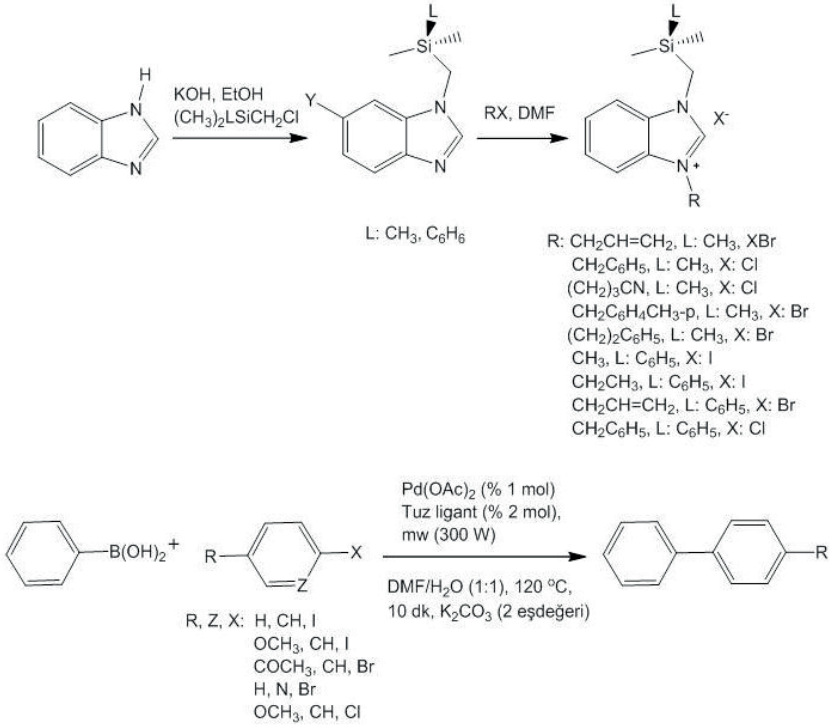

Şekil 4.5. Silisyum taşıyan benzimidazolyum halejenürler ve SM tepkimelerinde ligant etkileri

Heck, Sonoghashira, Buchwald-Hartwig ve Suzuki-Miyaura eşleşme tepkimelerinde de Pd varlığında kullanılan N-ftalimidoetil gruplarına sahip benzimidazolyum bromürler (Şekil 4.6) tepkime verimlerinin dikkate değer artışına sebep olmuştur. Özellikle SM tepkimelerinde aril bromürlerden % 86-96 izole verimler ile bifenil türevleri elde edilmiştir [51].

Bunların dışında $Pd(OAc)_2$ yanında ligant olarak kullanılan benzil, 3-fenilpropil ve alkanil köprü içeren benzimidazol tuzları ile fenilboronik asit, fenil-1,4-diboronik asit, 2- ve 3-halopiridinler, 1-bromonaftalin, aril klorür ve bromürlerin reaktif olarak kullanıldığı tepkimelerde yüksek verimler ile mikrodalga destekli SM tepkimelerinin katalizlenmesini dakikalar içerisinde sağlamışlardır [52-55].

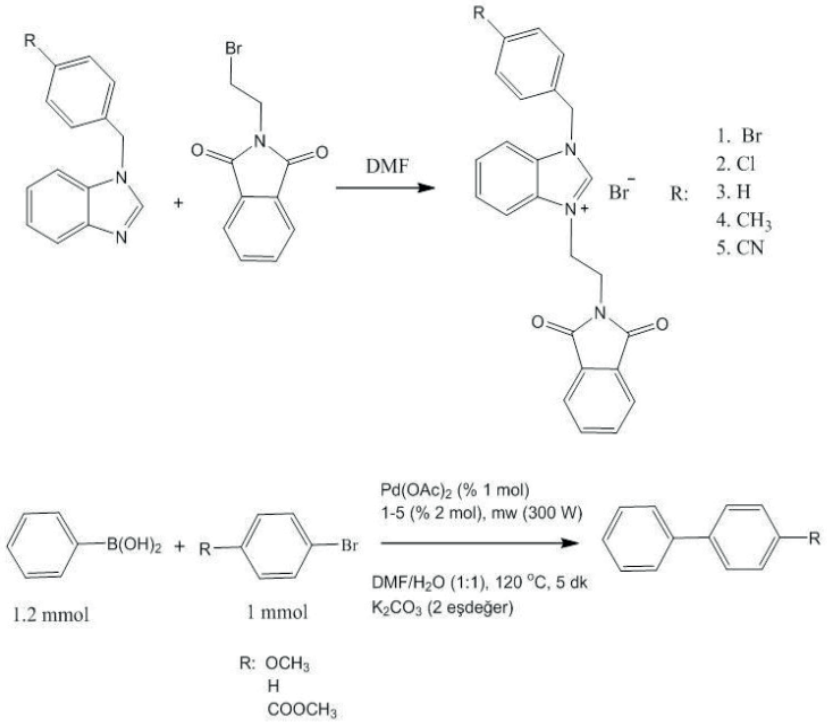

Şekil 4.6. N-ftalimidoetil grupları taşıyan benzimidazolyum halejenürler ve SM tepkimelerinde ligant etkileri

Özetle, NHC öncülü benimidazolyum halojenürler ve $Pd(OAc)_2$ dan oluşan homojen katalitik sistemler kullanılarak katalizlenen SM tepkimeleri birkaç saatlik tepkime sürelerinde ve ılıman koşullarda oldukça iyi verimler ile gerçekleştirilmektedir. Bununla birlikte tepkime olarak mikrodalga dielektrik ısıtma ile desteklenirse dakikalara hatta saniyelere düşen tepkime süreleriyle şaşırtıcı derecede verimli SM tepkimeleri gerçekleştirilmektedir.

Kaynaklar

1. D.A. Horton, G.T. Bourne, M.L. Smythe, *Chem. Rev.*, **2003**, 103, 893-930.
2. G.W. Bemis, M.A. Murcko, *J. Med. Chem.*, **1996**, 39, 2887-2893.
3. https://go.drugbank.com/unearth/q?query=biphenyl&button=&searcher=drugs.
4. N. Miyaura, A. Suzuki, *Chem. Rev.*, **1995**, 95, 2457-2483.
5. A. Suzuki, *Chem. Lett*., **2011**, 40, 894-901.
6. S.P. Stanforth, *Tetrahedron*, **1998**, 54, 263-303.
7. C. Zhang, J. Huang, M.L. Trudell, S.P. Nolan, *J. Org. Chem.* **1999**, 64, 3804-3805.
8. N. Miyaura, K. Yamada, H. Suginome, A. Suzuki, *J. Am. Chem. Soc.*, **1985**, 107, 972-980.
9. S. Akkoç, Y. Gök, İ. Özer İlhan, V. Kayser, *Current Org. Synth*., **2016**, 13, 761-766.
10. P. Ruiz-Castillo, S.L. Buchwald, *Chem. Rev.*, **2016**, 116, 12564-12649.
11. M.C. D'Alterio, E. Casals-Cruanas, N.V. Tzouras, G. Talarico, S.P. Nolan, A. Poater, *Chem. Eur, J.* **2021**, *27*, 13481-13493.
12. E.E. Martinez, C.A. Jensen, A.J.S. Larson, K.C. Kenney, K.J. Clark, S. Hadi Nazari, G.A. Valdivia-Beroeta, S.J. Smith, D.H. Ess, D.J. Michaelis, *Adv. Synth. Catal.* **2020**, *362*, 2876-2881.
13. F.P. Malan, E. Singleton, P.H. van Rooyen, M. Landman, *J. Organomet. Chem.,* **2016***,* 813, 7-14.
14. A. Suzuki, *Chem. Commun.*, **2005**, 38, 4759-4763.
15. M. Garcia-Melchor, A.A.C. Braga, A. Lledos, G. Ujaque, F. Maseras, *Acc. Chem. Res.* **2013**, 46, 2626-2634.
16. A. Suzuki, *J. Organomet. Chem.*, **1999**, 576, 147-168.
17. N.T.S. Phan, M. Van Der Sluys, C.W. Jones, *Adv. Synth. Catal.,* **2006**, 348, 609-679.
18. I.P. Beletskaya, F. Alonso, V. Tyurin, *Coord. Chem. Rev*., **2019**, 385, 137-173.
19. F. Mazars, G. Zaragoza, L. Delaude, *J. Organomet. Chem.*, **2022**, 987, 122489.
20. W.A. Herrmann, K. Öfele, D. v. Preysing, S.K. Schneider, J. Organomet. Chem. 6 87 (2003) 229–248.
21. S. Di ´ez-González, S.P. Nolan, *Top. Organomet. Chem*., **2007**, 21, 47-82.
22. M.G. Organ, G.A. Chass, D.-C. Fang, A.C. Hopkinson, C. Valente, *Synthesis*, 2008, 2776-2797.

23. P.P. Nair, A. Jayaraj, C.A. Swamy, *ChemistrySelect,* **2022**, *7*, e202103517, 1-20.
24. W.A. Herrmann, M. Elison, J. Fischer, C. Köcher, G.R.J. Artus, *Angew. Chem. Int. Ed. Eng.* **1995**, 34, 2371-2374.
25. C.J. O'Brien, E.A.B. Kantchev, C. Valente, H. Niloufar, N. Hadei, G.A. Chass, A. Lough, A.C. Hopkinson, M.G. Organ, *Chem. Eur. J.*, **2006**, 12, 4743-4748.
26. Böhm, V. P. W.; Gstöttmayr, C. W. K.; Weskamp, T.; Herrmann, W. A. J. Organomet. Chem. 2000, 595, 186-190.
27. C. Zhang, J. Huang, M.L. Trudell, S.P. Nolan, *J. Org. Chem*., **1999**, 64, 3804-3805.
28. A. Fürstner, A. Leitner, *Synlett*, **2001**, 290-292.
29. K. Arentsen, S. Caddick, F. Geoffrey, N. Cloke, A.P. Herring, P.B. Hitchcock, *Tetrahedron Lett.*, **2004**, 45, 3511-3515.
30. M.R. Kumar, K. Park, S. Lee, *Adv. Synth. Catal*., **2010**, 352, 3255- 3266.
31. P.N. Muskawar, P. Karthikeyan, S.A. Aswar, P.R. Bhagat, S. Senthil Kumar, *Arab. J. Chem.,* **2016**, *9*, 1765-1778.
32. Ü. İşçi, M. Aygün, R. Sevincek, Y. Zorlu, F. Dumoulin, *Turk. J. Chem*., **2015**, 39, 1300-1309.
33. C-C. Chiu, H-T. Chiu, D-S. Lee, T-J. Lu, *RSC Adv.*, **2018**, 8, 26407-26415.
34. T. Wang, T-R. Wei, S-J. Huang, Y-T. Lai, D-S. Lee, T-J. Lu, *Catalysis*, **2021**, 11, 817, 1-13.
35. S. Demir Düşünceli, M.H. Şahan, M. Kaloğlu, E. Üstün, İ. Özdemir, *J. Chin. Chem. Soc*., **2022**, 69, 1937-1953.
36. M. Yiğit, *Molecules,* **2009***, 14,* 2032-2042.
37. İ. Özdemir, Y. Gök, N. Gürbüz, E. Çetinkaya, B. Çetinkaya, *Synth. Commun*., **2004**, 34, 4135-4144.
38. C.O. Kappe, *Chem. Soc. Rev.*, **2008**, 37, 1127-1139.
39. I.D. Kostas, G.A. Heropoulos, D. Kovala-Dmertzi, P.N. Yadav, J.P. Jasinski, M.A. Demertzis, F.J. Andreadaki, G. Vo-Thanh, A. Petit, A. Loupy, *Tetrahedron Lett*., **2006**, 47, 4403-4407.
40. N.E. Leadbeater, M. Marco, *J. Org. Chem.,* **2003**, *68*, 888-892.
41. M. Larhed, A. Hallberg, *J. Org. Chem*. **1996**, 61, 9582-9584.
42. J. Westman, *Org. Lett.* **2001**, 3, 3745-3747.
43. A. Stadler, A.C. Kappe, *Eur. J. Org. Chem.,* **2001**, 919-925.
44. O. Navarro, H. Kaur, P. Mahjoor, S.P. Nolan, *J. Org. Chem.,* **2004**, *69*, 3173-3180.
45. A. Dolsak, K. Mrgole, M. Sova, Catalysis, 2021, 11, 439, 1-16.

46. K. L. dos Santos Castro, P.G. de Lima, L.S.M. e Miranda, R.O.M.A. de Souza, *Tetrahedron Lett*., **2011**, 52, 4168-4171.

47. L. shen, S. Huang, Y. Nie, F. Lei, *Molecules,* **2013**, *18*, 1602-1612.

48. Ü. Yılmaz, N. Şireci, S. Deniz, H. Küçükbay, *Appl. Organometal. Chem.,* **2010**, *24*, 414-420.

49. Ü. Yılmaz, H. Küçükbay, N. Şireci, M. Akkurt, S. Günal, R. Durmaz, M. Nawaz Tahir, *Appl. Organometal. Chem.* **2011**, *25*, 366–373.

50. H. Küçükbay, N. Şireci, Ü. Yılmaz, S. Deniz, M. Akkurt, Z. Baktır, O. Büyükgüngör, Turk. J. Chem., 2012, 36, 201-217.

51. H. Küçükbay, Ü. Yılmaz, K. Yavuz, N. Buğday, Turk. J. Chem., 2015, 39, 1265-1278.

52. Ü. Yılmaz, S. Deniz, H. Küçükbay, N. Şireci, *Molecules* **2013**, *18*, 3712-3724.

53. Ü. Yılmaz, H. Küçükbay, S. Türktekin Çelikesir, M. Akkurt, O. Büyükgüngör, Turk. J. Chem., 2013, 37, 721-733.

54. Ü. Yılmaz, H. Küçükbay, Naturengs, 2020, 1, 47-52.

55. Ü. Yılmaz, H. Küçükbay, Turk. J. Chem., 2018, 42, 1706-1719.

Chapter 6

A Pilot Study of Radionuclides Analysis of Human Placenta According to Different Ages

Oğuz Kağan Köksal[1]

Ömer Söğüt[2]

Fazıl Avcı[3]

Sultan Şahin Bal[4]

Abstract

In this study, radionuclides Th-232, K-40, Na-22, Eu-152, Ra-226, and Bi-207 were detected in placenta samples from 24 mothers who gave birth between the ages of 20 and 49. A NaI gamma detector with an ORTEC-branded scintillator that measures 7.62 cm x 7.62 cm and has a crystalline thallium-doped yield of 2% at 0.5 MeV and 1.3% at 2 MeV was used to test radionuclides. For 86400s, the placenta samples were counted (24 hours). Using Maestro-32 software, the peak areas in the obtained spectra were captured, entered into the proper equations, and the radionuclide activity concentrations were computed as Bq/g. Th-232, K-40, Na-22, Eu-152, Ra-226, and Bi-207 activity concentrations were determined based on different ages. Th-232, K-40, Na-22, Eu-152, Ra-226, and Bi-207 activity concentrations were found, and they varied depending on the radionuclide's age. These concentrations ranged from 8.470.20 to 34.911.27 Bq/g for Ra-226, from 0.781.03 to 25.581.03 Bq/g for Th-232, from 5.100.35 and 32.371.66 Bq/g for K-40, from 4.620.66 and 14. In order to develop the methodology for a more in-depth analysis, this pilot study evaluated the capability to identify particular radionuclides in placentea samples.

1 Adıyaman University Faculty of Engineering Department of Electrical and Electronics Engineering, 02040 Adıyaman, Türkiye.

2 Kahramanmaraş Sütçü İmam University, Faculty of Arts and Science, Department of Physics, Kahramanmaraş, 46100 Türkiye.

3 Republic of Turkey Ministry of Health, Provincial Health Directorate of Konya, Akşehir State Hospital, Türkiye

4 Bitlis Eren University, Faculty of Arts and Science, Department of Physics, Bitlis, Türkiye.

https://doi.org/10.58830/ozgur.pub252.c1217

1. Introduction

The placenta is the additional embryonic tissue that arises during pregnancy between the uterine mucosa and the chorion of the progeny for the development and protection of the offspring. The organ responsible for facilitating the exchange of nutrients, oxygen, and other substances between the mother and the fetus is the placenta. Most people tend to think of this exchange as a technique to alter the location where the mother's blood and the baby' blood shift. The mother's blood does not, however, combine with that of the fetus. From the outset of pregnancy, there is chemical communication between the mother and the fetus, and these hormonal and chemical messages continue to be beneficial to the infant until birth. The nutrients and oxygen required for the development of new cell groups and tissues are carefully chosen by the placenta and transported to the fetus. The waste products that are produced are separated, though, and sent to the mother's body. Due to the extensive cellular division and differentiation that occurs during embryological development, prenatal life is regarded as the most delicate stage of human development. Because of this, exposure to any environmental toxins at this time can have serious consequences. Numerous people are exposed to environmental contaminants from numerous sources, such as radionuclides, heavy metals, organic hydrocarbons, and pesticides, as a result of rising industrial pollution and man-made or natural combustion activities around the world. It is acknowledged that these pollutants gradually worsen the public health and are particularly harmful throughout the era of growth and development. The fetus is far more vulnerable to teratogens than an adult is, even at modest exposure levels that normally do not affect the mother [1, 2]. Exposure can result in structural alterations that are permanent if it happens during organ development [3].

The environment and living things are highly at risk from radionuclides, which are radioactive materials that release ionizing radiation during the decay of active atoms [4]. The placental transmission mechanism of radioactive substances has garnered particular attention in research on the radiation load to which the human organism is exposed by the addition of radioactive nuclides.

It might be possible to see this issue from new angles by estimating some of the adverse impacts that radioactive elements might have on the fetal organism. However, it is also possible to learn more about the process by which these nuclides are incorporated into the developing organism [5]. As a result of the use of radiation, humans are exposed to radiation doses at various rates. However, humans often absorb radionuclides through inhalation,

food, and water. A significant portion of the exposure from natural sources falls under a specific form of internal radiation exposure where the bronchial epithelium is exposed to alpha particles from radon's short-lived offspring [6, 7, 8]. Since the main source of natural radioactivity in soil samples is typically identified by the activity of Ra-226, Th-232, and K-40, it is crucial to identify the level of natural radioactivity in the soil [9]. Due to the fact that these radionuclides can enter people through the food chain, natural radioactive substances like Th-232, Ra-226, and K-40 can reach dangerous radiological levels in some circumstances [10]. Th-232 and Ra-226 are the radionuclides that are among them that are the most dangerous. Determining the health dangers to a developing life, such as a fetus, is crucial for this reason. Drinks, food, and breath can all introduce radium, europium, and K-40 into the body, posing both internal and external risks. According to certain research, neonates absorb more radionuclides than older children and adults. It is considered that adult fractional absorption values greater than 0.5 correlate to 100% absorption in newborns and infants. It is generally agreed that infant absorption values between 0.5 and 0.01 in adults should be increased by a factor of two. Values of 0.001 or less in adults are accepted with a ten-fold increase [11].

In contrast, when an assessment is made for drug- and food-based transfers, drug and nutrient transfers are explained by mechanisms such as passive, facilitated diffusion, and active transmission [12, 13]. A tentative classification of transport mechanisms across the human placenta is based on (a) primary physiological significance of transferred substances, (b) relative transfer rates, (c) true transport mechanisms, and (d) equality or inequality in distribution [14]. The absence of nucleotides in food or medicine, however, does not sufficiently explain whether or not they transfer. According to our research, certain nucleotides were transported while others were not.

By investigating the identification of specific radionuclides in placentea samples, this pilot study sought to establish the methodology such as preparation of samples and radionuclide measurements and utilized statistics analysis for a more thorough investigation. It will also serve as a reference for upcoming research.

2. Material and Method

2.1. Preparation of Samples and Making Measurements

Nearly 578 kilometers to the southeast of Turkey's capital, Ankara, lies the Mediterranean city of Kahramanmaraş, which is 568 meters above sea level. The city is situated between the 36th and 37th east meridian and the 37th

and 38th north parallel. At 26 weeks, placenta samples from 24 women who gave birth between the ages of 20 and 49 were obtained in 2013 at the Sutçü Imam University (KSU) Faculty of Medicine, Department of Obstetrics and Gynecology. Donors don't reside close to any nuclear or mineral facilities, while living in the city's center. However, it's possible that the people who live in this community will eat the fish in a contaminated reservoir. After being collected, cleaned, and weighed, the samples were stored in an oven at a constant temperature of 105 °C for three weeks. The ashing operation was done at a steady temperature of 105°C to avoid the samples burning in the oven. The samples were prepared for measurements by being sieved through a 200-mesh sieve after being smashed in a mortar.

2.2. Radionuclide Measurements

Gamma ray spectrometry was used to measure the activity concentration of radionuclides in placenta samples using a 7.62 cm x 7.62 cm NaI(Tl) detector [14]. This gamma spectrometer offers an energy resolution of 8% for 662 keV and a relative counting efficiency of roughly 20%. For the accuracy of the results, it is crucial that the system efficiency calibration be completed before the measurement. Gamma sources Cs-137 (662 keV (85.1%)), Co-60 (1172 keV (99.86%), and 1332 keV (99.98%) were used for the efficiency calibration. The referenced study provides a thorough explanation of how the detector in this study was calibrated [15]. The gamma spectrum was examined using the ORTEC-provided Maestro-32 program. Every 86400 seconds, every sample was counted (24 hours). To prevent unintentional radiation exposure, the detector is encased in a lead shield. The activity concentrations of Th-232, K-40, Na-22, Eu-152, Ra-226, and Bi-207 radionuclides were computed as Bq/g using these fields in the equation shown below.

$$A = \frac{C}{\varepsilon \, x \, \gamma \, x \, t \, x \, m} \qquad (1)$$

where m (g) is the mass of the dried and prepared samples for measurement, A (Bq/g) is the radioisotope concentration, C (counts) is the net peak area, ε is the detector efficiency, t (86400 s) is the counting time, and γ is the absolute transition probability of -decay. The difference between the areas of the peaks visible in the spectrum and the areas of the peaks determined from the BKGR (background = basic count) count is the area value, which is represented as the net peak area (C) in the equation. Figure 1 shows a picture of the experimental setup used to take the measurements.

Additionally, Figure 2 displays the spectrum for S4, including the start and end points. The nuclides used in this study's analysis were subjected to the energies displayed below.

Na-22: 511.01 keV and 1274.53 keV (Na-23 photo-peak)

Eu-152: 121.78 keV, 344.27 keV, 841.54 keV, 963.34 keV, 970.30 keV, 1314.61 keV and 1389.00 keV (Eu-151 photo-peak)

Bi-207: 569.70 keV, 1063.66 keV and 1770.23 keV (Pb-207 photo-peak)

These radioisotopes have energy in the channels where the peaks in the spectra obtained from the analysis of the samples coincide. The device's library also contains the energy of these isotopes and their peaks.

2.3. Statistics

Table 1's results are all provided as average-error values (x-error). For the statistical analysis of various ages and radionuclide activity concentrations, the IBM SPSS 22 program was employed. The link between various ages and radioactive activity concentrations was examined using Pearson correlation analysis. The range of the correlation coefficient is from -1 to +1. A negative correlation, on the other hand, is defined as one of the variable pairs rising while the other declines, and it is defined as the correlation coefficient taking values between 0 and -1. A positive correlation, which ranges from 0 to 1, indicates that the two variables change in tandem. Additionally, whether negative or positive, the connection is stronger the closer the correlation coefficient is to +1 or -1. Table 2 provides the correlation coefficients between the various factors.

3. Results and Discussion

Table 1 lists the radionuclide concentrations found in the tissues of the human placenta. As seen from Table 1 and Figure 3, the radionuclide activity concentrations measured in placenta samples are varied in between 34.91±1.27 8.47±0.20 Bq/g for Ra-226, between 25.58±1.03 and 0.78±1.03 Bq/g for Th-232, between 32.37±1.66 and 5.10±0.35 Bq/g for K-40, between 14.36±1.09 and 4.62±0.66 Bq/g for Eu-152, between 18.92±0.80 and 1.50±0.07 Bq/g for Na-22 and between 28.47±0.11 and 1.05±0.20 Bq/g for Bi-207. Also, the net mass of the placenta samples are tabulated at the same table.

As seen from Table 1 and Figure 3, Ra-226 was detected in all of the placenta samples in "all different ages". The highest Ra-226 value measured

34.91 Bq/g in the 30 age ~~group~~ (S11), while the lowest value measured 8.47 Bq/g in the 31 years old (S12). Th-232 radionuclide could not be detected in samples S20, S21, S23, S31, S34, S39 and S40. However, the highest amount of Th-232 was measured as 25.58 Bq/g in the 36 years old (S17) and the lowest Th-232 amount was measured in the 49 years old (S24). K-40 radionuclide could not be detected in the placenta samples S23, S24, S26, S29, S33, S35, S36, S39 and S41. However, the highest amount measured to be 32.37 Bq/g in the 25 years old (S6), while the lowest amount was measured as 5.10 Bq/g in the 34 years old (S15). The Eu-152 radionuclide was detected in all placental samples. The highest concentration of Eu-152 was measured as 14.36 Bq/g in the sample no. S5 (24 years old) and the lowest amount of Eu-152 was measured as 4.62 Bq/g in the sample S17, that is, in the 36 years old. Na-22 radionuclide could not be detected in placental samples coded S7, S17, S18, S19 and S24. For all that, while the highest Na-22 radionuclide concentration was determined as 18.92 Bq/g in the S11 coded sample, the lowest Na-22 amount was measured as 1.50 Bq/g in the S13 coded sample. Finally, in only one sample (S17), the radionuclide Bi-207 could not be measured. The highest Bi-207 radionuclide concentration was measured to be 28.47 Bq/g in the sample numbered S19, and the lowest Bi-207 radionuclide amount was also detected in the S24 coded sample as 1.05 Bq/g.

The amount of each radionucloid versus age can be seen at Figure 3. Although there is no significant correlation with age, the variation trend of each nucleoid is similar when all age groups are taken into account.

4. Conclusion

The placenta formed by the extraembryonic tissue that develops between the baby's chorion and the uterine mucosa during pregnancy for the development and protection of the embryo/fetus.It provides nutrition, development, respiration and excretion of the embryo/fetus.During the development of the embryo, it secretes different hormones. The placenta, which acts as a lung from time to time, takes over kidney function from time to time. Therefore, the placenta performs a multifunctional task [12, 13] (web 1). Radionuclide activity concentrations of Th-232, K-40, Na-22, Eu-152, Ra-226 and Bi-207 were measured in placenta tissue samples taken from a total of 24 pregnant women aged 20 to 49 years. The radionuclide activity concentrations are varied in between 34.91±1.27 and 8.47±0.20 Bq/g for Ra-226, between 25.58±1.03 and 0.78±1.03 Bq/g for Th-232, between 32.37±1.66 and 5.10±0.35 Bq/g for K-40, between 14.36±1.09 and 4.62±0.66 Bq/g for Eu-152, between 18.92±0.80 and 1.50±0.07

Bq/g for Na-22 and between 28.47±0.11 and 1.05±0.20 Bq/g for Bi-207. Statistical analysis was performed for the correlation between Th-232, K-40, Na-22, Eu-152, Ra-226 and Bi-207 radionuclide activity concentrations and different ages. But, no statistically significant correlation was determined between different ages and radionuclide activity concentrations. The data obtained could not be compared since it is unclear from the literature whether radionuclide activity concentration measurements are done in human placental tissues. Due to the fact that it has not yet been established whether the mothers have radionuclides it is unclear whether the radionuclide activity concentrations measured in Table 1 and Figure 3 are harmful to human health. The human body contains radioisotopes in its natural state. It's not just K-40; other isotopes include I-129, uranium, thorium, carbon, polonium, etc. Radiological examinations of placentas that belonged to both the mothers and the fetuses were carried out. There were no additional evaluations or measurements of the mother.

In addition, the tendency of each nucleotide to decrease and increase in all different ages is similar to each other although there are different sources of radionuclides. This pilot study intended to establish the methods, such as sample preparation and radionuclide measurements, and used statistical analysis for a more in-depth investigation by looking into the identification of individual radionuclides in placentea samples. It will also be used as a source for future studies.

Acknowledgement

The Scientific Research Projects Coordination Unit at Kahramanmaraş Sütçü İmam University is gratefully acknowledged by the authors for providing financial support for the completion of this study. (Project no: 2014/1-5M).

Table 1. The radionuclide activity concentrations measured as Bq/g in placenta samples (mean ±error, n=3).

Samples	Age	Ra-226	Th-232	K-40	Eu-152	Na-22	Bi-207	Mass (kg)
S1	20	14.72±0.44	BDL	13.47±0.26	9.30±0.98	11.14±0.44	18.81±0.72	0,0780
S2	21	26.60±1.03	BDL	20.84±2.51	8.81±0.77	10.08±0.65	13.54±0.09	0,0760
S3	22	22.45±0.80	13.33±0.94	10.17±0.90	7.71±1.09	11.24±0.39	14.40±0.08	0,0784
S4	23	22.69±0.70	BDL	BDL	8.48±0.75	4.83±0.05	6.47±0.32	0,0835
S5	24	29.70±0.99	20.96±0.83	BDL	14.36±1.09	11.30±0.30	23.35±0.87	0,0789
S6	25	16.75±0.61	13.87±0.65	32.37±1.66	10.08±1.03	17.68±0.62	22.71±0.73	0,0713
S7	26	23.47±0.85	9.30±0.49	BDL	6.73±0.60	BDL	4.83±0.32	0,0868
S8	27	13.78±0.55	3.98±0.47	30.73±0.44	10.39±0.83	2.94±0.06	12.33±0.38	0,0799
S9	28	22.55±0.63	21.97±1.45	21.41±1.81	12.07±1.04	12.39±0.29	19.69±0.14	0,0704
S10	29	17.31±0.71	20.26±0.97	BDL	7.23±0.73	4.57±0.06	16.92±0.20	0,0793
S11	30	34.91±1.27	16.74±0.55	18.88±1.74	12.97±0.98	18.92±0.80	3.02±0.10	0,0701
S12	31	8.47±0.20	BDL	6.72±0.22	8.52±0.76	9.64±0.50	13.07±0.30	0,0741
S13	32	13.79±0.46	6.70±1.75	30.00±1.26	3.86±0.59	1.50±0.07	18.72±0.95	0,0803
S14	33	19.53±0.65	13.26±0.61	BDL	8.88±0.66	8.41±0.30	4.00±0.53	0,0789
S15	34	24.16±0.63	BDL	5.10±0.35	9.14±0.77	12.51±0.52	21.18±1.15	0,0739
S16	35	16.80±0.62	8.59±0.51	BDL	5.48±0.50	5.87±0.17	1.89±0.18	0,0749
S17	36	22.43±0.84	25.58±1.03	BDL	4.62±0.66	BDL	4.84±0.61	0,0500
S18	37	13.04±0.54	21.80±1.23	5.61±0.97	9.69±0.77	BDL	BDL	0,0743
S19	38	25.90±0.89	6.41±0.58	19.09±2.12	14.33±0.96	BDL	28.47±0.11	0,0748
S20	39	23.60±0.75	BDL	BDL	7.26±0.78	8.18±0.06	8.34±0.20	0,0707
S21	40	16.74±0.51	24.23±1.54	14.11±0.32	13.40±1.22	7.41±0.29	8.13±0.58	0,0626
S22	41	21.21±0.85	10.84±0.41	BDL	8.78±0.89	10.45±0.30	15.18±0.67	0,0742
S23	42	16.10±0.61	BDL	14.49±0.72	13.13±0.86	9.18±0.28	25.30±0.36	0,0764
S24	49	23.07±0.85	0.78±1.03	29.85±0.98	10.67±0.91	BDL	1.05±0.20	0,0731

BDL:Below Detection Limit

Table 2. Correlation Coefficients

Correlation	N	p	r	results
Age*Ra-226	24	0.690	-0.086	Relationship weak, not significant
Age*Th-232	17	0.749	-0.084	Relationship weak, not significant
Age*K-40	15	0.969	-0.011	Relationship weak, not significant
Age*Eu-152	24	0.589	0.116	Relationship weak, not significant
Age*Na-22	19	0.526	-0.155	Relationship weak, not significant
Age*Bi-207	23	0.421	-0.176	Relationship weak, not significant

Fig. 1. Experimental set up.

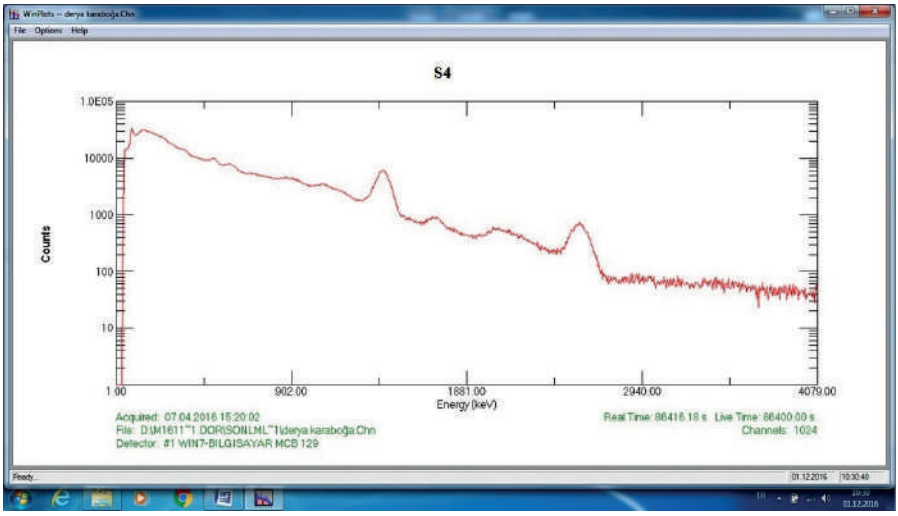

Fig. 2. The spectrum for S4 sample

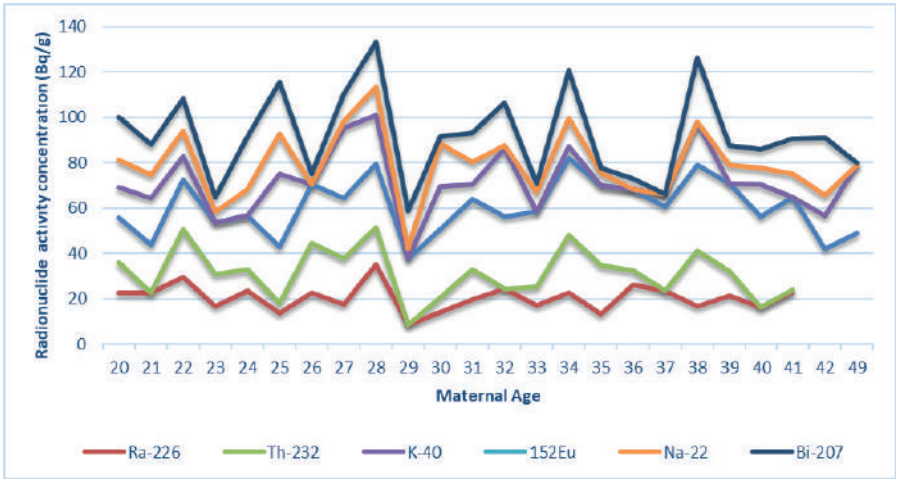

Fig. 3. Variation of each radionuclide according to different ages

References

1. Al-Saleh I, Shinwari N, Mashhour A, Mohamed GED, Rabah A. Heavy metals (lead, cadmium and mercury) in maternal, cord blood and placenta of healthy women. International journal of hygiene and environmental health. 2011;214:79-101.
2. Wells PG, Lee CJ, McCallum GP, Perstin J, Harper PA. Receptor-and reactive intermediate-mediated mechanisms of teratogenesis. Adverse Drug Reactions. 2010:131-62.
3. Sly PD, Flack F. Susceptibility of children to environmental pollutants. Annals of the new York Academy of Sciences. 2008;1140:163-83.
4. UNEP F. Global Assessment of Soil Pollution—Summary for Policy Makers. FAO Rome, Italy:; 2021.
5. Rajewsky B, Belloch-Zimmermann V, Lohr E, Stahlhofen W. 226Ra in human embryonic tissue, relationship of activity to the stage of pregnancy, measurement of natural 226Ra occurrence in the human placenta. Health Physics. 1965;11:161-9.
6. Radiation UNSCotEoA. Sources and effects of ionizing radiation, ANNEX B, Exposures from natural radiation sources. UNSCEAR 2000 REPORT, New York. 2000;1:97-9.
7. Omeje M, Adewoyin O, Joel ES, Ehi-Eromosele C, Emenike PC, Usikalu M, Akinwumi S, Zaidi E, Saeed MA. Natural radioactivity concentrations of 226Ra, 232Th, and 40K in commercial building materials and their lifetime cancer risk assessment in Dwellers. Human and Ecological Risk Assessment: An International Journal. 2018.
8. Sharama N, Sharama R, Virk H. Environmental radioactivity: A case study of Punjab. India, Advanced in applied science research. 2011;2:186-90.
9. NEA-OECD N. Exposure to radiation from natural radioactivity in building materials. NEA Group of Experts OECD. 1979.
10. Sabharwal AD, Bhupinder S, Kumar S, Singh S, Natural radioactivity levels (K, Th and Ra) in some areas of Punjab, India. 2012: Publisher.
11. Jackson P. Age-dependent doses to members of the public from intake of radionuclides: part 5 compilation of ingestion and inhalation dose coefficients (ICRP Publication 72). IOP Publishing; 1996.
12. Karaca T, Yörük M. Structure and function of ruminant placenta. Yüzüncü yıl Üniversitesi Veteriner Fakültesi Dergisi. 2010;21:191-4.
13. Kılıçoğlu Ç, Alaçam E. Veteriner doğum bilgisi ve üreme organlarının hastalıkları. Ankara Üniversitesi Veteriner Fakültesi Yayınları. 1985;403:6-26.

14. Şahin Bal S. The determination of concentrations of radioisotopes in some granite samples in Turkey and their radiation hazards. Radiation Effects and Defects in Solids. 2018;173:353-66.
15. Akkurt I, Gunoglu K, Arda S. Detection efficiency of NaI (Tl) detector in 511–1332 keV energy range. Science and Technology of Nuclear Installations. 2014;2014.

Web 1:https://www.bulenttiras.com/plasenta-nedir-ne-ise-yarar; (08.04.2022)

Bölüm 7

Combining Principal Normal Indicatrix Curves And Direction Curves With An Alternative Frame

İlkay Arslan Güven[1]

Fatma Çolak[2]

Abstract

This work examined the direction curves of principal normal indicatrix curves regarding a regular curve in Euclidean space of three dimension. The {N,C,W} frame was assigned as a new alternative frame for the mentioned curve. Investigating relationships among the main curve and direction curves using such novel alternative frame is an innovative approach. The Frenet members, curvature, torsion, harmonic curvature and geodesic curvature of direction curves were determined. Direction curve characterizations in the forms of the C-slant helix , slant helix and general helix were provided. In the end, the relevant figures for these curves were displayed.

1. Introduction

The primary field of differential geometry study that has received the most attention is curve theory. Curves come in many forms. Helix curves, such as those found in animal horns, seedpods, and plant shoots, are prevalent in nature. Additionally, the DNA molecule, which makes up the majority of genetic material, is made up of two chains that helix. These chains have couple helix shapes. Further, Salmonella and Escherichia coli flagella have helices. A screw is the most common example of a helix. It has a helical construction that converts rotation to motion along the axis. Computer graphics and the manufacturing of artificial helices from various materials both use helices.

1 Prof. Dr., Gaziantep University Art and Science Faculty Deparment of Mathematics, iarslan@gantep.edu.tr, 0000-0002-5302-6074

2 Master Student, Gaziantep University Graduate School of Natural and Applied Sciences Deparment of Mathematics, fatmacolak33@gmail.com, 0000-0003-4919-4793

https://doi.org/10.58830/ozgur.pub252.c1285

Ellipstic curves are additionally employed in cryptography. The role that curves play in surfaces is their most significant feature. Curves are useful for generating a surface concept, that works in physics, engineering, industry, and other fields.

One of curve theory's most alluring topics is the associated curve. Associated curves are defined as two or more curves that have a mathematical relationship to one another. These curves include Bertrand curve mates, Mannheim curve mates, adjoint curves and involute-evolute curve mates, among others.

Choi and Kim [3] recently suggested adding a new form of associated curve to the literature. They termed it the direction curve and described it such that the integral curve of an each Frenet vector in the mentioned curve. They gave relationships between related curves' curvature and torsion. They provided a canonical method to build these helices and characterized slant and general helices with regards to associated curves. In Minkowski space, direction curves were studied by Qian and Kim in [11]. Inspired by these direction curves, Macit and Düldül [10] utilized a Frenet curve's Darboux vector of a Frenet curve to find W-direction curves. The V-direction curve of a curve that is located on a surface covered by the Darboux frame was also defined. Kızıltuğ and Önder [7] explored the theory of direction curves in compact Lie groups of three dimension. Körpınar et al. [8] used a curve's Bishop frame to provide direction curves over again.

Another type of associated curve that has been extensively studied for a long time are spherical indicatrix curves. Kula and Yaylı [9] researched slant helices' spherical indicatrix curves. They discovered that these spherical helices are also spherical indicatrices. Şahiner [13] investigated the tangent indicatrix's direction curve and the relationship between spherical and direction curves. These curves belong to the allied curves class as well. Specific relationships between the curves' curvatures were provided. Techniques for obtaining the spherical helix, spherical slant helix, and general helix from the circle were discovered. In Şahiner [14], similar scenarios were examined for principal normal indicatrix curves.

Beside this, frames of curves are crucial to look at when studying curve theory because of their specifications. Examples of adapted curve frames abound. The most well-recognized and commonly used frame is the moving Frenet frame.

According to Uzunoğlu et al. [15], another newly defined attractive frame is $\{N, C, W\}$ which serves as an alternate moving frame. By treating

the principal normal vector N as a constant, such a frame represents the rotated state of a Frenet frame. It has a benefit over the Frenet frame in that the characterization of the slant helix may be expressed more succinctly with the new curvatures. The authors used the curve's curvature and torsion to establish new curvatures, f and g, while they were creating the $\{N, C, W\}$ frame. Regarding the strength of such new frame, they proposed the C-slant helix idea. Such kind of helix arises when the binormal and tangent indicatrix are both spherical slant helices. It was demonstrated that the C-constant precession curve is a C-slant helix and the C-slant helix's specific characterizations were developed. In the sense of the $\{N, C, W\}$ frame apparatus, they also provided the Frenet members of the indicatrix curves.

Our goal in this work is to investigate the combination of the $\{N, C, W\}$ frame, principal normal indicatrix curve and direction curves. We look into the characterizations of principal normal indicatrix curves' direction curves.

2. Basic Concept

Conte[illegible]ferentiable manifold M and an interval I, the differentiable function $\alpha: I \to M$ is referred to as the curve in differential geometry [12].

Three orthogonal vector fields are known as Frenet vectors for a regular curve α and $\alpha' \times \alpha'' \neq 0$. These vector fields are provided by

$$T = \frac{\alpha'}{\|\alpha'\|}, \quad \mathrm{N} = B \times T, \ \mathrm{B} = \frac{\alpha' \times \alpha''}{\|\alpha' \times \alpha''\|}. \tag{2.1}$$

The tangent vector T, the principal normal vector N and the binormal vector B are shown here. The curve's torsion and curvature are computed in the order of

$$\kappa = \frac{\|\alpha' \times \alpha''\|}{\|\alpha'\|^3}, \qquad \tau = \frac{\det(\alpha', \alpha'', \alpha''')}{\|\alpha' \times \alpha''\|^2} \tag{2.2}$$

and Frenet equations are valid as [12]

$$\begin{aligned} T' &= N, \\ N' &= -\kappa T + \tau B, \\ B' &= -\tau N \end{aligned} \tag{2.3}.$$

A new curve frame that follows a curve, the alternative $\{N, C, W\}$ frame, is described as

$$C = \frac{N'}{\|N'\|}, \qquad \mathrm{W} = \frac{\tau T + \kappa B}{\sqrt{\kappa^2 + \tau^2}} \quad .$$

Here; N is the unit principal normal vector of Frenet frame, C is the derivative of principal normal vector and W is the unit Darboux vector. The new curvatures f and g with respect to this new frame are provided by

$$f = \kappa\sqrt{1 + H^2} \quad , \qquad g = \sigma f \qquad (2.4)$$

where $H = \frac{\tau}{\kappa}$ is harmonic curvature of a curve and $\sigma = \frac{\kappa^2}{\left(\kappa^2 + \tau^2\right)^{3/2}}\left(\frac{\tau}{\kappa}\right)'$

is geodesic curvature of spherical image of principal normal indicatrix curve. According to Uzunoğlu et al. [15], the relationship between H and σ is also depicted as

$$\sigma = \frac{H'}{\kappa\left(1 + H^2\right)^{\frac{3}{2}}} \quad , \qquad \Gamma = \frac{\sigma'}{f\left(1 + \sigma^2\right)^{\frac{3}{2}}} \quad . \qquad (2.5)$$

Furthermore, when $H = \frac{\tau}{\kappa}$ is constant, a curve is referred to as a general helix, and the reverse is true [5]. Additionally, σ is constant if and only if it is a slant helix [6].

When a unit speed curve α has a vector field C that creates a constant angle $\theta \neq \frac{\pi}{2}$ with a fixed direction u , the curve is called a C-slant helix, in other words, $\langle C, u \rangle = \cos\theta = \text{constant}$ and the following equation holds for C-slant helix

$$\frac{\left(f^2 + g^2\right)^{\frac{3}{2}}}{f^2\left(\frac{g}{f}\right)'} = \tan\theta = \text{constant} \qquad (2.6)$$

where the constant angle θ is formed between the vector C and the fixed direction u [15].

Now, same basic notions about indicatrix curves will be given.

When curve's each Frenet frame vector is translated to the center of the unit sphere and gathering the end points of them, then indicatrix curves are created on the surface of the unit sphere. The tangent, principal normal and binormal vectors constitute the tangent, principal normal and binormal indicatrix curves, respectively, and the corresponding equations for these curves are shown as [12]

$$\begin{aligned} \alpha_T &= T, \\ \alpha_N &= N, \\ \alpha_B &= B \end{aligned} \tag{2.7}$$

Uzunoğlu et al. [15] gave the equations between the Frenet members of the principal normal indicatrix curve α_N and the curve α, if $\{T_N, N_N, B_N, \kappa_N, \tau_N\}$ is Frenet apparatus of the principal normal indicatrix curve, as;

$$\kappa_N = \sqrt{\sigma^2 + 1}, \quad \tau_N = \Gamma\sqrt{\sigma^2 + 1}. \tag{2.8}$$

and

$$\begin{aligned} T_N &= \frac{\kappa}{f}(-T + HB) \\ N_N &= \frac{\sigma}{\sqrt{\sigma^2+1}}\left[\frac{\kappa}{f}(HT + B) - \frac{1}{\sigma}N\right] \\ B_N &= \frac{1}{\sqrt{\sigma^2+1}}\left[\frac{\kappa}{f}(HT + B) + \sigma N\right]. \end{aligned} \tag{2.9}$$

The parametric curve that provides a unique solution to an equation system is known as an integral curve. If $\beta(t)$ is a parametric curve, Z is a vector field and if $\beta(t)$ solves the differential equation $\beta'(t) = Z(\beta(t))$, then $\beta(t)$ is referred to as an integral curve [12].

3. Direction Curves of Principal Normal Indicatrix Curve

This part includes the direction curves of principal normal indicatrix curves by using the apparatus of alternative frame $\{N, C, W\}$. Some characterizations and properties of these direction curves which are constructed by integrating the Frenet vectors of principal normal indicatrix curve are determined.

Let γ be a regular curve with Frenet frame $\{T, N, B\}$ and γ_N be the principal normal indicatrix curve of the curve γ. If the Frenet apparatus of γ_N is $\{T_N, N_N, B_N, \kappa_N, \tau_N\}$, then the following integral curves are called direction curves of principal normal indicatrix curve γ_N;

$$\begin{aligned} \phi_1 &= \int T_N, \\ \phi_2 &= \int N_N, \\ \phi_3 &= \int B_N \end{aligned} \tag{3.1}$$

Remark : Let s_1 and s_N be the arc length parameters of ϕ_1 and γ_N, respectively. Next, by differentiating and taking the norm the first equation in equation (3.1) with regard to s_1, we obtain $s_1 = s_N$. As a result, the arc length parameters of the principal normal indicatrix curve γ_N and the direction curves ϕ_1, ϕ_2 and ϕ_3 are equal.

Lemma 3.1: Let γ be a parametrized curve with arc length, γ_N be principal normal indicatrix curve of γ and ϕ_1 be T_N - direction curve of γ_N. Frenet apparatus of the direction curve ϕ_1 is given as

$$T_{\phi_1} = \frac{\kappa}{f}\left(-T + HB\right),$$

$$N_{\phi_1} = \frac{\sigma\kappa H}{f\sqrt{\sigma^2+1}}T - \frac{1}{\sqrt{\sigma^2+1}}N + \frac{\sigma\kappa}{f\sqrt{\sigma^2+1}}B,$$

$$B_{\phi_1} = \frac{H}{\sqrt{(H^2+1)(\sigma^2+1)}}T + \frac{\sigma}{\sqrt{\sigma^2+1}}N + \frac{1}{\sqrt{(H^2+1)(\sigma^2+1)}}B, \tag{3.2}$$

$$\kappa_{\phi_1} = \sqrt{\sigma^2+1} \qquad \text{and} \qquad \tau_{\phi_1} = \Gamma\sqrt{(\sigma^2+1)} \quad .$$

Proof: The results are simply derived by taking the derivative of the first equation in (3.1), utilizing equations (2.1), (2.2), (2.3), (2.4) and (2.5) and performing the necessary calculations.

Corollary 3.1: Let γ be a parametrized curve with arc length, γ_N be principal normal indicatrix curve of γ and ϕ_1 be T_N - direction curve of γ_N. T_N -direction curve of γ_N and principal normal indicatrix curve of γ overlap.

Proof: Observing equations (2.8), (2.9) and (3.2), we see that the Frenet apparatus of γ_N and ϕ_1 are same. Aside from this, if we take derivative of second equation of (2.7) and first equation of (3.1), use Frenet formulas and $\frac{ds}{ds_N} = \frac{1}{f}$, the result is apparent.

Theorem 3.1: Let γ be a parametrized curve with arc length, γ_N be principal normal indicatrix curve of γ and ϕ_1 be T_N - direction curve of γ_N. If the curve γ is general helix, then T_N - direction curve of γ_N is planar.

Proof: If γ is general helix, then $H = \frac{\tau}{\kappa}$ is constant. So, by the equation (2.5), we have $\Gamma = 0$. According to equation (3.2), it is obvious that torsion of ϕ_1 is zero.

Theorem 3.2: Let γ be a parametrized curve with arc length, γ_N be principal normal indicatrix curve of γ and ϕ_1 be T_N - direction curve of γ_N. The curve γ is C-slant helix if and only if T_N - direction curve of γ_N is general helix.

Proof: Contemplating equations (2.4) and (2.5), the harmonic curvature of ϕ_1 is obtained as $H_{\phi_1} = \Gamma$. Also using equation (2.6), we have $H_{\phi_1} = \Gamma = \frac{1}{\tan\theta}$. Thus if T_N - direction curve of γ_N is general helix, then H_{ϕ_1} is constant. So $\tan\theta = \text{constant}$ and we have the result.

Theorem 3.3: Let γ be a parametrized curve with arc length, γ_N be principal normal indicatrix curve of γ and ϕ_1 be T_N - direction curve of γ_N. The curve γ is slant helix if and only if T_N - direction curve of γ_N is planar.

Proof: If the curve γ is slant helix, then σ is constant. So by the equation (2.5), we get $\Gamma = 0$. By using the equation (3.2), the torsion of ϕ_1 is zero. Also the proof is true for the opposite option.

Lemma 3.2: Let γ be a parametrized curve with arc length, γ_N be principal normal indicatrix curve of γ and ϕ_2 be N_N - direction curve of γ_N. Frenet apparatus of the direction curve ϕ_2 is given as

$$
\begin{aligned}
T_{\phi_2} &= N_N = \frac{\sigma}{\sqrt{\sigma^2+1}}\left[\frac{\kappa}{f}(HT+B) - \frac{1}{\sigma}N\right], \\
N_{\phi_2} &= \frac{\kappa\left(\sqrt{\sigma^2+1}+\Gamma H\right)}{f\sqrt{\left(\sigma^2+1\right)\left(\Gamma^2+1\right)}}T + \frac{\Gamma\sigma}{\sqrt{\left(\sigma^2+1\right)\left(\Gamma^2+1\right)}}N + \frac{\kappa\left(-\sqrt{\sigma^2+1}H+\Gamma\right)}{f\sqrt{\left(\sigma^2+1\right)\left(\Gamma^2+1\right)}}B, \\
B_{\phi_2} &= \frac{H-\Gamma\sqrt{\sigma^2+1}}{\sqrt{\left(H^2+1\right)\left(\sigma^2+1\right)\left(\Gamma^2+1\right)}}T + \frac{\sigma}{\sqrt{\left(\sigma^2+1\right)\left(\Gamma^2+1\right)}}N \\
&\quad + \frac{H\Gamma\sqrt{\sigma^2+1}+1}{\sqrt{\left(H^2+1\right)\left(\sigma^2+1\right)\left(\Gamma^2+1\right)}}B,
\end{aligned}
\tag{3.3}
$$

$$\kappa_{\phi_2} = \sqrt{\left(\Gamma^2+1\right)\left(\sigma^2+1\right)} \quad \text{and} \quad \tau_{\phi_2} = \frac{\Gamma'}{f\left(\Gamma^2+1\right)}.$$

Proof: The results are simply derived by taking the derivative of the second equation in (3.1), utilizing equations (2.1), (2.2), (2.3), (2.4) and (2.5) and performing the necessary calculations.

Theorem 3.4: Let γ be a parametrized curve with arc length, γ_N be principal normal indicatrix curve of γ and ϕ_2 be N_N - direction curve of γ_N . If the curve γ is general helix, then N_N - direction curve of γ_N is planar.

Proof: If γ is general helix, then $H = \frac{\tau}{\kappa}$ is constant. So, by the equation (2.5), we have $\Gamma = 0$. Finally, the torsion of the curve ϕ_2 is zero, by considering equation (3.3).

Theorem 3.5: Let γ be a parametrized curve with arc length, γ_N be principal normal indicatrix curve of γ and ϕ_2 be N_N - direction curve of γ_N . The curve γ is C-slant helix if and only if N_N - direction curve of γ_N is planar.

Proof: Let the curve γ be C-slant helix. Then $\tan\theta = \text{constant}$, where θ is the angle between the vector field C and a fixed direction u. According to equations (2.4), (2.5) and (2.6) we have $\Gamma = \frac{1}{\tan\theta}$. Thus $\Gamma = \text{constant}$ and $\Gamma' = 0$. By the equation (3.3), the torsion of the curve ϕ_2 is zero and the result is clear.

Theorem 3.6: Let γ be a parametrized curve with arc length, γ_N be principal normal indicatrix curve of γ and ϕ_2 be N_N - direction curve of γ_N . N_N -direction curve can not be slant helix or general helix, if the curve γ is slant helix.

Proof: Considering equation (3.3), the harmonic curvature of the N_N -direction curve is obtained as

$$H_{\phi_2} = \frac{\Gamma'}{f\left(\Gamma^2+1\right)^{\frac{3}{2}}\sqrt{\left(\sigma^2+1\right)}}.$$

Also the σ function for being slant helix is

$$\sigma_{\phi_2}=\frac{1}{f}\frac{\left(\Gamma^2+1\right)\left(\sigma^2+1\right)}{\left(\left(\Gamma^2+1\right)\left(\sigma^2+1\right)+\left(\frac{\Gamma'}{f\left(\Gamma^2+1\right)}\right)^2\right)^{\frac{3}{2}}}\left(\frac{\Gamma'}{f\left(\Gamma^2+1\right)^{\frac{3}{2}}\sqrt{\left(\sigma^2+1\right)}}\right)',$$

Here, σ is constant if the curve γ is slant helix. Therefore $H_{\phi_2}=0$ and $\sigma_{\phi_2}=0$, consequently, N_N -direction curve can not be general and slant helices.

Example: Lets consider arc length parametrized and general helix curve

$$\gamma(s)=\left(\frac{\cos^2(s)}{\sqrt{2}},-\frac{\sin(s)\cos(s)}{\sqrt{2}},\frac{s}{\sqrt{2}}\right).$$

The principal normal indicatrix curve of γ is

$$\gamma_N(s)=\left(-\cos(2s),\sin(2s),0\right).$$

Then T_N -direction curve and N_N -direction curve of γ_N are found as

$$\phi_1(s)=\left(\frac{-\cos(2s)}{2}+c_1,\frac{\sin(2s)}{2}+c_2,c_3\right)$$

$$\phi_2(s)=\left(\frac{\sin(2s)}{2}+c_4,\frac{\cos(2s)}{2}+c_5,c_6\right)$$

where $c_i\in R,\quad 1\le i\le 9$.

It can be seen obviously that the curves ϕ_1 and ϕ_2 are planar, by calculating torsions of them. Thus we affirmed Theorem 3.1 and Theorem 3.4.

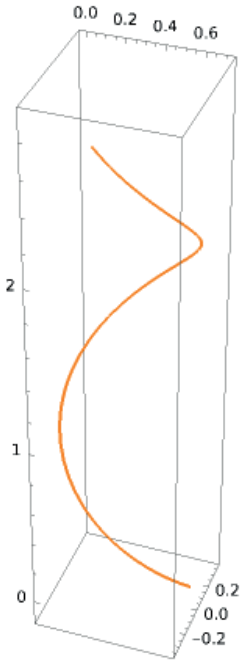

Figure 1. The curve γ **.**

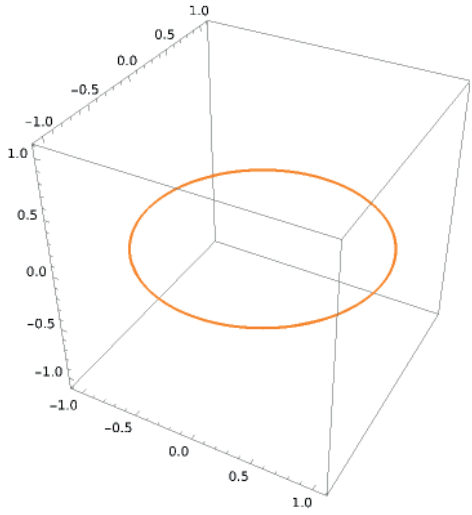

Figure 2. The curve γ_N **.**

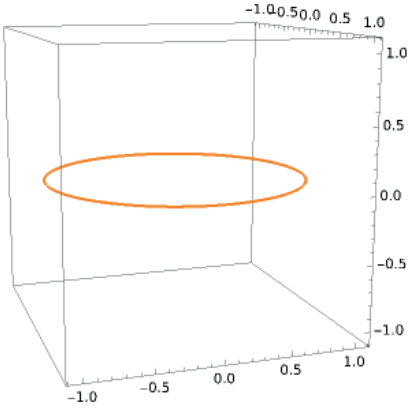

Figure 3. The curve ϕ_1 **.**

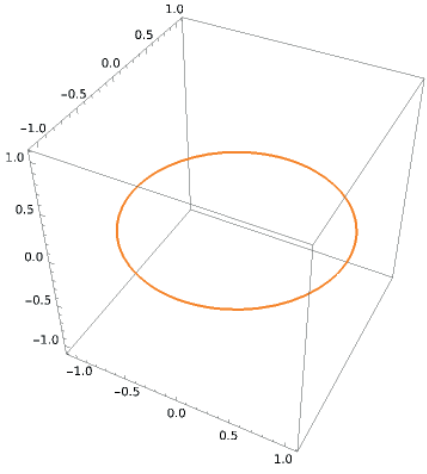

Figure 4. The curve ϕ_2 **.**

4. References

Ali, A.T. (2012). New special curves and their spherical indicatrix. *Global Journal of Advanced Research On Classical and Modern Geometries,* 1(2), 28-38.

Bishop, R.L. (1975). There is more than one way to frame a curve. *The American Mathematical Monthly*, 82(3), 246-251.

Choi, F.H. and Kim, Y.H. (2012). Associated curves of a Frenet curve and their applications. *Applied Mathematics and Computation,* 218, 9116-9124.

Do Carmo, M.P. (1976). Differential Geometry of Curves and Surfaces. Prentice Hall, Englewood Cliffs, NJ.

Gray, A., Abbena, E. and Salamon, S. (2006). Modern Differential Geometry of Curves and Surfaces with Mathematica, 3rd Edition, Chapman and Hall/CRC, New York.

Izumiya, S. and Takeuchi, N. (2004). New special curves and developable surfaces. *Turkish Journal of Mathematics,* 28, 153-163.

Kızıltuğ, S. and Önder, M. (2015). Associated curves of Frenet curves in three dimensional compact Lie group. *Miskolc Mathematical Notes*, 16(2), 953-964.

Körpınar, T., Sarıaydın, M.T. and Turhan, E. (2013). Associated curves according to Bishop frame in Euclidean 3-space. *Advanced Modeling and Optimization*, 15(3), 713-717.

Kula, L. and Yaylı, Y. (2005). On slant helix and its spherical indicatrix. *Applied Mathematics and Computation*, 169(1), 600-607.

Macit, N. and Düldül, M. (2014). Some new associated curves of a Frenet curve in E^3 and E^4 . *Turkish Journal of Mathematics*, 38, 1023-1037.

Qian, J. and Kim, Y.H. (2015). Directional associated curves of a null curve in Minkowski 3-space. Bulletin of the Korean Mathematical Society, 52(1), 183-200.

Struik, D.J. (1988). Lectures On Classical Differential Geometry, Dover, New York.

Şahiner, B. (2019). Direction curves of tangent indicatrix of a curve. *Applied Mathematics and Computation*, 343, 273-284.

Şahiner, B. (2018). Direction curves of principal normal indicatrix of a curve. *Journal of Technical Sciences*, 8(2), 46-54.

Uzunoğlu B., Gök, İ. and Yaylı, Y. (2016). A new approach on curves of constant precession. *Applied Mathematics and Computation*, 275, 317-323.

Yılmaz, B. (2016). Rektifiyan Eğriler ve Geometrik Uygulamaları. Ankara Üniversitesi Fen Bilimleri Enstitüsü Doktora Tezi.

Matematik ve Fen Bilimleri Üzerine Araştırmalar-III

Research on Mathematics and Science- III

Editör: Doç. Dr. Adile Akpınar

ÖZGÜR YAYINLARI

ISBN 978-975-447-766-5